Expressive and response dimensions of human emotion: neural mechanisms

Tien-Wen Lee

Thesis submitted for the degree of Doctor of Philosophy, August 2007

Department of Anatomy and Developmental Biology

University College London

UCL

ProQuest LLC
789 East Eisenhower Parkway
P.O. Box 1346
Ann Arbor, MI 48106-1346

Abstract

This thesis is about the neural mechanisms that underpin the expression of emotion in the human face and emotional modulation of behavioural responses.

I designed 5 integrated studies and used functional magnetic resonance imaging (fMRI) to address specifically the neural mechanisms underlying human facial expression and emotional response. This work complements studies of emotion perception and subjective affective experience to provide a more comprehensive understanding of human emotions.

I examined the neural underpinnings of emotional facial expression in three studies. I first demonstrated that emotional (compared to non-emotional) facial expression is not a purely motoric process but engages affective centres, including amygdala and rostral cingulate gyrus. In a second study I developed the concept of emotion contagion to demonstrate and verify a new interference effect (emotion expression interference, EEI). There is a cost (in reaction time and effort) to over-riding pre-potent tendency to mirror the emotional expressions of others. Several neural centres supporting EEI were identified (inferior frontal gyrus, superior temporal sulcus and insula), with their activity across subject predicting individual differences in personal empathy and emotion regulation. In a third study I examined an interesting phenomenon in our daily social life: how our own emotional facial expressions influence our judgment of the emotional signals of other people? I explored this issue experimentally to examine the behavioural and neural consequences of posing positive (smiling) and negative (frowning) emotional expressions on judgments of perceived facial expressions. Reciprocal interactions between an emotion centre (amygdala) and a social signal processing region (superior temporal sulcus) were quantified. My analysis further revealed that the biasing of emotion judgments by one's own facial expression works through changes in connectivity between posterior brain regions (specifically from superior temporal sulcus to post-central cortex).

I further developed two versions of an emotion GO/NOGO task to probe the impact of affective processing on behavioural responses. GO represents response execution and NOGO represents response inhibition. I therefore

investigated how different emotions modulate both these complementary response dimensions (i.e. execution and inhibition). This research line is pertinent to a major theme within emotion theory, in which emotion is defined in terms of response patterns (e.g. approach and withdrawal). My results confirmed that both emotional processing and induced emotional states have robust modulatory effects on neural centres supporting response execution and response inhibition. Importantly, my results argue for emotion as a context for response control.

My work extends our understanding of human emotion in terms of the nature and effect of its expression and its influence on response system.

I hereby declare that I have initiated, performed, and completed all aspects of the work described in this thesis by myself. This work includes conceptualization of the experimental questions, experimental design, execution of the experiments, data analyses, and write-up of the thesis.

Table of Contents

Figures

Tables

Abbreviations

ACC	Anterior Cingulate Cortex
BA	Brodmann Area
BOLD	Blood Oxygen Level Dependent
DCM	Dynamic Causal Modeling
EEI	Emotion Expression Interference
EMG	Electromyography
Eqn.	Equation
EPI	Echo Planar Imaging
fMRI	Functional Magnetic Resonance Imaging
GLM	General Linear Model
HRF	Haemodynamic Response Function
LFP	Local Field Potential
MNS	Mirror Neuron System
PC	Postcentral Cortex
PET	Positron Emission Tomography
PFC	Prefrontal Cortex
PM	Premotor Cortex
rCBF	Regional Cerebral Blood Flow
RT	Reaction Time
SMA	Supplementary Motor Area
SPM	Statistical Parametric Mapping
STS	Superior Temporal Sulcus

Acknowledgements

This thesis is supported by a Scholarship from Ministry of Education, Republic of China, Taiwan.

Chapter 1

Introduction to this thesis

Conceptual accounts of emotion embody experiential, perceptual, expressive and physiological modules (Izard et al. 1984) that interact with each other and influence other psychological processes, including memory and attention (Dolan 2002). Emotion induction (experience), emotion recognition (or perception) and emotion-accompanied physiological change have been explored in affective neuroscience (Critchley 2005; Phan et al. 2002; Wager et al. 2003). However, the neural underpinnings of emotional expression on the face and emotion-modulated changes in behaviour are still relatively under-investigated. These two dimensions are the main themes of this thesis.

I designed five integrated studies and used functional magnetic resonance imaging (fMRI) to address specifically the neural mechanisms underlying human facial expression and emotional response. This work complements studies of emotion perception and subjective affective experience to provide a more comprehensive understanding of human emotions.

1.1 EMOTIONAL EXPRESSION

1.1.1 Facial expression of emotion

Why do people express emotions on their faces? Charles Darwin was one of the most influential pioneers addressing this issue (Darwin 1872). In his evolutionary account, emotional expression originates in functional adaptations. Through association, modification and generalization shaped by evolutionary pressures, discrete patterns of facial expression developed, to be triggered in situations where the original function may no longer apply. Paul Ekman's observations of cross-cultural and cross-racial constancy in facial emotional expressions led to his *neurocultural theory*. This theory proposes that prototypical facial emotional expressions have arisen through natural selection and define *fundamental emotions* (Ekman 1972; Ekman et al. 1975). *Fundamental emotions* (anger, disgust, fear, happiness, sadness and surprise) are now established as principle dimensions within affective neuroscience and remain central to experiments in this thesis.

While facial emotions may speculatively be traced through vague and tortuous routes to origins in different "ancestral functions", the contemporary format of emotion expression on the face is doubtlessly functional for human beings. The *James-Lange theory of emotion* proposes physiological antecedents underpin emotional experience. In this context, facial movements (like other bodily changes) may be viewed as direct reactions to the emotional situation, subsequently contributing to the perception of emotion, rather than a consequence of being emotional (James 1894). Extension of James's theory leads to the *facial feedback hypothesis* (Tomkins 1981), which holds that that skeletomuscular or cutaneous feedback from facial expressions plays a casual role in regulating emotional experience and behaviour.

Tomkins proposed that an innate "affect program" emits message from the motor and physiological pathways to the body. The subsequent responses of the affected targets, such as the face and other organs, supply sensory feedbacks to the brain, which is experienced as emotion if reaching consciousness. The face, given its informative characteristics and prominent roles played in human emotions, was taken as a primacy for such feedback. Besides facial muscle, cutaneous, temperature and vascular receptors in the face were also assumed to play some minor roles in the facial feedback loop of emotion experience. Tomkins later modified his theory to downplay the facial muscles and focused on the facial skin. Other researchers extended and refined *facial feedback hypothesis* to dissociate global feeling states (pleasantness vs. unpleasantness, generated from brain stem, limbic system and hypothalamus), felt emotions (through facial feedback), and maintenance of emotions (through feedback from respiratory, cardiovascular and glandular systems) (Adelmann et al. 1989).

Ekman and co-workers (Ekman et al. 1980) observed that participants who actively smiled while watching positive films report themselves as happier than those who did not smile. Correspondingly, participants who produce angry, fearful or disgusted facial expressions when viewing a negative film reported subjectively greater negative affect. Given the frequent coupling of emotional experience and its emotional manifestation on face, several disambiguating strategies have been developed to test the *facial feedback hypothesis* empirically. For example, a directed facial action task and a non-obtrusive task were designed to eschew subjective awareness of posed facial expression which is concordant with a particular emotion style (Ekman et al.

1983; Soussignan 2002; Strack et al. 1988). Briefly, the directed facial action task requires the participants to follow muscle-by-muscle instructions that constitute specific facial expressions associated with different emotions; while the non-obtrusive task may ask the participants to hold a pencil in their mouth to either facilitate or inhibit the muscles typically associated with smiling without requiring subjects to pose a smiling face.

A causal relationship between facial feedback and experience of emotion is not always supported; a meta-analysis suggested the effect is only mild to moderate (Matsumoto 1987). Different emotional states may be induced and experienced without the need for facial or peripheral feedback. Thus, emotions can be generated through recollection of, or exposure to, emotion-laden material. If feedback from the periphery were necessary for differentiated emotional experience, blocking skeletomuscular activity would attenuate emotions (and their associated responses) and high-level spinal cord transection would result in diminished emotion experience and behaviours. In fact, both inferences have been disputed (Bermond et al. 1991; Girden 1943; Hoff et al. 1936). Emerging evidence validates the proposal that emotion and related constructs largely reside in the brain (Damasio et al. 2000; Dolan 2002). Feedback from the periphery might therefore play only a contributory role in modulating the intensity of emotion experience (Davidson et al. 2000). Nevertheless, there is broad empirical evidence for interactions between posed and observed facial expressions (Adelmann & Zajonc 1989), although the underlying neural mechanisms have previously remained uncertain.

Ekman's group further discovered that voluntary facial actions can generate emotion-specific autonomic responses (Ekman et al. 1983; Levenson et al. 1990) (an observation that is replicated in a recent report investigating cardio-respiratory activity; (Rainville et al. 2006)). Based on the close relationship between emotion experience, autonomic responses and facial expression, Ekman posited a "central, hard-wired connection between the motor cortex and other areas of the brain involved in directing the physiological changes that occur during emotion" (Ekman 1992). Posing emotion on the face is thus not purely a motoric process, yet the functional-specificity of the neural correlates resonating with facial emotion is largely unknown.

In addition to a purely affective interpretation (Ekman 1972), a wide range of meanings are attributed to facial movements, including *action readiness theory* (related but more fundamental issues are explored in this thesis, see next section; (Frijda 1986)), *motive-communication hypothesis* (Fridlund 1994), and *appraisal theory* (Scherer 2001). Closer inspection reveals that all these theories about emotional expression are not exclusive to each other; in fact, the meaning of facial expressions may be highly context-dependent (Parkinson 2005). Fridlund and co-workers highlighted the crucial role of social interaction in determining emotional expression on the face (Fridlund 1994). Expressed facial emotions thus influence or contribute to felt emotion, judgment of emotion of others and related social and physiological responses.

Evidence further suggests that emotions and facial expressions are 'contagious' in interactive milieu. This proposal is persuasively supported in my own facial electromyographical (EMG) studies: Viewing smiling and frowning faces implicitly activates the corresponding zygomaticus major muscle and corrugator muscle respectively in the viewer (Dimberg 1982; Dimberg 1986; Dimberg 1987; Dimberg 1990). One influential theory explains emotion contagiosity is "motor neuron system" (MNS). MNS, which is engaged when observing or performing the same action of others, has been proposed to play important roles in imitation (Rizzolatti et al. 2004). Mirror neurons, sensitive to hand and mouth action, were initially reported in monkey premotor, inferior frontal (F5) and inferior parietal cortices (Buccino et al. 2001; Ferrari et al. 2003; Rizzolatti & Craighero 2004; Rizzolatti et al. 2001). The human homologue of F5 covers part of the precentral gyrus and extends into the inferior frontal gyrus (Brodmann area 44 (BA 44), *pars opercularis*). In primates, including humans, the MNS is suggested as a neural basis for imitation and learning, permitting the direct, dynamic transformation of sensory representations of action into corresponding motor programmes. Despite the powerful explanatory strength of MNS, it is noteworthy that MNS theory is not an exclusive account. Dimberg et al. demonstrated the mild facial muscle activities may occur when viewing either facial or non-facial emotion-laden material (Dimberg 1986; Dimberg 1987; Dimberg 1990). In other words, emotion contagiosity is not necessarily restricted to MNS pathway, which was explored in this thesis.

Based upon emotion contagiosity, I hypothesized that this mimicry tendency (with 'resonant' patterns of neural activity; (Lee et al. 2006)) represents a pre-

potent response bias that would interfere with the ability to express a different opposing facial emotion (as exemplified by frowning to smiling faces or vice versa). It is clearly socially adaptive to have executive control over one's expression of emotion, enabling individuals to suppress, conceal or override pre-potent imitative responses. However, the responsible neural substrates for this expressive control are still unclear (Dimberg et al. 2002).

In this thesis, I used fMRI to investigate the neural mechanisms and neural substrates of three inter-related but uninvestigated issues, yet central to facial emotion expressions: imitative expression, controlled expression, and expression-biased emotion judgment; reflecting the way posed facial emotions interact externally and internally.

1.1.2 Emotion modulated behavioural responses

Positive and negative affective states have been linked to approach and withdrawal behaviours. The differential engagement of these facilitatory and inhibitory motivational systems is proposed to account for asymmetry in emotion-related brain activity (observed especially during electroencephalographic (EEG) studies; (Davidson 1995; Davidson et al. 1990)). The extension of this model has been influential in accounting for neurobiological mechanisms underlying personality, affective disposition, psychopathology, and trait/state reactions to emotion- and motivation- related constructs (Coan et al. 2004; Davidson et al. 2000).

However, adaptive social and motivational behaviour is also characterized by an ability to overcome stereotyped reactions and response patterns, permitting the expression of behavioural flexibility. Emerging evidence suggests a greater complexity to the relationship between discrete emotional states and response tendencies, indicating the independence of dichotomized motivational approach/withdrawal mechanisms and positive/negative affective representations within emotional brain systems (Harmon-Jones et al. 1998; Wacker et al. 2003).

The facial emotions of others not only signal affective states, but serve as dynamic social feedback cues with which to judge and regulate one's ongoing behaviour. An observed smiling face can encourage or reinforce behaviour, while an observed angry face can demand behavioural modification or inhibition. The relationship between positive and negative emotional signals to

approach and withdrawal behaviours represents a rather over-simplified dichotomy: Negative emotions, for example fear, may initiate fight, flight or freezing dependent upon both the context and individual differences (Bracha 2004). To date, very few imaging studies in humans have addressed how perceived emotions influence behavioural responses (Hare et al. 2005; Shafritz et al. 2006).

I accordingly developed two versions of an emotion GO/NOGO task to probe the impact of affective processing on fundamental behavioural responses. GO represents response execution and NOGO represents response inhibition. The participants performed GO/NOGO in sustained affective states for one task (emotion induction GO/NOGO) and in the presence of objective emotional signal for the other task (eye-gaze cued emotion GO/NOGO). I therefore investigated how different emotions modulate both these complementary response dimensions (i.e. execution and inhibition).

1.2 FUNCTIONAL IMAGING OF EMOTIONAL EXPRESSION

Functional neuroimaging of perception/recognition of emotional facial expressions of others generally reveals distributed network. Regions such as fusiform gyrus (fusiform face area) and superior temporal sulcus (STS) are typically viewed as visual nodes for generic processing of facial identity and changeable aspects and movements of faces including expression (Allison et al. 2000). Activities in both these regions are increased with facial stimuli of greater salience, though much evidence has suggested that emotional enhancement of fusiform activity is secondary to salience detection within amygdala (preferentially activated by with fearful faces) (Amaral et al. 1992; Vuilleumier 2005). STS detects and represents salient social features and probably forwards the representations to other brain regions for further processing (Adolphs et al. 1996). In contrast to commonality of STS and fusiform area across different fundamental emotions, neural specificity, to certain degree, has also been observed. For example, amygdala has been implicated preferentially for fear processing (Calder et al. 2001; LeDoux et al. 1988; Morris et al. 2001; Phelps et al. 2001; Scott et al. 1997); however, some evidence suggests that amygdalae also participate in the processing of other negative emotion, like anger (Scott et al. 1997), and positive emotion, like happiness (Kipps et al. 2007). Recognition of human signals of disgust involves ventral anterior insula and putamen (Calder et al. 2000; Krolak-

Salmon et al. 2003); while transient sadness increased neural activity at subgenual cingulate and anterior insula (Mayberg et al. 1999).

The functional imaging of emotional expression is still a young field in affective neuroscience. Imaging studies of facial emotion imitation have highlighted contributions from ventral premotor area, superior temporal gyrus, amygdala and insula (Carr et al. 2003; Ferrari et al. 2003; Leslie et al. 2004l). The ventral premotor area is situated at Brodmann area 44 (Broca's area on the left side). This area is viewed as a human homologue of premotor regions of macaque monkeys implicated in the mirror neuron system which, in turn, has been regarded as fundamental for action understanding and imitation (Rizzolatti & Craighero 2004). The role played by Broca's area (a language region) is thus extended to communication and empathy.

Imaging studies of behaviour manifestation modulated by emotion is rare. An emotional GO/NOGO paradigm is a suitable means to investigate this issue. Extant studies of emotion GO/NOGO typically tag emotion valences onto GO and NOGO cues, for example using happy face stimuli to signal GO trials and angry faces to signal NOGO trials, consistent with the theoretical relationship between approach and withdrawal response tendencies and positive and negative emotions. In such studies, the perceived emotion is either concordant or discordant with GO/NOGO contingencies (Hare et al. 2005; Shafritz et al. 2006). This contingent coupling of emotional information with response ensures that these studies probe aspects of emotion regulation and emotion-cognition interaction. However this task design does not permit an independent assessment of emotional influences on response execution and inhibition.

1.3 OUTLINES OF EXPERIMENTAL WORK

This thesis is organized into three parts.

In chapter 2, I summarize the principles of fMRI and analysis algorithms used in this thesis.

Chapter 3 to 5, I illustrate three studies that investigate facial emotion from three different perspectives. In chapter 3, I studied the imitation of facial expressions, incorporated three emotions and two ingestive comparisons to

identify emotion-specific imitating network. During scanning, the participants' facial movement was quantified from displacement of fiducial markers. These metrics were correlated with regional brain activity to highlight the neural centres resonant with magnitude of emotion expression (this work has been published; (Lee et al. 2007)). Chapter 4 demonstrates a new interference effect (emotional expression interference) and associated neural correlates. This interference effect is directly related to executive control of emotional expression, in contrast to the earlier investigation of emotion imitation - a facilitatory process (chapter 3 and published work; (Lee et al. 2006)). Chapter 5 highlights the neural mechanisms through which judgments of the emotions of others are biased by one's own actively posed facial emotion.

Chapter 6 and 7 describes two novel instantiations of emotional GO/NOGO studies: first, an eye-gaze cued emotional GO/NOGO task and, second, an emotion-induction GO/NOGO task. These two studies explicitly tested the emotional influences on fundamental motoric and withholding behaviours – response execution and inhibition.

FMRI studies entail MR physics and mathematical algorithms linking measured brain signals to neural activities. Before going into details about the neural activity mediating the expressive dimensions of emotion and their interaction with both affective and executive behaviours, it is appropriate for me to first describe the technical considerations and theoretical rationales underpinning these fMRI studies.

Chapter 2

Methods: Functional Magnetic Resonance Imaging (fMRI)

2.1 INTRODUCTION

All the experiments of this thesis adopted functional magnetic resonance imaging (fMRI). This chapter outlines the principles of this technique and summarizes the methods of neuroimaging data analysis. Haemodynamic functional neuroimaging methods such as fMRI and Positron Emission Tomography (PET) provide indirect measures of "brain activity". They are predicated on the coupling between increased neural activity, accompanied metabolic demand, and subsequent change in regional cerebral blood flow (rCBF) (review; Raichle 1998).

Neural activity can be investigated from many different angles: oscillation, action potential, sub-threshold depolarization, and local field potential (LFP) of neuronal population derived from summed synaptic excitation and synaptic inhibition, etc. FMRI is not able to differentiate all these neural activities; rather, they are all transformed into a single measurement: BOLD (blood oxygenation level-dependent) signal change which is used to infer brain activity. BOLD reflects the concentration of deoxygenated haemoglobin – the amount of deoxygenated haemoglobin per volume. The biological bridge between neural activity and BOLD is mediated by accompanied energy consumption and metabolites. Most fMRI scanning paradigm provides spatial resolution at around 8 to 50 mm^3, at least 10^6 neurons. BOLD signal thus reflects averaged behavior of neuronal populations, and is further modulated locally by oxygen consumption/supplement, flow velocity, and vascular constriction/dilation and so on. This chapter is divided into four sections: the neurovascular origins of fMRI signals, physical principles of fMRI (measurement of BOLD), haemodynamic modelling, and data analysis techniques.

2.2 NEUROVASCULAR ORIGINS of FMRI SIGNALS

Deoxygenate haemoglobin is an endogenous MRI contrast agent. The ferrous iron on the heme of deoxygenate haemoglobin is paramagnetic, but becomes diamagnetic in oxygenate haemoglobin. Paramagnetic substances have unpaired orbital electron; they become magnetized while the external magnetic field is on and become demagnetized once the field has been turned off. In

contrast, diamagnetic substances have no unpaired orbital electrons. When such a substance is placed in an external magnetic field, a weak magnetic field is induced in the opposite direction to external magnetic filed. The measurement of how magnetized a substance gets is named "magnetic susceptibility". If red blood cells containing deoxygenate haemoglobin were placed in the magnetic field used for MRI, there would be some filed distortion induced by the difference in the magnetic susceptibility relative to the surrounding. This susceptibility induced field shift or field distortion related to deoxygenate haemoglobin content is the source of BOLD contrast, and the change in the deoxygenate haemoglobin content associated with the brain activation can be detected in the MRI machine. The major factors affect the concentration deoxygenate haemoglobin include local oxygen consumption and flow state, discussed in the following paragraphs. As to the relationship between local magnetic susceptibility change and fMRI signal, see next section: 2.3 PHYSICAL PRINCIPLES OF FMRI.

Neuronal activity demands energy. Increases in neuronal activity cause an increase in glucose consumption (Kennedy et al. 1976; Wree et al. 1988). It is generally accepted that there is a "coupling" between neural activity, local glucose consumption, oxygen consumption, cerebral blood flow, oxygenate haemoglobin and deoxygenate haemoglobin, and capillary density. Nevertheless, given the simultaneous increase in oxygenate haemoglobin and deoxygenate haemoglobin, the cerebral oxygenation (the ration of oxygenate and deoxygenate haemoglobin) nearly kept constant. The above orchestrated change of physiological parameters is, however, only applied to brain activity at steady state; in other words, the physiological outcome after long-term adaptation. Instant and short-term challenge of the brain present different physiological pattern – this situation is pertinent to the fMRI studies because the experiment conducted in fMRI scanner is generally within 1 hour. Unlike traditional concept of "coupling", local consumption of oxygen under transient stimulation does not increase significantly, despite the increased local glucose consumption and the increased local cerebral blood flow (Raichle 1998). The local blood oxygenation thus rises, instead of decreases because the oxygen supplied from fully oxygenated blood via upstream dilated arterioles is much more than local oxygen consumption (Wenzel et al. 1996). As to the mismatch between glucose metabolism and oxygen consumption changes during brain activation, *oxygen limitation model* provides a plausible explanation (Buxton et al. 1997): Since during functional activation, cerebral blood flow increases are

mainly achieved by velocity increase or resistance reduction (not volume increase; the adaptive proliferation/expansion of vascular bed volume is negligible over short period of time), capillary transit time therefore decreases which, in turn, reduces oxygen extraction fraction. Namely, the gain of oxygen delivered to tissue from increased flow and enhanced oxygen gradient is partially cancelled out by reduced oxygen extraction fraction. The observed mismatch can thus be regarded as evidence for a tight coupling, rather than uncoupling between metabolism and blood flow. In line with this observation, anaerobic glycolysis had been proposed as an energy source for neural activity, which converts glucose to pyruvate, then to lactate with a net production of 2 ATPs. Evidence has been provided through in vivo microdialysis and magnetic resonance spectroscopy studies that a transient production of lactate occurs during brain activation (Fellows et al. 1993; Sappey-Marinier et al. 1992), manifested as a transient lactate peak.

However, contradictory evidence argues for increased oxidation of glucose by the brain. Data from PET, magnetic resonance spectroscopy, and from imaging of intrinsic optical reflectance signals in animals highlighted a significant increase in oxygen consumption during brain activation (Hyder et al. 1996; Malonek et al. 1996; Marrett et al. 1995). Recent accumulated evidence enables reconciliation of the two contrasting viewpoints, mediated by astrocytes. Astrocytes surround virtually all the intra-parenchymal capillaries and synaptic contacts; thus situated at an idea position for the interaction of neuronal activity and cerebral vasculature bed. Astrocytes possess receptors and reuptake sites for a variety of neurotransmitters, including excitatory neurotransmitter glutamate. Astrocytes also are enriched in glucose transporter, GLUT-1. During neuronal activation, astrocytes can sense released neurotransmitter like glutamate, which then triggers increased glucose uptake from capillaries (via GLUT-1). Glucose in astrocytes is then processed glycolytically to lactate by LDH_5 in an anaerobic way (Bonvento et al. 2002; Magistretti et al. 1999). Lactate is further transported into neuron via monocarboxylate transporters, and then converted to pyruvate by LDH_1. Pyruvate enters the TCA cycle – an oxidative step, generating 18 ATPs/lactate. The latter process indicates a metabolic "re-coupling" with increased oxygen consumption. Whether the transient glycolysis can be detected may thus depend upon the rapidity and degree of re-coupling between glycolysis in astrocytes and oxidative metabolism in neurons. The existence of transient non-oxidative glucose utilization would change the local cerebral oxygenation

and may help generate signals detectable by fMRI.

Increased local blood flow, which supplements fresh oxygenate haemoglobin as stated above, also contributes to BOLD signal. The factors induce regulatory adjustments of cerebral vessels are complicated, which can be categorized into intra-vascular and peri-vascular changes, with the latter of particular interest in general fMRI experiments. The local peri-vascular influence on neuron-vascular coupling can be further divided into ionic (functional) and metabolic factors. The most representative ion is potassium K^+, which is released into the extracellular space during neuronal activity (with concurrent influx of Na^+), as seen in a higher frequency of action potentials. Since the extracellular space in the brain is small (about 15%) and the intra/extracellular K^+ concentration gradient high, there is a considerable increase in the extracellular K^+, which in turn, dilates the cerebral vessels, reduces the resistance and increase the blood flow velocity. If there continues to be a mismatch between the oxygen/glucose demand and supply, H^+ and adenosine will trigger metabolically-induced vasodilatation. The initial increase of H^+ may have to do with lactate generation. Adenosine is the metabolic product of ATP mediated by ATPase, which restores electrical homeostasis by carrying K^+ back into and Na^+ out of the cells. Other factors affecting blood vessel resistance includes peri-vascular autonomic activities, serotonin, histamine, nitric oxide, and metabolites of arachidonic acid.

The temporal resolution of BOLD fMRI is considerably finer than that of PET, but still far away from neuronal timescale. The BOLD response to a transient change in metabolic activity is not instantaneous. Starting 1-2 seconds after the increase of metabolic activity, it takes 5-6 seconds to reach a peak and 15-30 seconds to return to baseline (Fransson et al. 1998a; Fransson et al. 1998b). Given the diverse neuronal, metabolic, neurovascular and haemodynamic responses and pathways involved, quantification of the relationship between BOLD signal and neuronal activity relies on models of physiological plausibility. The mathematical relationship between neural activity and BOLD response built upon state-of-art physiological ground is summarized in 2.4 HAEMODYNAMIC MODELLING. Nevertheless, a parsimonious way, at the sacrifice of accuracy and biological structure, to explore neural-BOLD relationship simply resorts to correlation. There are several electrophysiological parameters can be related to BOLD response, like spike activity, post-synaptic local field potential (LFP), power spectrum, etc.

Logothetis et al. (2001) used simultaneous recordings of spike activity, LFP and BOLD signals to show that BOLD signal amplitude correlated better with LFP than spike activity (Logothetis et al. 2001). Empirical evidence also suggests that the action potential firing activity of cortical cells contributes little to the metabolic demand of the brain, around 3% of the resting cortical energy consumption. The major determinant of neural oxygen and glucose consumption is the re-establishment of ionic concentrations via the Na^+-K^+ ATPase after synaptic activity, supporting the report of Logothetis et al. from metabolic perspective. The issue of how to integrate different neural activities (LFP, evoked potential, oscillation, sub-threshold depolarization, etc) within haemodynamic model remains to be investigated. Further work suggests that at very low and high synaptic activity there is a non-linear relationship between synaptic activity and rCBF (Norup Nielsen et al. 2001).

The incoming post-synaptic potential (LFP), however, can be either excitatory (around 70-80% of cortex) or inhibitory (around 20% of cortex). The inhibitory synaptic activity might decrease the BOLD by reducing net spike activities, and thus complicate the relationship of BOLD and LFP. Since both excitatory and inhibitory synapses demands energy consumption (Ackermann et al. 1984; Nudo et al. 1986), it is also reasonable to assume that inhibitory synaptic activity, like excitatory counterpart, would increase BOLD. Extant empirical evidence supported each of the above accounts (Heeger et al. 1999; Waldvogel et al. 2000). A recent model suggested that inhibition might increase BOLD response if there is a low prevailing level of excitation, but can reduce BOLD when excitation is generally high (Tagamets et al. 2001).

2.3 PHYSICAL PRINCIPLES OF FMRI

One of the pioneers of nuclear magnetic resonance theory was Felix Bloch of Stanford University, who won the Nobel Prize in 1946. He theorized that any spinning charged particle creates an electromagnetic field, with the magnetic component acting like a bar magnet. Quantum theory holds that atomic nuclei each have specific energy levels related to a property called "spin quantum number S". For example, the hydrogen nucleus has a spin quantum number S of ½ and with energy state ½ and -½. If there were even number of protons in a nucleus, every proton would be paired leaving net magnetic moment zero. When there is odd number of protons in a nucleus, there always exists one proton unpaired and gives a net magnetic field called "magnetic dipole

moment". Only nuclei with an odd number of protons or neutrons can be used for imaging in MR. In this thesis, MRI machine utilized the properties of hydrogen nucleus (proton), the most abundant atoms in the brain, to get both structural and functional signals.

When a proton is placed in a large external magnetic field (B_0), it not only spins about its own axis, but also rotates, wobbles or "precesses" about the axis of B_0 at an angular frequency ω, with ω equal to the product of a gyromagnetic ration γ and B_0, called Larmor equation:

$$\omega = \gamma * B_0 \qquad \text{(Eqn. 2.1)}$$

The gyromagnetic ratio γ for hydrogen protons is 42.6 MHz/Tesla. Further, around one in a million hydrogen spins will point to the same direction as B_0, called magnetization. When a group of protons wobble around in the external filed B_0, the out-of-phase component at the plane perpendicular to B_0 would be cancelled out, leaving a net magnetization vector M_0 along the direction of B_0. If there is a radiofrequency (RF) pulse transmitted along the direction perpendicular to B_0 at the same frequency of ω , then "resonance" occurs which adds on energy to the protons. Assume the oscillating magnetic field of RF pulse is B_1; M_0 begins to precess about the B_0 field at an angular frequency ω_1:

$$\omega_1 = \gamma * B_1 \qquad \text{(Eqn. 2.2)}$$

This results in a spiral motion of M_0 which pushes the system into a higher energy state, called "nutation". Once the RF pulse is turned off, the wobbling spins at some flip angle gradually relax back toward its lowest energy state – along the direction of B_0. There are two independent processes during spins relaxation: increase (recovery) in magnetic strength along B_0, and decrease (decay) in magnetic strength at the plane perpendicular to B_0. These two processes are governed by T1 and T2 relaxation time respectively.

T1 is also called "spin-lattice relaxation time" which refers to the time it takes for the spins to give the energy they obtained from the RF pulse back to the surrounding lattice in order to go back to their equilibrium state. The larger the T1 relaxation time means the slower the recovery. T2 is also called "spin-spin relaxation time" which implies an inherent property of a tissue to make a difference in the magnetic homogeneity by proton-proton interaction, and then, renders the spins out of phase (decay). Longer T2 causes slower decay. T2* is similar to T2 but also consider the factor of external magnetic field inhomogeneity. T2 decay occurs 5 to 10 times more rapidly than T1 recovery.

T2* is always less than T2, and T2* decay is always faster than T2 decay. The relaxation times T1 and T2 are specific for different tissues. For T1: cerebrospinal fluid (CSF) > gray matter > white matter. For T2: cerebrospinal fluid (CSF) > white matter > gray matter. Various designs of pulse sequence (PS; below) can provide different tissue contrast for identification. Generally, receiver detects MR signals at the plane perpendicular to B_0. If there is no further interference after RF turn-off, the signal detected will be like a sinusoid wave.

A pulse sequence is a sequence of RF pulses applied repeatedly during an MR study. Embedded in it are the repetition time (TR) and echo time (TE; or echo delay time) parameters. Unlike T1 and T2, which are inherent properties of the issue and therefore fixed, TR and TE can be controlled and adjusted by the operator. TR is the time interval between the applications of two consecutive RF pulses. Instead of making the measurement immediately after the RF pulse, measurement is delayed for a short period of time. This short period of time is referred to as TE. For a pulse sequence with short TR and short TE, T1-weighted image is acquired where fat tissue (ex. scalp subcutaneous layer and white matter) is bright. If TR and TE are long, T2-weighted image is acquired where water (ex. CSF) signal is prominent. Long TR and short TE would reflect the density of proton in the tissue, named proton density weighed image. In this thesis, structure image is T1-weghted and functional image is T2-weighted, with the former providing anatomical detail for visualization and the latter recording BOLD signal time course. There are a large number of pulse sequences developed for various clinical and research purposes, like partial saturation PS, inversion recovery PS (for specific tissue suppression with initial 180° RF followed by 90° RF; the interval between the 2 RFs is denoted TI: inversion time), STIR (short TI recovery, ex. for fat suppression imaging), spin echo (most commonly used PS; with initial 90° RF followed by RF180° to rephase/refocus the dephased spins caused by external magnetic field inhomogeneity), fast spin echo, gradient echo, echo planar imaging (EPI; the pulse sequence used in fMRI, see below for detail), etc. As stated in section 2.1, magnetic susceptibility provided by deoxygenate haemoglobin induces local magnetic field inhomogeneity. Reduction of deoxygenate haemoglobin during brain activation prolongs local T2* and makes local hydrogen signal enhanced – fMRI BOLD signal.

The above formulation is for single voxel MR signal. However, construction of

MR images requires decoding 3-D spatial information, which is the function of MR machine "gradients". Generally there are 3 different gradients: the slice-select gradient (Gz; Z-direction), the read-out or frequency-encoding gradient (Gx; X-direction), and the phase-encoding gradient (Gy; Y-direction). A gradient is simply a magnetic field that changes from point to point, usually in a linear fashion. Hence, magnetic nonuniformity is temporarily created in a linear manner to obtain information about position. Slice-selection in MR acquisition simply utilized Larmor Equation, with Z-direction gradient providing slice-specific precessional angular frequency for protons. Delivery of a RF at specific bandwidth can excite a specific slice (at XY plane). The Gx gradient is applied during the time the echo is received, i.e., during read-out. Gy is used to induce phase shift and usually applied between the 90° and the 180° RF pulses or between the 180° pulse and the echo. Phase encoding step takes time because discrimination of each row in a slice requires a separate phase encoding for the total row number; ex. if we want to discriminate 256 rows, then we need to perform 256 phase encoding steps, taking time 256 * TR. The summed signal for each TR fills in one line in a set of rows referred to as the data space. K-space can be thought of as a digitized version of the data space. Fast spin echo reduces the scanning time by filling in the number of "echo train length" into K-space at one TR. Gradient-recalled echo shortens the scanning time by introducing partial flip angle technique. Once all the data in k-space is acquired, 2D Fourier transform of the k-space results in the magnitude (modulus) and phase image, with the former being the constructed structure imaging in this thesis (magnitude image is also the most often seen MR image).

Our functional images utilized EPI technique. Unlike other fast scanning techniques (like fast spin echo, gradient-recalled echo) that can be achieved via software updates, EPI requires hardware modifications and thus expensive. High performance Gx gradients are needed to allow rapid on and off switching of the gradients. Gy can be kept on continuously or applied briefly during the time when the readout gradient was zero, to induce progressive phase-shift. The basic idea is to fill in k-space in one shot (one TR). Temporal resolution (TR) is therefore reduced to 3 to 4 sec which allows tracing cerebral haemodynamic changes for functional studies.

MR signal is vulnerable to local field inhomogeneity; in particular, there are severe geometric distortions in regions where there is an air-tissue interface. I

adopted 3 procedures to enhance signal quality. First, I applied orbitofrontal pulse sequence, where the slices covered the whole brain are in an oblique orientation of 30 degrees relative to the anterior–posterior commissural line to optimize sensitivity of orbitofrontal cortex and medial temporal lobes (Deichmann et al. 2003). Second, a fieldmap was acquired to unwarp geometrically distorted EPI images (Andersson et al. 2001). Fieldmap requires short- and long- echo scans where phase change due to local magnetic field difference can be converted to frequency map (phase difference divided by echo time difference). According to Larmor equation, there is a linear relationship between local field strength and frequency, thus providing index for adjustment of magnetic filed inhomogeneity. Lastly, head movement was minimized during scanning by comfortable external head restraint.

2.4 HAEMODYNAMIC MODELLING

The haemodynamic model adopted in the analysis was presented by Friston et al (Friston et al. 2000). It is predicated on a substantial amount of previous theoretical work and empirical evidence. The haemodynamic model was utilized to construct haemodynamic response function (HRF) which was frequently used in the analysis of functional localization and, is part of the underlying algorithm for the state-of-art analysis of functional integration (i.e. dynamic causal modelling, see section 2.5.3.2 and in chapter 5).

This model is a single-input-single-output system with a stimulus function as input. The stimulus function is assumed to be a known variable linking synaptic activity and rCBF. The model illustrates the relationship from stimulus function to BOLD using four state variables, six parameters and four differential equations, described as below:

Four state variables:
f_{in}: inflow; s: flow inducing signal; v: volume;
q: deoxygenate hemoglobin voxel content

Six parameters:
ε: efficacy; κ_s: rate-constant for signal decay;
κ_f: rate constant for auto-regulatoy feedback;
τ: time constant of flow transit time; α: Grubb's

Four differential equations:

$$\dot{f}_{in} = s \qquad \text{(Eqn. 2.3)}$$

$$\dot{s} = \varepsilon * u(t) - \kappa_s * s - \kappa_f * (f_{in} - 1) \qquad \text{(Eqn. 2.4)}$$

$$\tau * \dot{v} = f_{in} - f_{out}(v);\ f_{out}(v) = v^{1/\alpha} \qquad \text{(Eqn. 2.5)}$$

$$\tau * \dot{q} = f_{in} * E(f_{in}, E_0) / E_0 - f_{out}(v) * q / v;\ E(f_{in}, E_0) = 1 - (1 - E_0)^{1/f_{in}} \quad \text{(Eqn. 2.6)}$$

f_{out}: outflow; $E(f_{in}, E_0)$: fraction of oxygen extracted from inflowing blood f_{out} can be derived from state variable v and parameter α directly; and $E(f_{in}, E_0)$ can be derived from variable f_{in} and E_0 directly.

The physiological meanings of the above 4 differential equations are straight forward. All the state variables are normalized relative to the resting state, hence without unit. Eqn. 2.4 addresses the auto-regulatory/self-feedback of flow inducing signal s. ε is the efficacy of stimulus u(t) which can be used to differentiate brain regions pertinent to the processing of a particular stimulus. In other words, the null hypothesis is that ε is zero assuming a particular voxel being irrelevant to the mental processing of a certain kind of stimulus. The relationship between f_{out} and v mediated by exponential $1/\alpha$ is the famous balloon-Windkessel model (Buxton et al. 1998; Mandeville et al. 1999), which states that outflow is a function of volume that models the balloon-like capacity of the venous compartment to expel blood at a greater rate when extended.

The output BOLD signal y(t) is:

$$y(t) = \lambda(v, q, E_0) = V_0 * (7E_0 * (1 - q) + 2 * (1 - q/v) + (2E_0 - 0.2) * (1 - v)) + e \quad \text{(Eqn. 2.7)}$$

V_0 is the resting blood volume fraction, and e is the observation error. The concentration term $(1-q/v)$ accounts for the nonlinear behavior of the haemodynamic model.

Given the measurement of BOLD signals, Bayesian inference procedure (under some priori) for nonlinear observation models can be provided by applying first order Taylor expansion of equation 2.7 and E-M algorithm.

Empirical evidence suggested that the results resorting to hidden-states (as described above) and Volterra expansion are comparable (Friston et al. 2000). Volterra kernels, in opposite to hidden state-space model, characterizes the input and output relationship without resorting to hidden state variables. Volterra series have been described as a "power series with memory" performing a high-order or "non-linear convolution" of the inputs to obtain an output.

2.5 ANALYSIS OF FUNCTIONAL NEUROIMAGING DATA

All image analysis was performed using Statistical Parametric Mapping software, SPM (Wellcome Department of Imaging Neuroscience, UCL, UK. http://www.fil.ion.ucl.ac.uk/spm). The fMRI experiments in Chapters 3 and 4 were analyzed using SPM2 and the fMRI experiment in Chapter 5 to 7 were analyzed using SPM5. The analysis of imaging time series can be grossly divided into: preprocessing and statistical analysis.

2.5.1 Preprocessing

The analysis of fMRI data starts with several consecutive steps of spatial transformation with the purpose to remove movement artifact, reduce unwanted variance, enhance signal to noise ratio, and so on. Voxel-wise multiple univariate analysis requires BOLD time course from a particular voxel correspondent to a specific anatomical location. However, despite restraints on head, experienced subjects still show displacement of up to several millimeters. Given the voxel size of EPI image is generally at millimeter level, the initial preprocessing step realigns the data to remove the effects of subject movement. Following realignment the data undergoes unwarping to reduce deformation at static state (with fieldmap) and deformation from susceptibility-by-movement interaction (with movement parameters derived from realignment). The EPI time series are then normalized (transformed into a standardized anatomical space for subsequent comparison) and spatially smoothed. Data from individual subjects were pre-processed independently.

Realignment: This step involves rigid body transformation to minimize the sum of squared difference of voxel intensity between successive scans and a reference scan (I assigned the first scan in this thesis). Suppose a function b_i (Eqn. 2.8) describing the difference between the source and reference images at particular voxel i with respect to a transformation parameter $\boldsymbol{q}$.

Gauss-Newton optimization scheme of $\boldsymbol{b}$ (Eqn. 2.9) is repeated to update $\boldsymbol{q}$ until the sum of squared difference no longer decreases (10^{-8}) or a fixed number of iterations (64) has reached (Woods et al. 1998). Then, the EPI image series are re-sampled using B-spline interpolation. Mean EPI scan is generated after all the EPI images have been realigned. (bold case indicating matrix or vector)

$$b_i(\boldsymbol{q}-\boldsymbol{\Delta q}) \simeq b_i(\boldsymbol{q}) - \Delta q_1 \frac{\delta b_i(\boldsymbol{q})}{\delta q_1} - \Delta q_2 \frac{\delta b_i(\boldsymbol{q})}{\delta q_2} \cdots \qquad \text{(Eqn. 2.8)}$$

Eqn. 2.8 is equivalent to the following matrix format

$$\boldsymbol{A} * \Delta \boldsymbol{q} \simeq \boldsymbol{b}$$

, where $\boldsymbol{A} = \begin{pmatrix} \frac{\delta b_1(\boldsymbol{q})}{\delta q_1} & \frac{\delta b_1(\boldsymbol{q})}{\delta q_2} & \cdots \\ \frac{\delta b_2(\boldsymbol{q})}{\delta q_1} & \frac{\delta b_2(\boldsymbol{q})}{\delta q_2} & \cdots \\ \vdots & \vdots & \ddots \end{pmatrix}$, $\boldsymbol{b} = \begin{pmatrix} b_1(\boldsymbol{q}) \\ b_2(\boldsymbol{q}) \\ \vdots \end{pmatrix}$

$$\boldsymbol{q}^{(n+1)} = \boldsymbol{q}^{(n)} - (\boldsymbol{A}^T\boldsymbol{A})^{-1}\boldsymbol{A}^T\boldsymbol{b} \qquad \text{(Eqn. 2.9)}$$

Unwarping: After rigid-body registration, movement-related variance may be still sizable, attributable to nonlinear effects or movement-by-susceptibility interaction. To deal with this residual variance, an unwarping procedure (implemented in SPM2 and SPM5) was applied to the EPI time series (Andersson et al. 2001). Unwarping deals with two different states: first, static state (resting); and second, movement state (during the formal experiment). Magnetic field deformation (deformation field) in static state is measured by fieldmap; while the "rate of change" with respect to displacement (derivative field) is modelled as a linear combination of cosine basis fields. Unwarping movement-by-susceptibility interaction involves solving an inverse problem to estimate the derivative field based on acquired EPI series and estimated realignment parameters, which is applied to reduce movement-related variance (Andersson et al. 2001). The above procedures can be incorporated into a function of magnetic filed with respect to movement, with the deformation field (fieldmap) part representing the zero order term and the derivative field part representing first order term of the correspondent Taylor expansion.

Normalization: To accommodate registering images from different subjects to the same co-ordinate system, functional images were spatially normalized onto the Montreal Neurological Institute (MNI) atlas based on the normalization parameter derived from registering mean functional scan (derived from realignment step) to EPI template provided by SPM2/SPM5. The normalization resorts to a hybrid approach, starting with linear (twelve parameter affine transformation), then followed by non-linear (discrete cosine basis function with 1176 parameters) spatial transformations (Friston et al. 1995). An estimation scheme of "*maximum a posteriori*" (MAP) solution (according to Bayes' rule) was used to maximize the product of the likelihood function and the prior function (Eqn. 2.10).

$$p(q \mid b) \propto p(b \mid q) * p(q) \qquad \text{(Eqn. 2.10)}$$

, where $p(q)$ is the prior probability of parameters q, $p(b|q)$ is the conditional probability that b is observed given q and, $p(q|b)$ is the posterior probability of q, given that measurement b has been made. The advantage of the Bayes' approach is the innate penalty to current estimate q when the variance is large.

For affine registration, the maximum likelihood updating of parameter q can be derived from the function of residual squared difference, the same form as Eqn. 2.9, with variance-covariance matrix $\sigma^2(A^TA)^{-1}$ under the assumption of equal variance for each observation and multiple-Gaussian distribution. The MAP estimate is simply the average of the prior and likelihood estimates, weighted by the inverses of their respective covariance matrices. Nonlinear matching is achieved by linear combination of three dimensional (orthogonal) discrete cosine basis functions. The nonlinear registration involves simultaneously minimizing the membrane energies of the deformation fields and again, the residual squared difference between the EPI images and template. The obtained parameters are used to resample EPI functional images by trilinear interpolation.

Smoothing: Friston (2003) summarized the four major motivations for smoothing the fMRI images from theoretical accounts (Friston 2003). First, matched filter theorem suggests that the optimal smoothing kernel corresponds to the size of expected effect, in this thesis the spatial extent of BOLD signal, which is around 2 to 5 mm. Second, central limit theorem supports that smoothing the data will render the distribution "more" normal and effect the subsequent parametric, in contrast to non-parametric, statistics.

Third, Gaussian random field theory, which is used to make corrected statistical inference, requires a reasonable lattice representation of the underlying error terms of Gaussian field. To achieve the end, the smoothness should be substantially greater than voxel size. Fourth, smoothing the data accommodates inter-subject differences in terms of anatomical variability at homological brain regions. In this thesis, the EPI functional images were spatially smoothed with an isotropic Gaussian kernel of 8 mm.

2.5.2 Statistical analysis of imaging data

Functional specialization and integration are two of the central tenets of imaging neuroscience. Functional specialization holds that anatomically distinct cortical and sub-cortical areas are specialized to perform certain aspects of perceptual, cognitive or motor programming. Functional integration, in contrast, speaks to the interaction between functionally segregated areas. Neuroimaging tool fMRI resorts to haemodynamic responses, which accompany mental processes, in investigating localization and integration of functions in the brain. A large variety of methods have been developed to explore both issues.

For functional specialization, the most popular approach is through massive univariate statistical tests for each voxels. The mathematical formulation linking measured BOLD response and administered psychological test is via design matrix construction, which may accommodate a wide range of psychological challenges and contexts. General Linear Model (GLM) provides a framework for subsequent parameter estimation (see below). The resultant statistical parameters are assembled into an image, named statistical parametric map (SPM). Since the probabilistic behaviors of neighboring voxels are not independent, Bonferroni correction is thus over-conservative given the voxel number for a SPM generally exceeds many thousands. The spatially extended statistical property of SPM can be framed within Gaussian random filed theory, which gives the expected Euler characteristic (EC) for a smooth statistical map that has been thresholded. At high threshold EC is either one or zero. The expected EC thus leads to the expected number of clusters above a given threshold, approximating the number of unlikely excursions or "blobs" in the SPM. Calculated EC in turn yields the height threshold. For convenience, the statistical values (student t-test SPM {t} or F test SPM {F}) are forcefully transformed into Gaussian field (SPM {Z}). In this thesis, the majority of the analyses are based on this conventional approach, with other detail described

in 2.5.2.1.

For functional integration, a common approach is multivariate analysis which unveils a distributed "pattern" of neurophysiological changes, like eigenimage analysis, multidimensional scaling, MANCOVA with CVA, partial least square, etc. Interaction between neural nodes can also be investigated by "connectivity". The concept of connectivity is not new, which can be further clarified with "functional connectivity" and "effective connectivity" (Friston et al. 1993a; Friston et al. 1993b). Functional connectivity is defined by temporal correlation between remote neural nodes; whereas effective connectivity is causal, which models the influence one neural node exerts on the others or models the interaction (ex. through bilinear terms, see below). Effective connectivity can be investigated in static system, ex. psycho-physiological interaction and structure equation modelling, or dynamic system, ex. Kalman filter and multivariate autoregressive models. Among all these various models of effective connectivity, dynamic causal model (DCM) is an outstanding and state-of-art approach. In this thesis, I applied DCM analyses in chapter 5 to investigate the modulatory effect of emotion expression on emotion judgment. The algorithm behind DCM is summarized in 2.5.2.2.

2.5.2.1 Conventional SPM analysis

In conventional SPM analysis, design matrix and contrast setup play crucial roles. The design matrix is applied to all the voxels, which can be thought of as allowing inputs to be connected to all regions and discount interactions among regions (see 2.5.2.2 for comparison). The design matrix is partitioned into effects of interest, confounds and error. The main effects of different psychological inputs can be modelled as stick functions in separate columns of the design matrix. The variability of a particular psychological input is entered as parametric modulator, which is centre-meanned. To approximate the measured haemodynamic response, each stick functions and parameteric modulators are further convolved with pre-determined HRF (Friston et al. 2000). Session effect, covariates (ex. movement parameters derived from realignment step), and low frequency drift (modelled as linear combination of discrete cosine sets) of magnetic filed are treated as confounds. The GLM is applied to obtain the effect of interest, with the null hypothesis that the coefficient of irrelevant voxel is zero (Eqn. 2.11).

$$Y = X * \beta + e \qquad \text{(Eqn. 2.11)}$$
$$\beta = (X^T X)^{-1} X^T Y$$

If design matrix X is rank deficient, there are infinitely many parameter sets β fitting the same model. In this case, Moore-Penrose pseudoinverse was adopted to solve the equation, which is constrained by minimum L_2 norm of β.

To localize function in the brain, cognitive subtraction is a common strategy which isolates a specific psychological construct by calculating the difference between two (or several) tasks. Substantiation of cognitive subtraction is through contrast setup by a vector or matrix "c", mathematically reflected as $c^T\beta$. Since over-parameterized model is occasionally encountered in neuroimaging studies, it is imperative to consider only the contrasts that are invariant over the space of possible parameters. Valid contrast can be tested by Eqn. 2.12.

$$c^T = c^T(X^TX)^{-1}X^TX \qquad \text{(Eqn. 2.12)}$$

In other words, $c^T\beta$ is constant if c^T is unchanged by post-multiplication with $(X^TX)^{-1}X^TX$.

Statistical inferences are made about the size of the effects of interest in relation to the error variance using F (ANOVA or ANCOVA; SPM{F}) or T (SPM{T}) statistics. However, the error term (e in Eqn. 2.11) generally does not conform to independent and identical distribution (i.i.d) because fMRI data exhibits short range serial temporal correlations. The error structure was modelled with first degree auto-regressive process (AR(1)) and solved within ReML (restricted maximum likelihood) framework with corrected (effective) degrees of freedom. Although the design matrix is applied to every voxel, the variance is assumed to be different between voxels.

The above calculation plus the application of random filed theory constitutes the major part of first level analysis, and provides individually based SPM. Generalization of result to the whole population requires second level analysis, with a similar analytic structure as in Eqn. 2.11. In second level analysis, the observation Y is replaced by concatenating the individual contrast(s) of interest $c^T\beta$. The design matrix makes correspondent change according to the contrast of interest, and the error term reflects between subject variability. In this thesis, all the analytic results are at population (second) level. The resultant coordinates from SPM were transformed into standardized anatomic space (Talairach et al. 1988).

2.5.2.2 Dynamic Causal Model (DCM)

DCM is a source reconstruction tool to identify a nonlinear dynamic system, which combines a causal model and haemodynamic response model (section 2.4). The causal model is a realization of Fleiss fundamental equation (Eqn. 2.13), which describes the causal relationship between the outputs and the recent history of the inputs;

$$\dot{z} = f(z, \theta, u) \qquad \text{(Eqn. 2.13)}$$

, where z represents state variables, θ are the parameters of the model, and u is the input. DCM embodies two types of perturbation of an interconnected system made of representative neural nodes (Friston et al. 2003). The first type of perturbation is modelled as the imposition of a direct influence on a specified neuroanatomical region, for example V1 responding to visual stimuli. The second type exerts its effect vicariously by changing the coupling between neural nodes. For example, attention may modulate the connectivity of V1 to V5 during the perception of moving objects (Penny et al. 2004a). Accordingly, DCM differentiates the extrinsic and intrinsic connectivity strength of a system and also permits the modulation of connectivity as a function of experimental contexts. DCM achieves this through a generalization of the conventional linear model into bilinear model manipulations. In DCM, the state is the neuronal response, and the causal model (function f in Eqn. 2.13) is expressed as in Eqn. 2.14:

$$\dot{z} \approx Az + \sum u_j B^j z + Cu \qquad \text{(Eqn. 2.14)}$$

Matrix A is a connectivity (mixing) matrix describing the connectivity among the regions in the absence of input. Matrix B^j induces the change in intrinsic coupling from the jth input. Multiplication of the element of B^j and u_j constitutes the bilinear interaction term. Matrix C represents the extrinsic influences on inputs on neuronal activity.

DCM further incorporates a biologically plausible generative model - haemodynamic forward model (section 2.4) that relates the state variables to measured haemodynamic (BOLD) responses. The variable z in Eqn. 2.14 replaces the variable ε *u(t) in Eqn. 2.4. With some constraints on the coupling parameters (priors, described below), the estimation of connectivity in current DCM employs a full Bayesian framework. Assume that matrix A has diagonal -1 to represent auto-decay and the matrix A is scaled by a factor σ. The largest real eigenvalue (Lyapunov exponent) of matrix A should be less than zero to make the system stable, instead of diverging exponentially to infinite values. For a fixed value ξ of the squared sum of the off-diagonal

elements of matrix A, the largest eigenvalue is reached when all the off-diagonal elements are the same. Conditional upon the chi-square distribution of ξ in terms of probability (say, probability of ξ greater than some value is less than 0.05), an upper limit of ξ provides the priori variance of the elements of matrix A, which is also applied to matrix B. The prior unbiased estimates of the elements in matrix A (except diagonal) and B are set to zero. The prior expectation of σ is set to one, compatible with the time constant of between-region interaction ranges from a few hundred milliseconds to several seconds. Under the assumption of Gaussian, the variance of σ is determined by assigning the probability that σ is less than zero (say, lower than 0.05). The prior estimates of the elements of C are set to zero and the variances are set to one. Priors for the biophysical (haemodynamic) parameters are empirically determined (Friston et al. 2000). DCM accordingly enables making inference of connectivity parameters from measured BOLD time series. Adopting Akaike's Information Criterion (AIC) and Bayesian Information Criterion (BIC), Bayesian scheme further permits model averaging, inferential deduction and model comparison.

DCM surpasses classical between-region correlation/coupling analysis in several aspects. First, the derived connectivity is effective as opposed to functional; in other words, it is causal. The connectivity in DCM further provides sensible physiological meaning. The units of connections are per unit time and correspond to rates. A strong connection indicates an influence from other neural nodes is quick or with a small time constant. Second, DCM model is a sophisticated nonlinear source reconstruction tool with updated physiological constraints and haemodynamic model. Third, DCM is framed with Bayesian framework which allows making statistical inferences and model comparison (Penny et al. 2004a). The optimal model is selected by considering both model-fitting and parameter regularization. Fourth, DCM is able to disambiguate the influence from perturbing (extrinsic) and contextual inputs, with the latter modelled by bilinear coupling which allows the change of connectivity due to top-down influence or under various psychological/experimental contexts. This flexibility is particularly useful in neuroimaging studies of factorial design. For example, attention may modulate the connectivity of V1 to V5 while perceiving moving objects (Penny et al. 2004a). Although other methods, like structure equation models, also make inference about effective connectivity, DCM is preferred for fMRI studies due to its emphasis on neurodynamics, which in turns causes haemodynamic change

(Penny et al. 2004b). In structure equation model, the connectivity change is derived directly from observed haemodynamics. As to the DCM modelling of chapter 5 in this thesis, facial emotion stimuli are perturbing/extrinsic inputs, and the actively posed facial expressions provide psychological context - contextual inputs, where facial emotion judgment is biased.

The relationship between DCM and conventional SPM is addressed here. In fact, conventional SPM is a special case of DCM. Setting the variance of matrix A and B in Eqn. 2.14 to zero discounts all the interaction between neural nodes; and matrix C is correspondent to the design matrix in Eqn. 2.11. Eqn. 2.11 can thus be viewed as the ability (i.e. efficacy) of input to excite neural activity in each voxel. Current DCM generally hosts 4 to 6 neural nodes to allow reasonable computation burden and calculation validity. The representative time course of each neural node is extracted from first eigenvariate of all the voxels within the region of interest.

Chapter 3

Imitating expressions: Emotion-specific neural substrates in facial mimicry

---

3.1 INTRODUCTION

In this chapter, I investigated the neural correlates associated with imitating emotional facial expression, with non-emotional facial expressions as a comparison.

In dynamic social interactions, the perception of another's facial expression can induce a 'contagious' or complementary subjective experience and a corresponding facial musculature reaction, evident in facial electromyography (EMG) (Dimberg 1990). Further, the relationship between facial muscle activity and emotional processing is reciprocal: Emotional imagery is accompanied by changes in facial EMG that reflect the valence of one's thoughts (Schwartz et al. 1976). Conversely, intentionally adopting a particular facial expression can influence and enhance subjective feelings corresponding to the expressed emotion (Adelmann et al. 1989; Ekman et al. 1983). To explain this phenomenon, Ekman proposed a "*central, hard-wired connection between the motor cortex and other areas of the brain involved in directing the physiological changes that occur during emotion*" (Ekman 1992).

Neuroimaging studies of emotion typically probe neural correlates of the perception of emotive stimuli or of induced subjective emotional experience. A complementary strategy is to use objective physiological or expressive measures to identify activity correlating with the magnitude of emotional response. Thus, activity in the amygdala predicts the magnitude of heart rate change (Critchley et al. 2005) and electrodermal response to emotive stimuli (Phelps et al. 2001; Williams et al. 2004). Facial expressions are overtly more differentiable than internal autonomic response patterns. In the present study, I used the objective measurement of facial movement to index the expressive dimension of emotional processing.

My approach hypothesizes that the magnitude of facial muscular change during emotional expression 'resonates' with activity related to emotion processing (Ekman 1992; Ekman et al. 1983). Thus, I predicted that brain activity correlating with facial movement, when subjects adopt emotional facial expressions, will extend beyond classical motor regions (i.e. precentral gyrus,

premotor region, supplementary motor area) to engage centres supporting emotional states. Recently, a 'mirror neuron' system (MNS; engaged when observing or performing the same action) has been proposed to play important role in imitation, involving the inferior frontal gyrus, Brodmann area 44 (BA 44) (Rizzolatti et al. 2004). While clinical studies suggest right hemisphere dominance in emotion expression, neuroimaging evidence is equivocal (Blonder et al. 2005; Borod 1992; Carr et al. 2003; Leslie et al. 2004). One focus of my analysis was to clarify evidence for right hemisphere specialization in BA 44 for emotion expression.

I measured regional brain activity using functional magnetic resonance imaging (fMRI) while indexing facial movement during imitation of emotional and non-emotional expressions (see Materials and Methods). Subjects were required to imitate dynamic video stimuli portraying angry, sad and happy emotional expressions and non-emotional (ingestive) expressions of chewing and licking. Evidence suggests that facial expressions may intensify subjective feelings arising from emotion-eliciting events (Adelmann & Zajonc 1989; Dimberg 1987). I therefore predicted that neural activity, besides motor regions and MNS, would correlate with the magnitude of facial movement during emotion mimicry. Moreover, I predicted that activity within regions implicated in representations of pleasant feeling states and reward (including ventral striatum) would be enhanced during imitation of happy expressions, activity within regions associated with sad feeling states (notably subcallosal cingulate cortex) would be enhanced during imitation of sad faces (Mayberg et al. 1999; Murphy et al. 2003; Phan et al. 2002), and regions associated with angry feeling/aggression modulation (putatively, ventromedial prefrontal region) would be enhanced while imitating angry faces (Damasio et al. 2000; Dougherty et al. 2004). Further, since facial movement communicates social motives, I also predicted the engagement of brain regions implicated in social cognition (including superior temporal sulcus) during emotion mimicry (Frith et al. 1999; Parkinson 2005; Wicker et al. 2003).

3.2 MATERIALS AND METHODS

3.2.1 Subject, task design and experimental stimuli

I recruited eighteen healthy right-handed volunteers (mean age, 26 years; 9M, 9F). Each gave informed written consent to participate in an fMRI study approved by the local Ethics Committee. Subjects were screened to exclude history or evidence of neurological, medical, or psychological disorder including substance misuse. None of the subjects was taking medication.

Since facial emotional expressions are highly dynamic signals (Kilts et al. 2003), my experimental stimuli consisted of short movies of five dynamic facial expressions (representing anger, sadness, happiness, chewing and licking), performed by four male and four female models. The eight models were selected from 13 models whose movies were identified as intended facial expressions by another independent expert. All of the models prepared personal scripts to facilitate generation of corresponding expressions and received training before videotaping and half had previous acting experience or drama background. Only movies reaching 100% consensus were taken as experimental stimuli in this thesis. Subjects performed an incidental sex-judgement task, signalling the gender of the models via a two-button, hand-held response pad. To ensure subjects focused on the faces, the hair was removed in post-processing of the video stimuli, see Figure 3.1 (i).

Figure 3.1

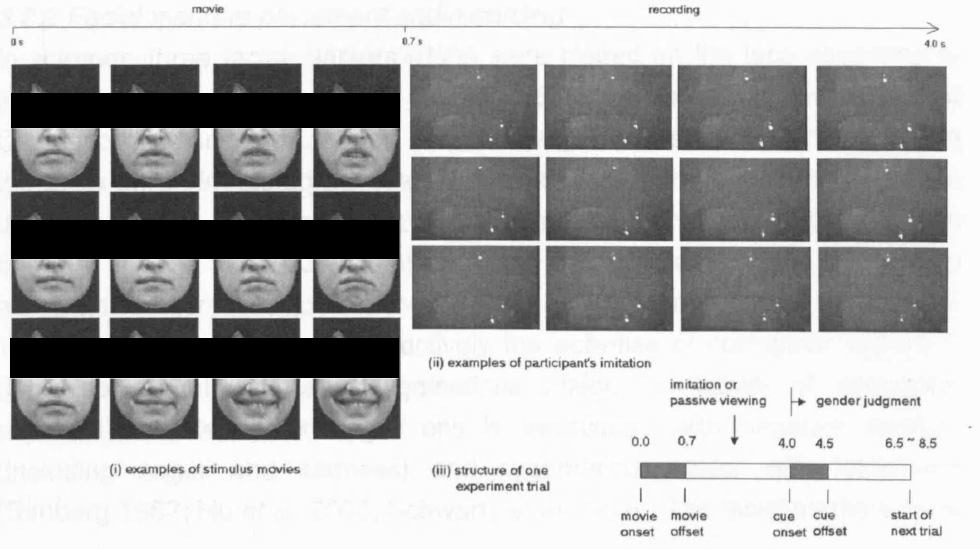

Figure 3.1 Examples of (i) experimental stimuli and, (ii) recorded frames of participant's imitation of the three facial expressions. From top row to bottom, they are angry, sad and happy, respectively. The structure of one experiment trial is illustrated in (iii).

The experiment was split into three sessions each consisting of eight interleaved blocks. A block was either imitation (IM), where the subjects imitated the movies, or passive viewing (PV), where the subjects just passively viewed the video stimuli. Within each block, there were two trials for each facial expression and the order of the trials was randomized. Thus, each subject viewed a total of twenty-four trials of IM or PV for each facial expression. In the imitation IM blocks, the subjects were instructed to mimic as accurately as possible the movements depicted on video clips.

On each trial, the video (movie) clip lasted 0.7 seconds. Four seconds after the movie onset, a white circle was presented on the screen for 0.5 seconds to cue the response (gender judgment). On IM blocks, the subject imitated the facial expression during the interval between the movie offset and gender response cue. Trial onset asynchrony was jittered between 6.5 to 8.5 seconds (average 7.5 seconds) to reduce anticipatory effects. Each session lasted twelve minutes and thirty seconds. The whole experiment lasted approximately forty minutes and the trial structure is illustrated in Figure 3.1 (iii). The leading block of the three sessions was either IM-PV-IM or PV-IM-PV, counter-balanced across subjects.

3.2.2 Facial markers placement and recording

In scanner, three facial markers (dots) were placed on the face according to the electrodes sites suggested in facial EMG guidelines by Fridlund and Cacioppo (Fridlund et al. 1986). The first dot, D1, was affixed directly above the brow on an imaginary vertical line that traverses the endocanthion, while the second, D2, was positioned 1 cm lateral to, and 1 cm inferior to, the cheilion, and the third, D3, was placed 1 cm inferior and medial to the midway along an imagery line joining the cheilion and the preauricular depression. Their movement conveyed respectively the activities of corrugator supercilii, depressor anguli oris and zygomaticus major. Activity of corrugator supercilii and depressor anguli oris is associated with negative emotion (including anger and sadness) and zygomaticus major with happiness (Dimberg 1987; Hu et al. 2003; Schwartz et al. 1976). The facial markers were

located on the left side of face consistent with studies reporting more extensive left hemiface movement during emotional expression (Rinn 1984). The dots were made from highly reflective material (3M™ Scotchlite™ Reflective Material), and were 2 mm in diameter, weighing 1mg. I adjusted the eye-tracker system to record dot position using infrared light luminance in darkness. The middle part of the subject's face was obscured by part of the head coil. Dot movement was recorded on video (frame width x height, 480 x 720 pixels; frame rate, 30 frames per second), see Figure 3.1 (ii). Analysis of facial movement used a brightness threshold to delineate the dot position from the central point of the marker. Dot movement was calculated as the maximal deviation from baseline within 4 seconds after stimulus onset; where the baseline was defined as the average position of the dot ion the preceding 10 video frames. During imitation of sadness and anger the magnitude of facial change was taken from the summed movement of D1 and D2. During imitation of happiness, facial change was measured from movement of D3 and, for chewing and licking from D2. I adopted the simplest linear metric of movement in the analyses. Movie segments of five seconds were constructed for each imitation trial post-experiment. Each segment was visually appraised by the experimenter to identify correct and incorrect responses and exclude the presence of confounding 'contaminating' movements.

3.2.3 fMRI data acquisition

I acquired sequential T2*-weighted echoplanar images (Siemens Sonata, 1.5-T, 44 slices, 2.0 mm thick, TE 50 ms, TR 3.96 s, voxel size 3*3*3 mm^3) for blood oxygenation level dependent (BOLD) contrast. One hundred and ninety-six whole-brain images were obtained over 13 min for each session. The first five echoplanar volumes of each session were not analyzed to allow for T1-equilibration effects. A T1-weighted structural image was obtained for each subject to facilitate anatomical description of individual functional activity after co-registration with fMRI data.

3.2.4 fMRI data analysis

I used software SPM2 on a Matlab platform (Mathwork, IL) to analyze fMRI data. The analytic flows and underlying principles have been described in chapter 2. Separate design matrices were constructed for each subject to model, firstly, presentation of video face stimuli as event inputs (delta functions) and, secondly, the magnitudes of movement of dots on the face as parametric inputs. For clarity, in the following context I refer to the resultant statistical

parametric maps (SPMs) of the former "*categorical SPM*" and the latter "*parametric SPM*". Data from 16 subjects were entered in the *parametric SPM* analyses; two subjects were excluded because of incomplete video recordings of facial movement.

Error responses representing trials in which a subject incorrectly imitated the video clip were detected from recorded movies and modelled separately within the design matrix. Activity related to stimulus events was modelled separately for the five different categories of facial expressions using a canonical haemodynamic response function (HRF) with temporal and spatial dispersion derivatives (to compensate for discrepant characteristics of haemodynamic responses). In *categorical SPM* analyses, contrast images were computed for activity differences of imitation minus passive viewing for each stimulus category. These were entered into group level (second-level) analyses employing an analysis of variance (ANOVA) model.

Second-level random effect analyses were performed separately as F-tests of event-related activity *(categorical SPM)* and as F-tests of the parametric association between the facial movements *(parametric SPM)*. The statistical threshold was set at 0.05, corrected, for the former, and at 0.0001, uncorrected, for the latter. The threshold of spatial extent of cluster size was set at 3 voxels, which was applied throughout this thesis. I made an assumption that ingestive facial expression and emotional facial expression were not comparable in terms of underlying mental processes, and consequently avoided a subtraction logic (e.g. smiling minus chewing) commonly employed in neuroimaging studies. To constrain the analysis to brain regions specific to imitation of *emotion* processing, I used an exclusive mask representing the conjunction of activity elicited by the two *ingestive* facial expressions (IGs) in both *categorical SPM* and *parametric SPM.* I examined parameter estimates of peak coordinates to distinguish activations from deactivations in F-tests.

3.3 RESULTS

3.3.1 Behavioural performance

Subjects imitated emotional and ingestive facial expression from the video clips with greater than 90% accuracy (error rates for angry faces 7.1%, sad faces 3.8%, happy face 1.6%, chewing face 6.3% and licking face 1.9%). Movement of each of the three facial markers reflected the differential imitation of facial expressions conditions (D1, $F(1,15) = 5.66$ ($P = 0.016$); D2, $F(1,15) = 5.507$ ($P = 0.007$) and; D3, $F(1,15) = 17.828$ ($P < 0.001$) under sphericity correction). Since the facial markers were very light in weight, no subject remembered that there were three dots on the face after scanning.

To test for the possibility of confounding head movement during expression imitation trials, I assessed the displacement parameters (mm) used in realignment calculations during pre-processing of function scan time series (entered for each subject within SPM). For IM and PM blocks: -0.009 (SD 0.037) and 0.004 (SD 0.042) along the X direction, 0.091 (SD 0.086) and 0.114 (SD 0.071) along the Y direction, and 0.172 (SD 0.147) and 0.162 (SD 0.171) along the Z direction. The mean rotation parameters (rad) for IM and PM blocks are 0.0002 (SD 0.0030) and -0.0011 (SD 0.0035) around pitch, 0.0002 (SD 0.0010) and 0.0000 (SD 0.0013) around roll, and 0.0001 (SD 0.0007) and -0.0003 (SD 0.0008) around yaw. For the above six parameters, paired T-tests of IM and PV do not reach statistical significance (df = 17).

3.3.2 Activity relating to emotional imitation (categorical SPM)

Bilateral somatomotor cortices (precentral gyrus, BA 4 and 6) were activated during imitation of all the five emotional and ingestive facial expressions, compared to passive viewing. Imitation of emotions (IEs), compared to imitation of ingestive facial expressions (IGs), enhanced activity within the right inferior frontal gyrus (BA 44) (Figure 3.2, Table 3.1; all the Tables in this chapter are listed from page 47 to 54). A condition by hemisphere (contrasting subject-specific contrast images with the equivalent midline-'flipped' images) did not reach statistical significance (*P* value 0.001, with region of interest analysis at BA 44), consistent with relative lateralization of BA 44 emotion-related response. Bilateral BA44 activity was observed in *categorical SPM* at an uncorrected *P* value 0.0001.

Figure 3.2

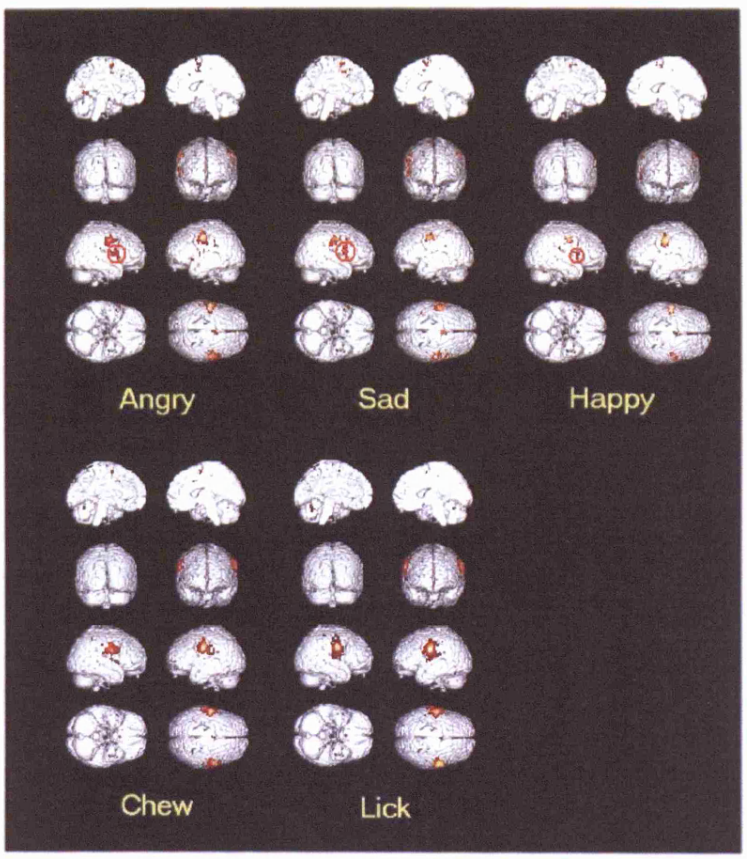

Figure 3.2 The rendered view of activation maps for imitation of the five facial expressions contrasted with passive viewing (*P* < 0.05, corrected). Red circles highlight that the response of right inferior frontal region was common to imitation of emotional facial expressions.

In addition to BA44, the three IE conditions all evoked activity within medial prefrontal gyrus (BA 6), anterior cingulate cortex (24/32), left superior temporal gyrus (38) and left inferior parietal lobule (BA 40). Emotion-specific activity changes patterns were also noted in these categorical analyses: Imitation of angry facial expressions was associated with selective activation of the left lingual gyrus (BA 18). Similarly, imitation of happy facial expressions was associated with selective activation of the lentiform nucleus (globus pallidus) ($P<0.05$, corrected. Activity related to non-emotional IGs was used as an exclusive mask; Table 3.2).

Electrophysiological evidence suggests that passive viewing of emotional facial expressions can evoke facial EMG responses reflecting automatic motor mimicry of facial expressions (Dimberg 1990; Rizzolatti & Craighero 2004). I tested whether passive viewing of expressions (in contrast to viewing a static neutral face) evoked activity within the mirror neuron system (MNS). I failed to observe activation within MNS at the threshold significance of $P < 0.05$,

corrected (or even at P < 0.001, uncorrected; Table 3.3). However, at this uncorrected threshold, enhanced activity was observed within precentral gyrus across angry, happy and chewing conditions

3.3.3 Activity relating to facial movement in emotional imitation (parametric SPM)

During all five (emotional and ingestive) expression imitation conditions, facial movement correlated parametrically with activity in bilateral somatomotor cortices, (prefrontal gyrus, BA 4/6). Moreover, when imitating the three *emotional* expressions (IE conditions), facial movement correlated with activity within the inferior frontal gyrus (44), medial frontal (BA 6) and the inferior parietal lobule (39/40) in a pattern resembling that observed in the *categorical* SPM analysis (Figure 3.3). After taking conjunction of parametric SPM of ingestive expression as an exclusive mask (Table 3.4), I also observed right insula activation across all three IEs. Interestingly, the categorical activation within anterior cingulate cortex (BA 24/32) did not vary parametrically with movement during these IE conditions.

Figure 3.3

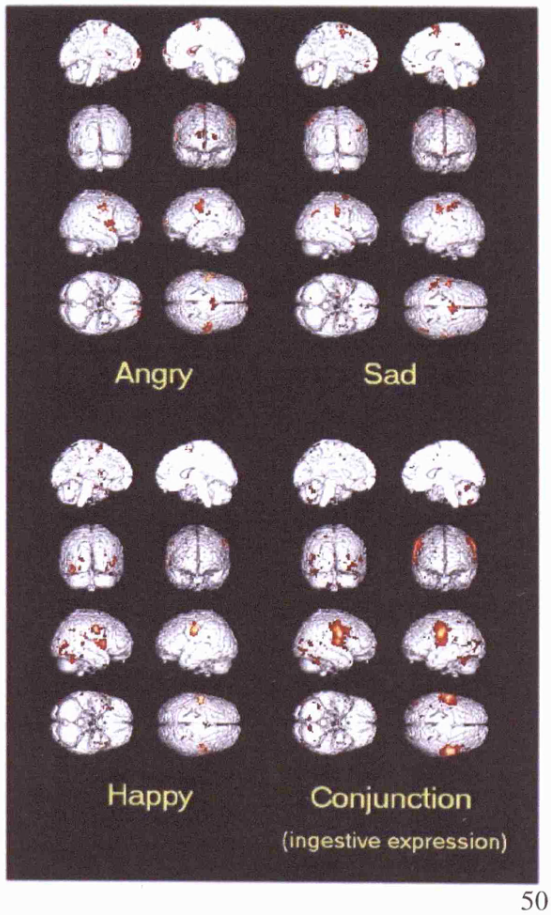

Figure 3.3 The rendered view of activation maps showing significant correlation between regional brain activity and movement of facial markers ($P < 0.0001$, uncorrected). The conjunction (right lower panel) was computing using a conjunction analysis of ingestive expressions, chewing and licking.

I were able to further dissect distinct activity patterns evoked during imitation of each emotional expression (IE trials) that correlated with the degree of facial movement (analyses were constrained by an exclusive mask of the non-emotional IG-related activity). Ventromedial (BA 11) prefrontal cortex, bilateral superior prefrontal gyrus (BA 10) and bilateral lentiform nuclei reflected parametrically the degree of movement when imitating angry facial expressions (but were absent in *categorical SPM* analysis of anger imitation even when the statistical threshold is also set at the same uncorrected 0.0001 level). Conversely activity with the lingual gyrus was absent in *parametric SPM* but was present in *categorical SPM* analysis.

Again ventromedial prefrontal gyrus (BA 11) covaried with facial movement during imitation of sad facial expression, representing an additional activation compared with *categorical SPM*. Since the activation of BA 11 was present in imitation of sad and angry faces, but absent in imitation of happy, chewing and licking faces, it may reflect specific, perhaps empathetic, processing of negative emotions. This argument was supported by a specific contrast of [angry + sad – happy], which showed enhanced activity at ventromedial prefrontal gyrus with coordinate [-6, 28, -14] and z-value 3.86. Other activated areas in *parametric SPM* during imitation of sad expression included rostral anterior cingulate (BA 32) and right temporal pole (BA 38).

The degree of facial movement during imitation of happy facial expressions correlated parametrically with activity in bilateral lentiform nucleus, bilateral temporal pole (BA 38), bilateral fusiform gyri (BA 37), right posterior superior temporal sulcus (BA 22), right middle occipital gyrus (BA 18), right insula (BA 13) and, notably, left amygdala (Figure 3.4, Table 3.5).

Figure 3.4

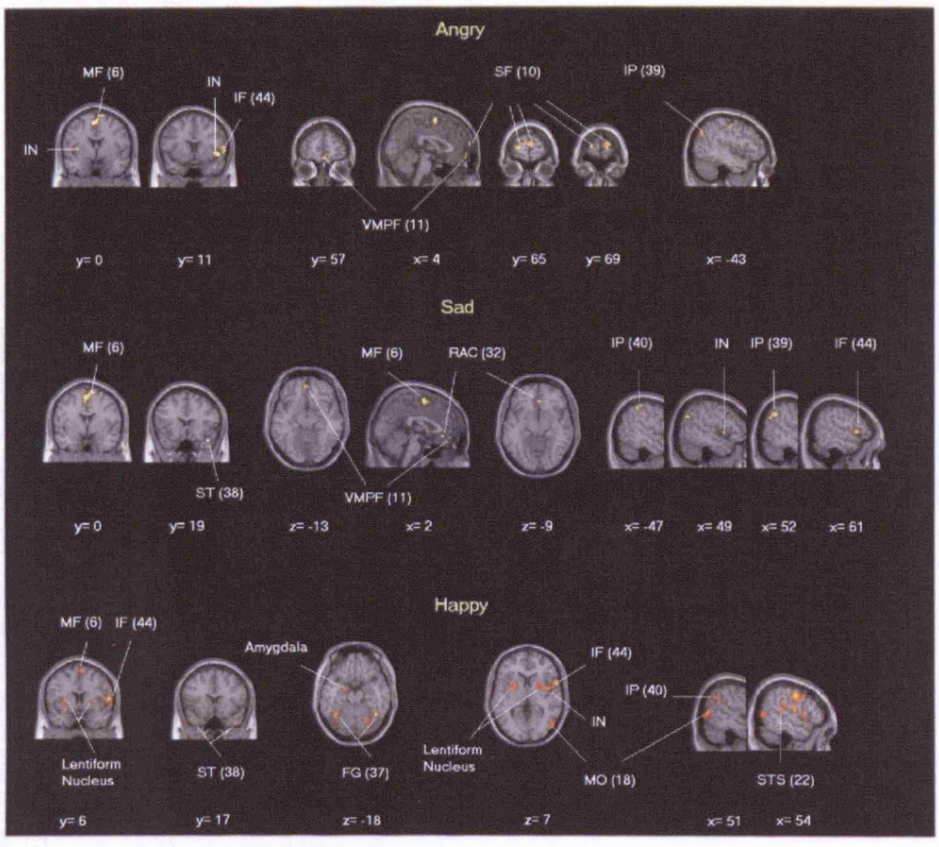

Figure 3.4 Brain regions showing significant relationship with movement of facial markers during emotion-imitation after application of exclusive non-emotional mask (conjunction of chew and lick). For coronal and axial sections, right is right and left is left. Positive x coordinate means right and negative means left.

Abbreviations (Brodmann's area): IF (44), inferior frontal gyrus; IN (13), insula; IP (39), inferior parietal lobule; MF (6), medial frontal gyrus; MO (18), middle occipital gyrus; RAC (32), rostral cingulate cortex; SF (10), superior frontal gyrus; ST (38), superior temporal gyrus; STS (22), superior temporal sulcus; VMPF (11), ventromedial prefrontal cortex.

Table 3.1 Sites where neural activation was associated with imitation of the five facial expressions contrasted with passive viewing

Brain area (BA) [a]	Stereotaxic coordinates [b]			Z score (BA)	Stereotaxic coordinates			Z score (BA)	Stereotaxic coordinates			Z score (BA)
	Imitation of angry faces				*Imitation of sad faces*				*Imitation of happy faces*			
Left precentral gyrus (4/6)	-53	-7	36	7.15	-48	-1	41	5.98	-50	-7	36	6.41
Right precentral gyrus (4/6)	53	-4	36	6.67	56	-10	39	5.99	45	-10	36	6.16
Right postcentral gyrus (40)									65	-25	21	5.38
Right middle frontal gyrus (9)					50	13	35	5.19				
Right inferior frontal gyrus (44)	59	4	8	5.92	59	7	13	6.17	59	12	8	5.36
Anterior cingulate cortex (32)	3	19	35	5.28	0	8	44	5.51				
Medial frontal gyrus (6)	3	0	55	5.63	6	9	60	5.52	0	-3	55	5.79
Left inferior parietal lobule (40)	-53	-33	32	5.69								
Left lingual gyrus (18)	-18	-55	3	6.41								
Left insula	-39	-3	6	5.89								
Right lentiform nucleus									24	3	3	5.85
	Imitation of chewing faces				*Imitation of licking faces*				*Conjunction of imitation of ingestive expressions*			
Left precentral gyrus (6)	-50	-7	31	7.60	-50	-7	28	>10	-53	-7	31	>10
Right precentral gyrus (6)	53	-2	25	6.46	56	-2	28	>10	53	-4	28	>10
Right precentral gyrus (44/43)	59	3	8	5.36 (44)	50	-8	11	5.60 (43)				

Right postcentral gyrus (2/3)	59	-21	40	4.93	53	-29	54	5.01	62	-21	37	6.50
Anterior cingulate cortex (32)	6	13	35	5.13								
Medial frontal gyrus (6)	0	0	55	5.84	0	0	53	5.40	6	3	55	5.31
Right superior temporal gyrus (38)									39	16	-26	6.04[†]
Left insula					-42	-6	6	5.72	-42	-6	3	6.48
Right insula	39	-5	14	5.08	36	-5	11	4.94	39	0	0	6.33

[a] BA, Brodmann designation of cortical areas

[b] Values represent the stereotaxic location of voxel maxima above corrected threshold ($P < 0.05$)

Relative activation was observed for all the above peak coordinates (with the exception of superior temporal gyrus [†]), as indicated by positive parameter estimates for canonical haemodynamic response above ninety percent confidence intervals.

Table 3.2 Sites where neural activation was specifically evoked during imitation of the three emotional facial expressions contrasted with passive viewing [a]

Brain area (BA) [a]	Stereotaxic coordinates [b]			Z score (BA)	Stereotaxic coordinates			Z score (BA)	Stereotaxic coordinates			Z score (BA)
	Imitation of angry faces				*Imitation of sad faces*				*Imitation of happy faces*			
Left precentral gyrus (4/6)	-45	-9	45	6.74	-48	-1	41	6.02	-45	-9	45	6.42
Right precentral gyrus (4/6)	42	-13	39	5.82	56	-16	37	5.55	48	-4	42	5.38
Left precentral gyrus (43)	-53	-11	12	5.53								
Right postcentral gyrus (40)									65	-25	21	5.48

Left inferior frontal gyrus (44/47)	-45	11	-4	5.19 (47)	-50	7	7	5.25 (44)	-48	16	-4	4.94 (47)
Right inferior frontal gyrus (44)	56	9	11	6.12	59	9	13	5.85	59	12	8	5.52
Right middle frontal gyrus (9)	56	8	36	5.84	50	13	35	5.19				
Anterior cingulate cortex (24/32)	3	19	35	5.47	0	8	44	5.54	0	13	32	4.96
Medial frontal gyrus (6)	3	0	55	5.76	6	9	60	5.53	0	-3	55	5.92
Left inferior parietal lobule (40)	-53	-33	32	5.91	-39	-41	55	5.39	-59	-31	24	4.89
Left superior temporal gyrus (38)	-45	11	-6	5.19	-50	6	0	5.25	-48	14	-6	4.94
Left lingual gyrus (18)	-18	-55	3	6.61								
Left insula	-39	-3	6	6.08								
Right insula	36	9	8	5.37								
Right lentiform nucleus									24	3	3	5.85

[a] Conjunction of the two ingestive facial expressions, chew and lick with corrected threshold $P < 0.05$, is taken as an exclusive mask

[b] BA, Brodmann designation of cortical areas

[c] Values represent the stereotaxic location of voxel maxima above corrected threshold ($P < 0.05$)

Table 3.3 Sites where neural activation was associated with observation of the five facial expressions contrasted with observation of static neutral faces

Brain area (BA) [a]	Stereotaxic coordinates [b]			Stereotaxic coordinates			Stereotaxic coordinates		
			Z score			Z score			Z score
	Observation of angry faces			*Observation of sad faces*			*Observation of happy faces*		

Left precentral gyrus (6)	-42	-7	31	3.46								
Right precentral gyrus (8)									45	19	35	3.72
Anterior cingulate cortex (24)	12	-7	45	3.83								
Medial frontal gyrus (10)	-3	58	-5	3.87								
Left superior temporal gyrus (38)	-33	22	-24	3.31								
Right superior temporal gyrus (22)									59	-54	19	4.14
Right middle temporal gyrus (21)									56	-10	-17	3.79
Right fusiform gyrus (20)					42	-19	-24	3.38				
	Observation of chewing faces				*Observation of licking faces*							
Right precentral gyrus (6)	67	1	19	3.94								
Left superior parietal lobule (7)					-6	-64	58	3.25				
Left inferior parietal lobule (40)					-53	-48	30	3.84				
Left middle temporal gyrus (38)					-50	2	-28	4.42				

[a] BA, Brodmann designation of cortical areas

[b] Values represent the stereotaxic location of voxel maxima above uncorrected threshold ($P < 0.001$) and spatial extent more than 3 voxels

Table 3.4 Sties of neural activation associated with facial movements in ingestive facial expressions

Brain area (BA) [a]	Stereotaxic coordinates [b]			Z score (BA)	Stereotaxic coordinates			Z score (BA)	Stereotaxic coordinates			Z score (BA)
	Imitation of chewing faces				*Imitation of licking faces*				*Conjunction of imitation of ingestive expressions*			
Left precentral gyrus (4/6)	-50	-7	28	6.13* (6)	-50	-7	25	6.30* (6)	-56	-10	31	7.69 (4)*
Right precentral gyrus (6)	56	-2	25	6.31*	53	-7	36	6.03*	56	-2	28	Inf*
Medial frontal gyrus (6)	3	0	55	4.99*								
Left superior parietal lobe (7)	-18	-64	58	4.12	-18	-64	56	4.44	-18	-61	53	4.47
Right inferior parietal lobule (40)	53	-28	26	4.92*	53	-28	24	4.01				
Left superior temporal gyrus (39)									-53	-52	8	4.26
Right superior temporal gyrus (22/38)					39	19	-31	4.13 (38)	59	11	-6	4.72 (22)
					59	8	-5	3.96 (22)				
Right middle temporal gyrus (37/39)	59	-58	8	5.15* (39)	53	-69	12	5.29* (39)	59	-64	9	6.24 (37)*
Left fusiform gyrus (37)	-39	-62	-12	4.75	-45	-50	-15	4.31	-48	-47	-15	4.65
	-42	-50	-10	4.36								
Right fusiform gyrus (19/37)	45	-56	-15	5.01 (37)*	36	-56	-15	4.22 (37)	42	-50	-18	5.48 (37)*
	33	-76	-9	4.42 (19)								
Right lingual gyrus (19)					24	-70	-4	4.52				
Left middle occipital gyrus (19)	-42	-84	15	4.95*	-42	-87	7	4.71	-48	-78	4	5.50*
					-45	-76	-6	4.11	-30	-87	15	4.28

Right middle occipital gyrus (19)					30	-81	18	4.68	30	-81	18	5.50*
Left inferior occipital gyrus (18)									-33	-82	-11	4.65
Right inferior occipital gyrus (18/19)					48	-77	-1	4.46 (18)	45	-79	-1	5.40 (19)*
Left insula	-45	-17	4	4.46	-50	-37	18	4.86*	-48	-37	18	5.33*
Right insula	45	8	-5	4.18	45	-8	14	5.00*	45	-8	14	6.51*
Left lentiform nucleus	-27	-3	3	4.70								

[a] BA, Brodmann designation of cortical areas

[b] Values represent the stereotaxic location of voxel maxima above uncorrected threshold ($P < 0.0001$)

* indicates the Z score is also above corrected threshold ($P < 0.05$)

Table 3.5 Sites where neural activity showed selective correlations with facial movements during imitation of each of the three emotional facial expressions [a]

Brain area (BA) [a]	Stereotaxic coordinates [b]			Z score (BA)	Stereotaxic coordinates			Z score (BA)	Stereotaxic coordinates			Z score (BA)
	Imitation of angry faces				*Imitation of sad faces*				*Imitation of happy faces*			
Left precentral gyrus (4)	-45	-12	45	4.13					-45	-16	39	5.87*
Right precentral gyrus (4/6)	45	-4	44	4.74 (6)					39	-16	37	5.63 (4)*
									42	-4	33	4.49 (6)
Left precentral gyrus (43)									-53	-8	11	4.47
Left postcentral gyrus (2/3/40)	-53	-19	23	4.73 (3)	-56	-21	43	4.49 (2)	-59	-19	20	4.58 (40)

Right postcentral gyrus (40)	53	-28	21	4.18								
Left superior frontal gyrus (10)	-21	64	2	4.79								
Right superior frontal gyrus (10)	18	67	8	4.63								
Left superior frontal gyrus (6)					-12	-2	69	3.88				
Right superior frontal gyrus (6)	9	6	66	4.78	9	3	66	4.51				
Left inferior frontal gyrus (44/47)	-57	6	5	4.62 (44)	-30	20	-14	4.12 (47)				
Right inferior frontal gyrus (44/45)	56	7	13	4.63 (44)	59	15	2	4.15 (45)	56	9	8	5.91 (44)*
Ventral medial prefrontal cortex (11)	3	55	-15	4.26	-3	46	-12	3.97				
Rostral anterior cingulated cortex (32)					3	34	-9	4.25				
Medial frontal gyrus (6)	-3	0	53	5.02*	3	0	58	4.73	9	6	60	4.79
Anterior cingulate cortex (24)									-6	-16	39	4.43
Posterior cingulate gyrus (31)					6	-42	33	4.22	6	-36	40	4.55
Left inferior parietal lobule (39/40)	-48	-65	36	4.29	-45	-35	54	4.38 (40)				
Right inferior parietal lobule (39/40)					48	-62	34	4.45 (39)	50	-56	36	4.51 (40)
									56	-28	26	4.56 (40)
Left superior temporal gyrus (38)									-45	13	-26	4.47
Right superior temporal gyrus (38)					42	16	-24	4.89	39	16	-34	4.21
Left middle temporal gyrus (21)									-65	-33	-11	4.47
Left middle temporal gyrus (37)									-45	-67	9	4.21
Right superior temporal sulcus (22)									53	-32	7	4.30
Right inferior temporal gyrus (20)									59	-36	-13	4.30
Left fusiform gyrus (37)	-39	-56	-12	4.34					-39	-56	-12	4.84*
Right fusiform gyrus (37)									42	-56	-12	5.35*

Right parahippocampal gyrus (28)					21	-13	-20	4.43				
Left cuneus (18)									-21	-95	13	4.38
Left middle occipital gyrus (18)									-21	-82	-6	4.20
Right middle occipital gyrus (19)									50	-69	9	4.79
Left insula	-37	3	5	4.26								
Right insula	47	8	-5	4.78	45	9	0	4.10	42	0	6	5.21*
Left caudate nucleus									-15	12	13	4.38
Right caudate nucleus									21	21	3	4.13
Left lentiform nucleus	-24	0	-8	4.03					-24	6	5	4.72
Right lentiform nucleus	21	12	8	4.28					27	0	0	4.39
Left amygdale									-21	-4	-15	4.87*

[a] Conjunction of the two ingestive facial expressions, chew and lick with uncorrected threshold $P < 0.0001$, is taken as an exclusive mask

[b] BA, Brodmann designation of cortical areas

[c] Values represent the stereotaxic location of voxel maxima above uncorrected threshold ($P < 0.0001$)

* indicates the Z score is also above corrected threshold ($P < 0.05$)

3.4 DISCUSSION

This study highlights the inter-relatedness of imitative and internal representations of emotion by demonstrating engagement of brain regions supporting affective behaviour during imitation of emotional, but not non-emotional, facial expressions. Moreover, this study applies novel methods to the interpretation of neuroimaging data in which metrics for facial movement delineate the direct coupling of regional brain activity to expressive behaviour.

Explicitly imitating the facial movements of another person non-specifically engaged somatomotor and premotor cortices. In addition, imitating both positive and negative emotional expressions was observed to activate the right inferior frontal gyrus, BA 44. The human BA 44 is proposed to be a critical component of an action-imitation 'mirror neuron' system: Mirror neurons were described in non-human primates and are activated whether one observes another performing an action or when one executes the same action oneself. Mirror neurons, sensitive to hand and mouth action, are reported in monkey premotor, inferior frontal (F5) and inferior parietal cortices (Buccino et al. 2001; Ferrari et al. 2003; Rizzolatti & Craighero 2004; Rizzolatti et al. 2001). The human homologue of F5 covers part of the precentral gyrus and extends into the inferior frontal gyrus (BA 44 *pars opercularis*). In primates, including humans, the MNS is suggested as a neural basis for imitation and learning, permitting the direct, dynamic transformation of sensory representations of action into corresponding motor programmes. Thus explicit imitation, as in this study, maximizes the likelihood of engaging the MNS. At an uncorrected statistical threshold ($P = 0.0001$, uncorrected), I observed activation of bilateral inferior frontal gyri and inferior parietal lobules for all the five imitation conditions (Buccino et al. 2001; Carr et al. 2003; Leslie et al. 2004), concordant with current knowledge of imitation network (Rizzolatti & Craighero 2004).

Nevertheless, I had also predicted activation of the MNS, albeit at reduced magnitude, during passive viewing, but were unable to demonstrate this, even at a generous statistical threshold ($P = 0.001$, uncorrected). Across other studies, evidence for passive engagement of BA44 *pars opercularis* when watching facial movements is rather equivocal (Buccino et al. 2001; Carr et al. 2003; Leslie et al. 2004). One factor that may underlie these differences is

attentional focus: In this study, the subjects performed an incidental gender discrimination task so that attention was diverted from the emotion. In fact it is plausible that the human MNS is necessarily sensitive to intention and attention, to constrain adaptively any interference to goal-directed behaviours from involuntarily mirroring of signals within a rich social environment.

The right, and to a lesser extent the left, inferior frontal gyrus was engaged during imitation of emotional facial expressions. In fact, despite clinical anatomical evidence for the dependency of affective behaviours on the integrity of right hemisphere, including prosody and facial expression (Borod 1992; Gorelick et al. 1987; Ross et al. 1979), I showed only a relative, not absolute, right lateralized predominance of BA 44 activation. Besides the MNS, there are other possible accounts for enhanced activation within inferior frontal gyri. It is possible, for example, that the imitation condition (relative to passive viewing) enhances the semantic processing of emotional/communicative information, thereby enhancing activity within inferior frontal gyri (George et al. 1993; Hennenlotter et al. 2005; Hornak et al. 1996; Kesler-West et al. 2001; Nakamura et al. 1999). Activation of BA44 would thus reflect an interaction between facial imitative engagement and interpretative semantic retrieval.

I also observed emotion-specific engagement of a number of other brain regions, notably inferior parietal lobule (BA 40), medial frontal gyrus (BA 6), anterior cingulate cortex (BA 24/32, ACC) and insula. Each of these brain regions is implicated in components of imitative behaviours: The inferior parietal lobule supports ego-centric spatial representations and cross-modal transformation of visuospatial input to motor action (Andersen et al. 2002; Buccino et al. 2001). Correspondingly, damage to this region may engender ideomotor apraxia (Grezes et al. 2001; Rushworth et al. 1997). Similarly, the medial frontal gyrus (BA 6, SMA) is implicated in the preparation of self-generated sequential motor actions (Marsden et al. 1996) and dorsal ACC is associated with voluntary and involuntary motivational behaviour and control including affective expression (Critchley et al. 2003; Devinsky et al. 1995; Rushworth et al. 2004). In monkeys, SMA and ACC contain accessory cortical representations of the face and project bilaterally to brainstem nuclei controlling facial musculature (Morecraft et al. 2004). PET evidence suggests a homology between human and nonhuman primate anatomy in this respect (Picard et al. 1996). Lastly, insula cortex, where activity also correlated with

magnitude of facial muscular movement during emotional expressions, is implicated in perceptual and expressive aspects of emotional behaviour (Carr et al. 2003; Phillips et al. 1997). Insula cortex is proposed to support subjective and empathetic feeling states yoked to autonomic bodily responses (Critchley et al. 2004; Singer et al. 2004b). It is striking that that the activation of these brain regions (particularly BA 44 *pars opercularis* and insula which contain primary taste cortices (O'Doherty et al. 2002; Scott et al. 1999)), was not strongly coupled to the imitation of ingestive expressions (Table 3.4 and 3.5). However, this observation of emotional engagement of a distributed matrix of brain regions during imitative behaviour highlights the primary salience of communicative affective signals (compared to non-communicative ingestive actions) to guide social interactions. In this regard, I hypothesise that cinguloinsula coupling supports an affective set critical to this apparent selectivity of prefrontal and parietal cortices.

In addition to defining regional brain activity patterns mediating social affective interaction, a key motivation of this study was to dissociate, using emotional mimicry, neural substrates supporting specific emotions. These effects were most striking when the magnitude of facial movement was used to identify 'resonant' emotion-specific activity. Thus, across the imitation of three emotions, enhanced activity within right insular region might reflect representation of feelings states that may have their origin in interoception (Critchley et al. 2004). Correlated activity at bilateral lentiform nuclei in the imitation of angry faces might reflect goal-directed behaviour (Hollerman et al. 2000). Anger-imitation also engaged bilateral frontal polar cortices (BA10). The frontal poles are implicated in a variety of cognitive functions including prospective memory and self-attribution (Ochsner et al. 2004; Okuda et al. 1998). Nevertheless, underlying these roles BA10 is suggested to support a common executive process, namely the "voluntary switching of attention from an internal representation to an external one ..."(Burgess et al. 2003). Within this framework, BA 10 activity may be evoked during anger imitation since subjects are required to suppress pre-potent reactive responses in order to affect a confrontational external expression (inducing activity within BA 10). Recently, Hunter *et al.* (Hunter et al. 2004) reported bilateral frontal poles activation during action execution which further suggests that in this study, bilateral BA 10 activation in the imitation of anger might be related to the prominent behaviour dimension of anger expression. I did not notice significant

activity at amygdala either in the categorical or in the parametric analysis (Scott et al. 1997).

Activity within ventromedial prefrontal cortex (VMPC) correlated significantly with the degree of facial muscle movement when mimicking both angry and sad expressions (Figure 3.4), suggesting a specific association between the activity of this region and expression of negative emotions (Damasio et al. 2000). A direct relationship was also observed between activity in the adjacent rostral ACC, very close to subgenual cingulate, and facial muscular movement during imitation of sadness. This region is implicated in subjective experience of sadness and with dysfunctional activity during depression (Liotti et al. 2000; Mayberg et al. 1999).

In contrast, the more subjects smiled in imitation of happiness (degree of movement of zygomatic major), the greater the enhancement of activity in cortical and subcortical brain regions including the globus pallidus, amygdala, right posterior superior temporal sulcus (STS) and fusiform cortex. This pattern of activity suggests recruitment in the context of positive affect of regions ascribed to the 'social brain' (Brothers 1990). The globus pallidus is a striatal region implicated in dopaminergic reward representations (Ashby et al. 1999; Elliott et al. 2000) and affective approach behaviours (Arkadir et al. 2004). It is interesting that basal ganglion activation was observed in imitation of angry and happy faces but not in imitation of sad faces, where both emotions carry on approaching action tendency. The right posterior STS is particularly implicated in processing social information from facial expression and movement (Frith & Frith 1999; Perrett et al. 1982). The recruitment of this region during posed facial expression further endorses its contribution to emotional communication beyond merely a sensory representation of categorical visual information. The preferential recruitment of these visual cortical regions when imitating expressions of happiness emphasizes the importance of reciprocated signalling of positive affect to social engagement and approach behaviour; signals of rejection in effect may turn off 'social' brain regions. This argument is particularly pertinent when considering activation evoked in the left amygdala when smiling: Although much literature is devoted to the role of amygdala in processing threat and fear signals, the region is sensitive to affective salience and intensity of emotion, independent of emotion-type (Buchel et al. 1998; Hamann et al. 2002; Morris et al. 2001; Morris et al. 2002; Winston et al. 2003). A recent report revealed that the ability

of happiness recognition correlates with amygdala volume (Kipps et al. 2007). Thus, reciprocation of a smile (a signal of acceptance and approach) permits privileged access to social brain centres. Smiling may thus represent a more salient and socially-committing (or perhaps risky) behaviour than imitation of other expressions.

The mechanisms underlying the resonance between emotional facial movements and neural activities are still not clear. "Facial feedback hypothesis" suggested that it was the feedback from various receptors in the face that contributes to neural activities at emotion network. The peripheral receptors may comprise of musculo-skeletal, vascular, thermo-regulatory, and cutaneous origins (Adelmann & Zajonc 1989). Conversely, actively-posed emotion expression on the face may engage the process of self-generating emotion which is also expected to activate emotion-related neural network. These two pathways are analogous to "bottom-up" and "top-down" processes and can be disambiguated by various strategies. For example, a directed facial action task and a non-obtrusive task were designed to eschew subjective awareness of posed facial expression which is concordant with a particular emotion style (Ekman et al. 1983; Soussignan 2002; Strack et al. 1988). The directed facial action task requires the participants to follow muscle-by-muscle instructions that constitute specific facial expressions associated with different emotions; while the non-obtrusive task may ask the participants to hold a pencil in their mouth to either facilitate or inhibit the muscles typically associated with smiling without requiring subjects to pose a smiling face. Since facial feedback hypothesis is not the main focus of this thesis, these tasks were not tested and thus not included in this thesis. A more parsimonious bi-directional/associative mechanism was proposed by Ekman: a "*central, hard-wired connection between the motor cortex and other areas of the brain involved in directing the physiological changes that occur during emotion*" (Ekman 1992). Ekman's model explains the frequently observed reciprocality in emotion literature: emotion expression facilitates emotion perception and felt emotion; emotional states facilitate emotion expression; emotion perception activates emotion-correspondent facial muscles and facilitates emotion induction (Adelmann & Zajonc 1989; Dimberg 1982; Dimberg 1986; Dimberg 1987; Dimberg 1990; Ekman 1992; Ekman 1993; Ekman et al. 1983; Izard et al. 1984; Sutton et al. 1997).

A specific consideration is that even though this parametric analysis explored neural activity correlating with facial movements, my findings do not constitute direct evidence for the causal generation of emotions by facial movements. Nevertheless, the context of this experiment (expression mimicry) embodies social affective interaction and is distinct from intentional 'non-emotional' muscle-by-muscle mobilization of posed facial expression (Ekman et al. 1983). By highlighting modulation of neural activity in brain regions implicated in emotional processing, my findings supplement and extend data showing that "facial efference", when congruent with emotional stimuli, can modulate subjective emotional state (Adelmann & Zajonc 1989). In addition to experiential, reactive and social cognitive dimensions, emotions interact with psychological constructs and their underlying neural mechanisms (Dolan 2002; Ekman 1997). Consequently interpretations of the results of my parametric analysis may extend beyond social affective inferences to include interactions with other cognitive functions, including concurrent mnemonic, anticipatory, psychophysiological processes and so on (Ekman 1997); however, the evidence supporting their relationship with facial expression is either inconsistent or lacking. Nevertheless, my results endorse the proposal that emotional facial mimicry is not purely a motoric behaviour but engages distinctive neural substrates implicated in emotion processing. Another limitation of this study was that facial expressions of emotion tend to engage the whole face, whereas ingestive expressions affect the mouth region and tongue in particular. Even though not optimal, choosing ingestive expressions as control was because of the difficulty to find facial movements concordant with emotion but did not carry emotion. Nevertheless, these might contaminate my results in brain regions showing differential motoric somatotopy and neural networks carrying out ingestive function. My design therefore did not provide an ideal context where subtraction of different conditions can isolate a single cognitive operation, also named "cognitive insertion" (Caplan et al. 2004; Price et al. 1997). Furthermore, although smoothness is a preferred pre-processing step (chapter 2) it may mask nearby activation foci during subtraction. For example, different but close sub-regions at anterior insula may host emotion processing and ingestive functions. Similarly, different sub-regions at inferior frontal cortex may host mirror neuron system and neural node for emotion expression. Subtraction of smoothed images in this study may mask meaningful findings. I therefore took an alternative approach and restricted my analysis to the areas masked out by common ingestive functions which was

derived from a conjunction mask calculated from chewing and licking contrasts.

3.5 CONCLUSION

To summarize, this study defines shared and dissociable substrates for affective facial mimicry. I highlight, first, the primacy of affective behaviours in engaging action-perception (mirror-neuron) systems and, second, a subsequent valence-specific segregation of emotional brain centres. At a methodological level, this study illustrates how the magnitude of facial muscular movements can enhance sensitivity in identification of emotion-related neural activity. The face conveys abundant information communicating internal emotional state to inform hermeneutically social cognition and the dynamics of human interaction (Singer et al. 2004a).

Chapter 4

Controlling emotional expression: Behavioural and neural correlates of non-imitative emotional responses

---

4.1 INTRODUCTION

In contrast to the previous chapter relating to the imitation of emotional expressions, I investigated the neural responses relating to the expression of an emotion that is discordant to the observed expression.

It is recognized that the ability to inhibit and correct pre-potent responses is a central feature of executive function, enabling the adaptive control of behaviour beyond immediate stereotyped responses and reactions. The development of response control and associated behavioural flexibility, evident in phylogenetic evolution and in human maturation, suggests that it mediates behavioural advantages. Within experimental psychology, response control is typically examined using facilitation/interference paradigms. Congruence of behavioural cue with a pre-potent response is facilitatory, reflected typically as a reduction of reaction times (RT's). Conversely, overcoming pre-potent psychological or behavioural tendency to execute an alternative intended response is manifest as a 'cost', reflected experimentally in prolonged RT's.

Behavioural interference tasks have explored a variety of contexts: The most widely known is the Stroop Colour -Word Task (MacLeod 1991). In the Stroop task, subjects view words describing different colours (e.g. blue, red, etc), and are required to name the colour of the ink in which the words are printed. Ink colour and response may be congruent (e.g. the word blue printed in blue ink) or incongruent (blue printed in red ink). The interference effect on incongruent trials reflects a cost in suppressing the pre-potent response to read the colour word. Interference in other aspects of cognition (e.g. counting Stroop; (Bush et al. 1998; Hayward et al. 2004)) and emotion processing (e.g. emotional Stroop; (Bentall et al. 1990; Compton et al. 2003; Malhi et al. 2005; Williams et al. 1996)) have been explored using Stroop-like conflict tasks. Moreover, since behavioural conflict is typically expressed at the level of response, a number of studies have focused on competition within spatial and motor response dimensions (e.g. Simon task; (Fitts et al. 1954; Maclin et al. 2001)). Nevertheless, while interference effects

are observable across perceptual, cognitive, emotional and motoric domains, it remains unclear whether a common neural mechanism mediates an ability to override pre-potent responses. Indeed, there is evidence for both common (Peterson et al. 2002) and dissociable (Whalen et al. 1998) neural substrates mediating response-competition.

In the present study, I extended Stroop effect to the under-explored dimension of emotion expression interference (EEI). The ability to control and contain the evoked emotional responses is important for adaptive emotional behaviour (Gross 1998). Emotional facial expressions represent potent social cues and empirical evidence suggests that emotions and facial expressions are 'contagious'. Thus, in facial electromyographical (EMG) studies, viewing smiling and frowning faces implicitly activate corresponding zygomaticus major muscle and corrugator muscle respectively in the viewer (Dimberg 1982; Dimberg et al. 2002). I hypothesized that this mimicry tendency (with 'resonant' patterns of neural activity; (Lee et al. 2006)) represents a pre-potent response bias that would interfere with the ability to express a different opposite facial emotion (frowning to smiling faces or vice versa).

First, I performed a facial EMG study, where the subjects viewed video clips depicting happy or angry emotional expressions while directed to express a concordant or discordant facial emotion (i.e. smile or frown), Second, following the EMG study (which validated the presence of an interference effect), I applied functional magnetic resonance imaging (fMRI) to delineate brain regions responsible for this EEI effect. I predicted that EEI would require extra expressive and inhibitory effort, reflected in enhanced activity within motor-related region and inferior frontal cortex (Carr et al. 2003; Lee et al. 2006; Leslie et al. 2004). Moreover, inhibition of pre-potent emotional expressions EEI is likely to be facilitated by enhanced self-generated representation of the appropriate (intended) emotional feeling states (e.g. by recruiting activity within regions such as right anterior insula cortex; (Critchley et al. 2004; Reiman et al. 1997)). Lastly, to examine stimulus-response (S-R) compatibility (conceptually distinct from stimulus-stimulus (S-S) compatibility; (Fitts & Deininger 1954; Simon et al. 1990)) in affective and non-affective contexts, I also included a modified 'Simon' task to serve as a non-emotional comparison of the interference effect (Valle-Inclan 1996; Wascher et al. 1996).

4.2 MATERIALS AND METHODS

4.2.1 Subjects, experimental stimuli and questionnaires

I recruited thirty-two volunteers for the EMG study (mean age, 22.7 years; 14M, 18F), and fourteen among them for the fMRI study (mean age, 23.8 years; 7M, 7F). Each gave informed written consent approved by the local Ethics Committee. Subjects were screened to exclude history or evidence of neurological, medical, or psychological disorder including substance misuse. None of the subjects was taking medication.

Since facial emotional expressions are highly dynamic signals (Kilts et al. 2003), I utilized short movies instead of static pictures as stimuli. Experimental stimuli consisted of 700 ms video clips of two dynamic facial expressions portraying anger and happiness from ten male and ten female models. Each movie was further processed by SmartMorph (http://meesoft.logicnet.dk/SmartMorph/) to create 4 different intensities of emotional expression: 25%, 50%, 75% and 100%. In detail, SmartMorph is a semi-automatic way to perform successive spatial warping between images. A crucial advantage of the semi-automatic algorithm is that it allows setting corresponding landmarks on the to-be-warped images to make the transformation in high validity and quality. The successive images were selected along the degrees of 25%, 50%, 75% and 100% transformation and compiled back into movies. These four intensities provided a stimulus platform for the subject to make subjective emotion intensity judgments (Figure 4.1 (i)). In total, I constructed 160 different movies from 20 different identities.

I administered two questionnaires to subjects to probe the relationship between EEI effects and two related dimensions, namely: Empathy Quotient (EQ) and Emotion Regulation Questionnaire (ERQ; (Gross et al. 2003); (Lawrence et al. 2004)). EQ comprises three subscales: cognitive empathy, emotion reactivity (close to the concept of emotion empathy) and social skills. ERQ includes subscales of reappraisal and suppression. Since the central themes of EEI involve the relationship between contagiousness of emotion expression (emotion empathy) with expressive control (suppression), I was particularly interested in the emotion reactivity subscale of the EQ (EQ-er) and suppression subscale of the ERQ (ERQ-s).

Figure 4.1

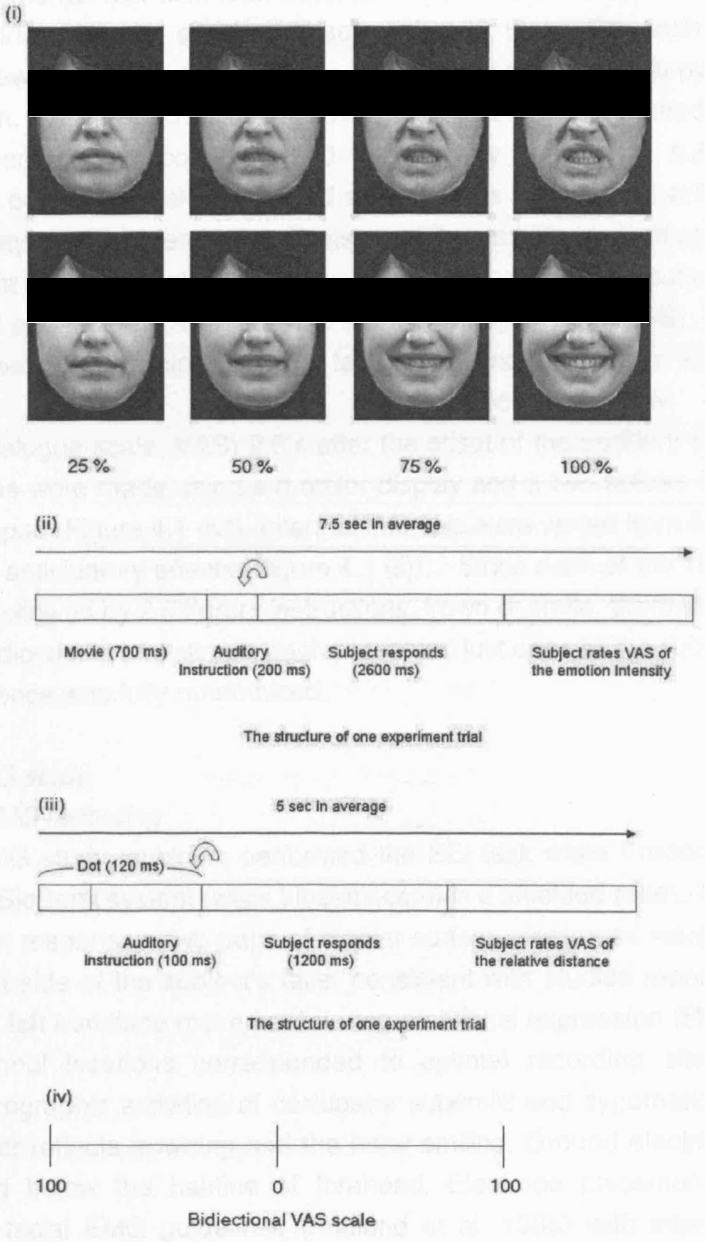

Figure

4.1 Examples of experimental stimuli (i), and the structure of a single trial for emotion expression interference task (ii) and Simon Task (iii). The VAS scale used is illustrated in (iv).

4.2.2 Emotional expression interference (EEI) task

The experimental EEI task was identical in both the EMG and fMRI studies and comprised of two sessions, each with 160 trials. On each trial, the subject viewed a movie clip depicting a different intensity of happy or angry expression. At the end of each movie, the subject was required to either frown or smile in response to 200 ms auditory cue. The subject was instructed before the task to respond as quickly as possible (to enhance the automaticity of interference effects). The auditory instruction was concordant or discordant with the expression in the movie, resulting in both congruent and incongruent trials; i.e. smiling to happy faces (SS), smiling to angry faces (SF), frowning to happy faces (FS), and frowning to angry faces (FF). Subjects performed an emotion intensity judgment (visual-analogue-scale, VAS) 2.6 s after the offset of the auditory instruction. Responses were made using a monitor display and a two-button, hand-held response pad (Figure 4.1 (iv)). Intertrial intervals were varied from 6.5 to 8.5 s to reduce anticipatory effects (Figure 4.1 (ii)). Since each of the 160 movies could be followed by 2 different instructions, frown or smile, there were a total of 320 audio-visual trial stimuli, each presented just once to the subjects. The trial sequence was fully randomized.

4.2.3 EMG study

4.2.3.1 EMG recording

In the EMG study, subjects performed the EEI task while I recorded facial EMG via BioSemi system (www.biosemi.com) in a shielded room. To register movement responses, two pairs of bipolar surface electrodes were attached on the left side of the subject's face, consistent with studies reporting more extensive left hemiface movement during emotional expression (Rinn 1984). The regional locations corresponded to optimal recording sites for the electromyographic activities of corrugator supercilii and zygomaticus major. The former reflects frowning and the latter smiling. Ground electrodes were positioned below the hairline of forehead. Electrode placement followed standard facial EMG guidelines (Fridlund et al. 1986) with inter-electrode distance 1 cm. Sample rate was set at 2048 Hz.

4.2.3.2 EMG data analysis

EMG data was band-pass filtered between 10 and 500 Hz and full-wave rectified. The data were smoothed using a root-mean-square analysis with 60

ms window. An eight second epoch was segmented for each experimental trial (from 1 s before the commencement of each movie). Onset latency was defined by more than 3 standard deviations (SDs) above the baseline level (average of the 100ms before the commencement of the trial) for a minimum of 50 ms.

Outlying data (rejected trials) were defined as trials where averaged latency exceeded three standard deviations away from the mean, where EMG activity onset occurred before the auditory instruction, or rating of opposite emotion. The filtered and smoothed EMG data were visually checked to verify the automatically identified onsets, missing responses and the rejected trials.

4.2.4 fMRI study

4.2.4.1 Emotional expression interference (EEI) and Simon Task

A random subset (N=14) subjects of the EMG subjects took part in the fMRI study. Each subject performed the EEI task over 2 sessions, with 256 trials in total, in an identical manner to the facial EMG study. In a third session, the subjects performed a non-emotional interference task; a modified Simon task with similar design structure to the emotion expression (EEI) task. This task served as a comparison for non-emotional interference effects. In this task, the subject was required to fixate on a central cross, which was constantly displayed on the screen. An auditory instruction (100 ms; the content was 'left' or 'right') 50 ms came after the visual presentation of a white dot (120 ms duration) at a location either the left or right of the central fixation cross. The distance of the white dot was variable; ranging from 25 to 90 percent of the half-width of monitor. This variability in distance embodied the parametric properties of facial stimuli in the earlier EEI task. The subject was requested to press the left or right button as quickly as possible according to the auditory instruction. Thus, the subject's response was either to the same (concordant) or opposite (discordant) position relative to the viewed dot. After responding, the subject rated the perceived distance of the dot from the central cross on a VAS scale, 1.2 s after the offset of the auditory instruction (Figure 4.1 (iii) and (iv)). Trial length ranged from 4 to 6 s and (mean 5 s). There were 128 trials in total and the trial sequence was randomized. Thus, the Simon Task design shared with the emotion judgment (EEI) task the following requirements: the subject (1) passively viewed stimuli with different parametric attributes; (2) made a rapid forced-choice response to an auditory

instruction, in a manner either concordant or discordant with the visual stimuli, and; (3) referred to an internal/invisible standard.

Before fMRI scanning, all the subjects received 15 minutes of training in both tasks. During training, correct response rates for both the emotion (EEI) and the modified Simon task were higher than ninety-five percent (a video camera was used to record responses to confirm performance accuracy in the emotion expression task).

4.2.4.2 fMRI data acquisition

I acquired sequential T2*-weighted echoplanar images (Siemens Allegra, 3-T, 44 slices, 2.0 mm thick, TE 0.65 ms, TR 2.86 s, voxel size 3*3*3 mm3) for blood oxygenation level dependent (BOLD) contrast. Three hundred and twenty whole-brain images were obtained over 16 min for the two emotion sessions and 240 images over 12 minutes for the Simon session. The first 5 echoplanar volumes of each session were not analyzed to allow for T1-equilibration effects. A T1-weighted structural image was obtained for each subject to facilitate anatomical description of individual functional activity after co-registration with fMRI data.

4.2.4.3 fMRI data analysis

I used SPM2 analysis software to analyze acquired fMRI data. In individual subject analyses, low-frequency drifts and serial correlations in the fMRI time series were respectively accounted for using a high-pass filter (constructed by discrete cosine basis functions) and non-sphericity correction, created by modelling a first degree autoregressive process. Error responses were defined as the trials in which a subject misclassified the video clips/dots (i.e. where happy movie were rated as angry) or pressed the button opposite to the auditory instruction in the Simon task. Errors were modelled within the design matrix. For the emotion (EEI) task, activity related to stimulus events was modelled separately for the four different categories (SS, SF, FS, FF) using a canonical haemodynamic response function (HRF) with temporal and spatial dispersion derivatives (to compensate for discrepant characteristics of haemodynamic responses). In the analysis of the Simon task, I modelled the concordant and discordant conditions with the same three haemodynamic basis functions in a similar statistical model to the EEI task analysis for comparison. Additionally, individual correlational maps for concordant and discordant conditions were constructed voxel-by-voxel from the correlation

coefficient of linearly detrended measured BOLD effects and acquired emotion intensity ratings of the stimuli (aligned in time and convolved with a canonical HRF). Contrast images for interference effects ([SF+FS-SS-FF] for the EEI task and [discordant–concordant] for Simon task) and the two correlation maps (discordant and concordant) were entered into group level (second-level) analyses using an analysis of variance (ANOVA) model.

The second-level group analyses (random effects with non-sphericity correction) were explored separately using F-tests of event-related activity reflecting interference in the EEI and Simon tasks. Voxel-wise statistical threshold was set at $P < 0.001$, uncorrected. To constrain this analysis to brain regions specific to EEI processing, I used an exclusive mask derived from Simon task. A 'discordant minus concordant' T-test was used in the analysis of the correlation maps to explore the brain regions showing parametric EEI. For the above brain image analyses, the spatial extent threshold was set at 3 contiguous voxels.

4.3 RESULTS

4.3.1 EMG study

Inspection of individual data revealed a parametric relationship between the latency of EMG response onset and the viewed and rated perceived intensity of emotion in both frowning and smiling conditions. This significant trend was most prominent when combining concordant and discordant conditions (illustrated in Figure 4.2). Thus, EMG onset latency decreased with increasing emotion intensity in the concordant conditions (frowning to frowning faces, smiling to smiling faces), and increased with increasing emotion intensity in the discordant conditions (frowning to smiling faces, smiling to frowning faces). Across subjects, the average correlation coefficients of EMG onset latency and rated emotion intensity were: 0.3165 for FC (SD = 0.155, $P < 0.001$, df = 31) and -0.3998 for SC (SD = 0.154, $P < 0.001$, df = 31).

In response to the stimuli depicting frowning, mean EMG onset latency for concordant responses was 364.2 ms (SD 93.1) and for discordant responses was 452.3 ms (SD 103.7). Similarly, in response to smiling stimuli, mean EMG onset latency for concordant responses was 325.8 ms (SD 97.5) and for discordant responses was 444.3 ms (SD 133.7). To highlight this congruency effect, I took the extreme 20% (each of smiling and frowning) stimuli with the strongest emotion intensity ratings and the 20 % of trial stimuli with the lowest emotion intensity ratings (rating around zero) for concordant and discordant trials and analyzed the difference in average EMG onset latency. The four paired-samples T-tests all reached statistical significance with P values less than 0.001, verifying both interference and facilitation effects; see Table 4.1. The average error rate on the EEI task was 7.5% comprising missing/wrong responses, contamination of baseline due to early muscle activities or blinks, and rating of opposite emotion valence. The error responses were excluded from the analysis.

I also explored the relationship between EMG latency and inter-individual differences in emotional style (EQ). Across subjects, the emotion reactivity subscale of Empathy Quotient (EQ-er) correlated significantly with EMG onset in concordant condition, with correlation coefficient -0.415 for frowning ($P = 0.018$) and 0.476 for smiling ($P = 0.006$), but not in discordant condition, with correlation coefficient -0.294 for frowning ($P = 0.102$) and 0.128 for smiling condition ($P = 0.484$).

Figure 4.2

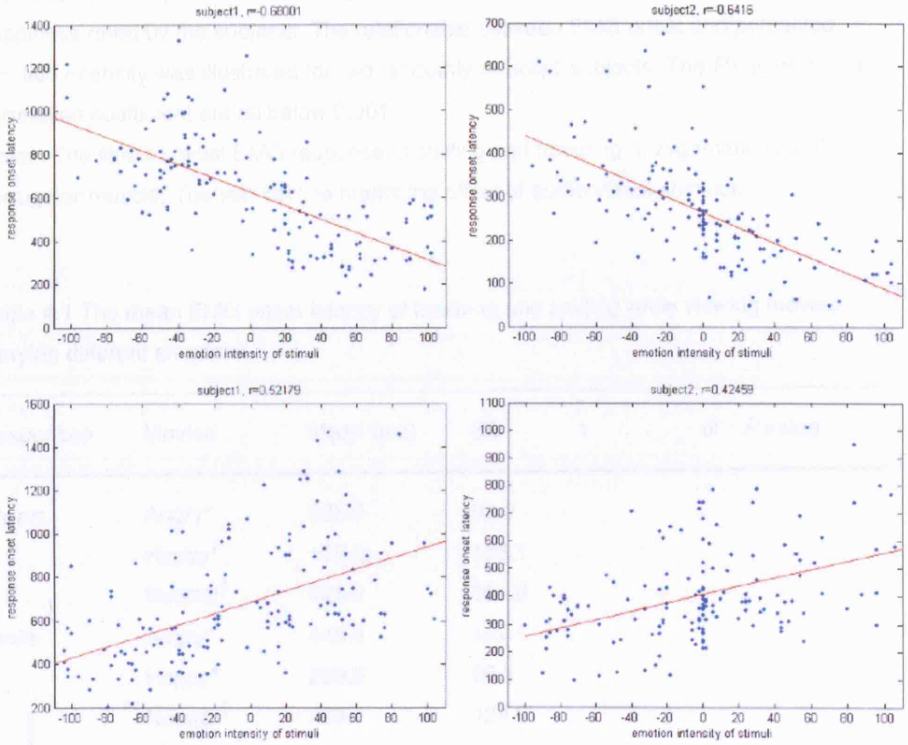
subject1, r=-0.68001
response onset latency
emotion intensity of stimuli
subject2, r=-0.6415
response onset latency
emotion intensity of stimuli
subject1, r=0.52179
response onset latency
emotion intensity of stimuli
subject2, r=0.42458
response onset latency
emotion intensity of stimuli

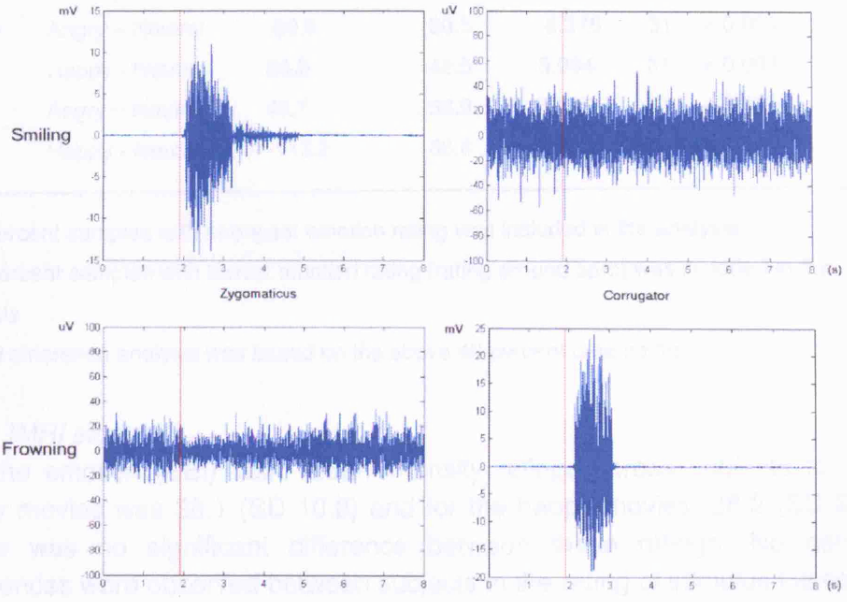
Smiling
mV
Zygomaticus
uV
Corrugator
(s)
Frowning
uV
mV
(s)

Figure 4.2 Upper: The ordinate is the EMG onset latency (ms) and the abscissa is the rating of emotion intensity. Positive and negative values indicate the degree of anger and happiness rated by the subjects. The relationship between EMG onset and perceived emotion intensity was illustrated for two randomly selected subjects. The *P* values of the correlation coefficient are all below 0.001.
Lower: The filtered facial EMG response of smiling and frowning at zygomaticus and corrugator muscle. The vertical line marks the offset of audio-visual stimulus.

Table 4.1 The mean EMG onset latency of frowning and smiling while viewing movies carrying different emotions

Responses	Movies	Mean (ms)	SD	t	df	*P* value
Frown	Angry*	335.6	93.9			
	Happy*	455.2	105.1			
	Neutral†	425.2	101.0			
Smile	Angry*	449.8	129.1			
	Happy*	289.9	96.5			
	Neutral†	403.1	124.6			
Paired Differences						
Frown	Angry – Neutral	-89.6	60.5	-8.376	31	< 0.001
	Happy - Neutral	30.0	42.5	3.994	31	< 0.001
Smile	Angry – Neutral	46.7	56.9	4.640	31	< 0.001
	Happy - Neutral	-113.2	66.6	9.614	31	< 0.001

* 20 percent samples with strongest emotion rating was included in the analysis
† 20 percent samples with lowest emotion rating (rating around zero) was included in the analysis
Paired difference analysis was based on the above 40 percent data points

4.3.2 fMRI study

For the emotion (EEI) task, mean intensity ratings across subjects for the angry movies was 38.1 (SD 10.8) and for the happy movies, 38.2 (SD 8.4). There was no significant difference between these ratings. No gender differences were observed between subjects in the rating of stimulus intensity.

In the Simon Task, mean reaction times for concordant and discordant

conditions were 445.7 and 509.8 ms respectively ($P < 0.001$, $t = 5.162$, $df = 13$). In contrast to behavioural results of the EEI study, correlations between stimulus dot position and motor reaction time in the Simon Task did not reach statistical significance. The average response error rate across subjects was 9%.

4.3.2.1 Brain activity relating to emotional expression interference (EEI)

Brain regions demonstrating significant differential activity during EEI (incongruent vs. congruent responses) included motor cortex, ventrolateral prefrontal cortex, lingual gyrus, and right anterior insula (see Figure 4.3 and Table 4.2 for detail). Interestingly, significant activity changes within genual or dorsal anterior cingulate cortex were not evoked by EEI. Because of the difficulty implementing accurate facial EMG within the 3T MRI environment, I could not identify all error responses in EEI, nor provide brain activation map of error responses in EEI. However, participants were over-trained in the task before scanning, where performance exceeded 95%, and during scanning the error rate of EEI score (i.e. mis-assigning positive emotions as negative and vice versa) was 1.3%.

Figure 4.3

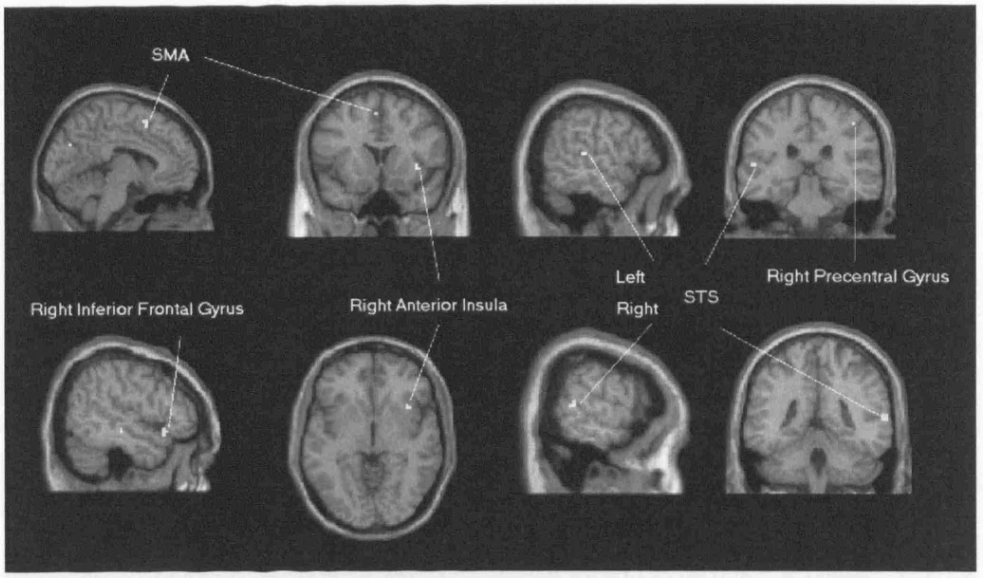

Figure 4.3 For coronal and axial sections, right is right and left is left.
Abbreviations: SMA, supplementary motor area; STS, superior temporal sulcus.

Table 4.2 Sites where neural activation was associated with interference effect of emotion expression ($P < 0.001$, uncorrected)

Brain area (BA) [b]	Stereotaxic coordinates [c]			Z score
Right precentral gyrus (4)	45	-24	48	3.82
Right inferior frontal gyrus (47)	50	17	-11	3.25
Supplementary motor area (6)	-3	9	55	3.60
Left superior temporal sulcus (22)	-53	-29	10	3.56
Right superior temporal sulcus (22)	65	-40	8	3.49
Right middle temporal gyrus (21)	50	-24	-9	3.66
Left lingual gyrus (18)	-21	-76	-11	3.93
Left cuneus (7)	-9	-71	31	3.84
Right anterior insula	36	12	-1	3.74
Thalamus	6	-32	4	3.66
Right cerebellum (semi-lunar lobule)	24	-75	-37	3.73

After taking the SPM of Simon Task ($P = 0.01$, uncorrected) as an exclusive mask, the result is exactly the same

4.3.2.2 Brain activity relating to interference effect of Simon Task

The Simon Task provided a non-emotional comparison for this EEI task. Conflict and interference during the Simon Task evoked changes in fronto-striatal activity. Modulation of activity within visual association cortices, left posterior insula and cerebellum was also observed (Figure 4.4 and Table 4.3). Taking the SPM of Simon Task as an exclusive mask (even under a generous statistical threshold, uncorrected $P < 0.01$, see below), the EEI SPM remains unchanged, suggesting limited overlap in the neural substrates for overcoming emotional and non-emotional response conflicts. No response interference effect was observed in dorsal anterior cingulate cortex (dACC) during the Simon Task, yet, strikingly, error responses caused robust dACC activation (uncorrected P value < 0.001) (Figure 4).

Figure 4.4

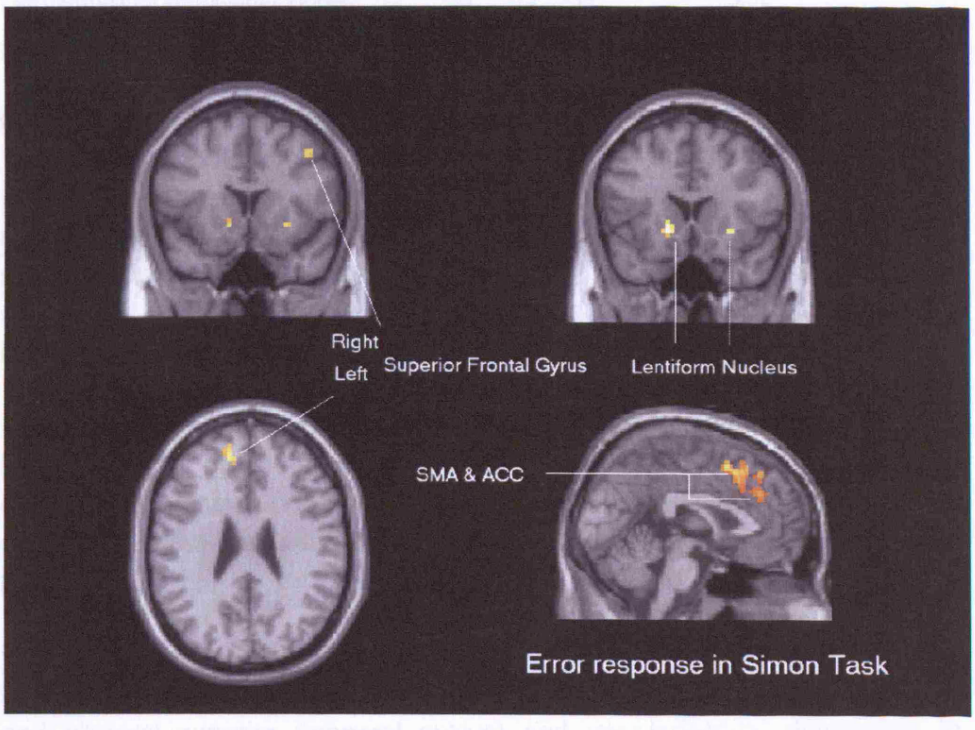

Figure 4.4 For coronal and axial sections, right is right and left is left.

The brain activities related to error response of Simon task is illustrated at the right lower corner.

Abbreviations: SMA, supplementary motor area; ACC, anterior cingulate cortex.

Table 4.3 Sites where neural activation was associated with interference effect of Simon Task (uncorrected, $P < 0.001$)

Brain area (BA) [b]	Stereotaxic coordinates [c]			Z score
Left superior frontal gyrus (9)	-12	48	22	3.81
Right superior frontal gyrus (9)	42	16	38	3.46
Right superior temporal gyrus (22)	50	-6	-2	3.27
Right parahippocampal gyrus (36)	30	-35	-8	3.75
Right fusiform gyrus (37)	45	-53	-20	3.50
Left precuneus (7)	-9	-71	42	4.21
Left insula	-45	-0	-3	4.10
Left lentiform nucleus	-15	17	-6	4.42
Right lentiform nucleus	27	17	-6	3.73
Left cerebellum (semi-lunar lobule)	-33	-72	-39	3.58

4.3.2.3 Brain correlation map

I predicted that interference (EEI) effects would be amplified by increases in perceived emotion intensity of the viewed facial stimuli. To test this I constructed brain correlation maps of EEI (by correlating brain activity and subjective rating, see Method) and calculated the contrast of discordant and concordant conditions. As with the categorical EEI analysis, activity within inferior frontal gyrus (BA 47), right anterior insula, and superior temporal sulcus was modulated during EEI, as a function of the perceived emotional intensity of the facial expressions. In addition, bilateral middle frontal gyri and left orbitofrontal gyrus also demonstrated this parametric aspect of conflict in emotional expression (Table 4.4). As to the Simon Task, since the dot position did not modulate the interference effect, further correlation analyses were not performed.

Within this second level analyses, I also explored the predictive relationship between activity during EEI (in right anterior insula, right inferior frontal gyrus and bilateral superior temporal sulcus) and inter-individual differences in emotional style (EQ, ERQ). Across subjects, the emotion reactivity subscale of Empathy Quotient (EQ-er) correlated significantly with activity within left superior temporal sulcus ($P = 0.007$). Similarly, the suppression subscale of Emotion Regulation Questionnaire (ERQ-supp) correlated with EEI-related activity within right inferior frontal gyrus ($P = 0.017$). These rating and correlation results are summarized in Table 4.5.

Table 4.4 Correlation map constructed from intensity rating and brain responses (discordant > concordant; uncorrected, $P < 0.001$)

Brain area (BA) [b]	Stereotaxic coordinates [c]			Z score
Left inferior frontal gyrus (9)	-53	13	24	3.26
Left inferior frontal gyrus (47)	-42	26	-4	3.58
Right inferior frontal gyrus (47)	48	23	-11	3.45
Left middle frontal gyrus (9)	-30	25	37	3.55
Right middle frontal gyrus (9)	45	25	26	3.35
Right middle frontal gyrus (6)	42	14	55	3.36
Right medial frontal gyrus (6)	9	-23	56	4.11
Right orbitofrontal gyrus (11)	27	43	-15	3.40
Left superior temporal sulcus (22)	-53	-38	7	3.55
Left middle temporal gyrus (37)	-48	-44	-3	3.69
Right anterior insula	39	17	-11	4.01
Left cerebellum (tuber)	-33	-83	-29	3.42
Left cerebellum (uvula)	-3	-65	-27	3.73

Table 4.5 The rating results of ERQ and EQ and the correlation coefficients with activity at four regions of interest.

	ERQ-supp	EQ-er	Mean score of rating	
Right inferior frontal gyrus	0.62 *	-0.39	ERQ-reap	31.64
Right anterior insula	0.29	0.23	ERQ-supp	13.71
Left superior temporal sulcus	0.30	-0.68**	ERQ-all	45.36
Right superior temporal sulcus	-0.26	0.09	EQ-ce	12.50
			EQ-er	11.21
			EQ-ss	6.86
			EQ-all	38.36

EQ: Emotion Regulation Questionnaire

ER: Empathy Quotient

reap: reappraisal, supp: suppression, ce: cognitive empathy, er: emotion reactivity, ss: social skills, all: total score

* $P = 0.017$; ** $P = 0.008$

4.4 DISCUSSION

This study explored a novel Stroop-like effect; namely, emotion expression interference (EEI). This interference effect highlights automatic emotional conflict at the level of stimulus-response (S-R) compatibility. In this behavioural facial EMG study, I showed facilitation and interference effects on emotional expression from reaction times (RT's). Besides, the EMG onset in concordant condition correlated negatively with the personal emotion reaction, reflected in the subscale 'emotional reactivity' of Empathy Questionnaire (EQ-er reflects the tendency to react emotionally to the emotions of others; Lawrence et al., 2004), implying that people with higher emotional empathy respond faster to others' facial expressions. In this neuroimaging study, I show that EEI is mediated by an emotion-related sensorimotor network that includes bilateral superior temporal sulcus (STS), right anterior insula, right inferior frontal gyrus (IFG) and supplementary motor area (SMA). This neural activation pattern differs from observations in classical Stroop/interference paradigms. Notably, within these experimental subjects, this profile did not overlap with interference-related activity engendered by the Simon Task. I also illustrated that conflict-related neural activity within IFG, right anterior insula and STS was directly sensitive to the perceived intensity of emotional expression stimuli, further endorsing the role of these regions in emotion expression interference at the level of stimulus-response conflict.

It is highly possible that the EEI originates at the level of mimicry, requiring an individual to overcome the intrinsic imitative tendency evoked by the emotional facial expression of another. The underlying mechanism for this 'emotion contagion' effect, highlighted by a series of EMG studies (Dimberg 1982), is still under debate. Measurement of the mimicry tendency at response level does not necessarily mean that it goes through motoric mimicry. For example, specific facial EMG pattern can also be aroused to non-face emotional stimuli (Dimberg 1986). Various social or emotional behaviours automatically become active in the presence of relevant behaviour or stereotyped-group features (Bargh et al. 1996). Further, the automatic mimicry is shaped by personal characteristics (Sonnby-Borgstrom 2002). These observations point to heterogeneous pathways underlying mimicry tendency which are not exclusive to each other. In other words, the emotion contagion may work through emotional, motoric, cognitive evaluative channels, or in combination. My previous study (chapter 3) of imitating emotional facial expressions highlighted

the involvement of both motoric and emotional (notably amygdala) centres (Lee et al. 2006). EEI is likely to engage both emotional and motoric pathways.

At a psychological level, the EEI effect may reflect the greater motoric effort required to overcome a pre-potent imitative facial expression in order to express a discordant emotion. Correspondingly, the brain regions observed in association with EEI include right IFG (BA 47), precentral gyrus and medial prefrontal cortex (BA 6). The latter location (for facial movement) reinforces the notion of somatotopy within SMA (Chainay et al. 2004). The pars opercularis within right IFG, BA 44, is implicated in imitation network and regarded as part of a mirror neuron system (Carr et al. 2003; Lee et al. 2006; Rizzolatti et al. 2004). Mirror neurons, cells sensitive to both observed and self-initiated actions, provide a putative neural substrate for imitative behaviour and simulatory representations of others. EEI may reflect the engagement of this mirror neuron system wherein the expression of discordant facial emotion overrides a pre-potent automatic mimicry or mirror neuron response. In an earlier study, I demonstrated enhanced activity within right BA 44 during emotional facial mimicry that reflected parametrically the degree of facial musculature movement (Lee et al. 2006). Interestingly, in the present study, EEI-related activity within right IFG extended into the neighboring, BA 47, and demonstrated a parametric relationship with intensity of conflicting emotion. One interpretation, arising from this previous study and those of others (Eisenberger et al. 2003; Hariri et al. 2000; Lee et al. 2006), is a modulatory role of BA 47 in suppressing implicit/automatic mimicry or mirror responses generated within BA 44.

One strategy that subjects may have drawn upon to overcome interference during perception of a discordant emotional expression, is the engagement and amplification of representations of the intended expression. Within this imaging data, the activity of one brain region, right anterior insula, putatively reflected this compensatory representational enhancement. Right anterior insula is implicated in second-order representations of emotional state, including feelings arising from the interpretation of interoceptive responses and self-generated emotion (Critchley et al. 2004; Reiman et al. 1997). In contrast, recognition and experience of disgust engages insula at a more ventral region (Calder 2003; Calder et al. 2000; Krolak-Salmon et al. 2003). In the present study, right anterior insula activation was observed during EEI (both categorically and parametrically), reflecting at least the emotional effort

required for discordant expressive responses. This account is concordant with the general notion that the insula is preferentially involved in the evaluative, experiential or expressive aspects of internally generated emotions (Phan et al. 2002; Reiman et al. 1997).

I had not predicted a priori that STS activity would be engaged during the expression conflict task. STS is implicated in sensory processing of changeable aspects of face stimuli, including facial expressions (Puce et al. 1998; Winston et al. 2004) and corresponding representations of social signals (rather than motoric expression). Nevertheless, in chapter 3 (in which subjects mimicked facial expressions) I observed a parametric relationship between STS activity and magnitude of imitative facial movement (Lee et al. 2006). Together, these two studies demonstrate a role for STS that surpasses passive processing and representation of social signals. Rather STS cortical activity is context-sensitive, in that it is modulated as a function of the facial expression held by the subject. In EEI, increased STS activity may facilitate processing and appraisal of social reactions evoked by the volitional expression of a discordant emotion.

Stimulus-response conflict and interference were not associated with enhanced dorsal anterior cingulate cortex (dACC) activity in either the emotion expression task or the Simon Task. In cognitive tasks, dACC activity is implicated in control processes that include attentional demand, executive control, error detection, response monitoring, response inhibition, set-shifting, attentional selection, strategy formation and autonomic control (Bush et al. 2000; Carter et al. 1999; Critchley et al. 2003; Critchley et al. 2005; Gehring et al. 2001; Paus et al. 1998). Interference effects do not always evoke activity enhancement in dACC / preSMA. Thus during a Simon interference task, Maclin et al. proposed that ACC is particularly engaged where there is a conflict across modalities whereas within modality conflict is processed in regions dedicated to that specific functional modality (Maclin et al. 2001). Besides, it has been reported that ACC does not show differential responding when events occurred with equal frequency, as in this design (Braver et al. 2001). My own observation during the Simon Task may endorse these views, observing fronto-striatal activity changes consistent with previous reports (Rubia et al. 2006).

The imaging findings of EEI may reflect three component mechanisms: enhanced motoric effort, subjective (actively generated) feeling state and enhanced social signal processing. Correspondingly, I examined the relationship between activity in right inferior frontal gyrus (BA 47), right anterior insula and bilateral superior temporal sulcus and inter-individual differences in behavioural and subjective emotional style. This observation that positive correlations between BA 47 activity and the suppression sub-score of ERQ supports an account in which BA 47 modulates (or inhibits) automatic emotional expressions, perhaps via connectivity between BA 44 and premotor region. Thus, individual differences in the ability to suppress emotional responses are reflected in BA47 activity during emotional expression interference. I also observed that activity in STS correlated negatively with individual scores of emotion reactivity (EQ-er reflects the tendency to react emotionally to the emotions of others; (Lawrence et al. 2004)). In the light of this extended integrative account of STS function, I suggest that a tendency towards enhanced emotional reactivity may enhance neural response or efficiency at STS to process social signals. As to the origins of the interference effect, it is still unclear. Besides chameleon effect which possibly engages mirror neuron system, mood congruency and conceptual priming effects should also be considered. The former can be tested in the designs eschewing the awareness of posed expression (Ekman et al. 1983; Strack et al. 1988). The latter can be tested in a design where the emotion-laden words (e.g. word Happy or word Angry) replace the emotion expression movies. Whether behaviour and neuroimaging results are similar across modalities is of great interest to the issue of EEI.

The EEI and Simon tasks represent different tasks, notably in type of stimuli, in mode of response and relative differences in the timing of cue and target. Each elicits a specific interference effect (emotion-response and cognition-response dimension respectively). There are therefore a number of contributing factors that may account for differences between the tasks in the neural substrates for interference. First, the processing of the stimuli themselves may confound activity relating to conflict, evoking distinctive patterns of brain activation, which was related to face-object and spatial sensory representations instead of to the interference effect per se. Nevertheless, I attempted to address this by matching closely perceptual and response level requirements within the two tasks. Thus, after subtraction of discordant and concordant conditions, the neural centres mediating interference effects should be identified

independently of presented stimuli and response demands. Further, if higher cognitive function (including different attention load) differentially modulated processing of stimulus-response mismatch, I would anticipate differential brain responses within fusiform face area and superior parietal regions. The absence of significant effects at these loci supports the validity of this contrasts. Second, in this design discordant and concordant conditions were balanced in terms of trial number (i.e. equal frequency), which minimized performance error and eliminated the possible confound of "frequency effect" in this interference brain map. As a consequence, the brain map of EEI did not interact with any cognitive effort required to overcome habitual responses inherent in design. Other studies have focused on this experimental manipulation of response competition (Braver et al. 2001). Third, while task difficulty may contribute to relative differences in interference-related brain activity, particularly within inferior frontal gyrus (BA 47; (Gould et al. 2003; Paus et al. 1998; Stricker et al. 2006), it is unlikely to account for the differences that I observed between EEI and Simon task activity. Behaviourally, both tasks produced correct response rates higher than 95 and 90 percent before and during experiments, indicating similar difficulty level. Further, correlation between the activity at BA 47 and STS with personal emotion regulation and empathy score underlines their roles in emotional expression control. Nevertheless, while I were unable to identify a common centre for processing interference of EEI and Simon, this null finding does not exclude the recruitment of common centres for processing response conflict at higher levels of task demand and difficulty. Interestingly, a recent fMRI paper of emotion go/nogo, where cognitive go/nogo served as a non-emotional comparison, also revealed distinct activation patterns (Shafritz et al. 2006). This observation complements this own evidence to imply that emotion response inhibition and interference recruit additional or distinct neural substrates to cognitive control tasks, and argue that there is no generic neural circuitry mediating all types of behavioural interference.

4.5 CONCLUSION

In this chapter, I demonstrated a novel interference effect at the level of expressed emotion with important implications for adaptive social and motivational behaviour. Using neuroimaging, I delineated centres of regional brain activity engaged during emotion expression interference and distinguished this activity pattern from activity engendered by non-emotional interference in a Simon Task. Emotion expression interference (EEI) enhanced activity across distributed neural substrates including anterior right inferior frontal gyrus (BA 47), supplementary motor area (facial area), posterior superior temporal sulcus and right anterior insula, reflecting motoric, perceptual and experiential modules of emotional processing. BA 47 and STS activity during EEI further predicted individual differences in personality measures of regulatory emotional control and reactive emotion empathy. This study highlights the neural specificity underlying emotion expression interference, complementing the findings of imitating emotion in chapter 3.

Chapter 5

Emotional judgments of others are biased by the observer's own facial expressions through changes in regional neural activity and connectivity

---

5.1 INTRODUCTION

Chapter 1 highlighted the enhancement of behavioural and neural responses when the observed facial emotion is the same as the one posed by the viewer. In fact, this phenomenon has long been recognized (Adelmann et al. 1989). In a similar way one's own facial expression can feed back to modulate activity within emotional brain regions to influence affective behaviours, including the emotional appraisal of others.

Ekman and co-workers (Ekman et al. 1980) observed that participants who actively smile while watching positive films report themselves as happier than those who did not smile. Correspondingly, participants who produce angry, fearful or disgusted facial expressions when viewing a negative film report subjectively greater negative affect. Interaction between posed and observed facial expressions has broad empirical support (Adelmann & Zajonc 1989), yet the underlying psychophysiological mechanisms remain uncertain. My previous two chapters (chapter 3 and 4) revealed that the active posing of emotional facial expressions engages, in addition to motoric regions, neural circuitry implicated in emotion processing and affective behaviour (Lee et al. 2007; Lee et al. 2006). In this chapter, I investigated empirically the interaction of posed emotion and emotion intensity judgment.

In this study, I undertook two functional magnetic resonance imaging (fMRI) experiments in the same individuals. The first experimental task defined the functional neuroanatomy of emotional appraisal of the intensity/saliency of dynamic facial expressions while the second described the interaction between observed and posed facial expressions (interaction: observed/posed; IP). I predicted that the judgment of emotional intensity requires the concurrent perception of emotional valence and a quantitative representation of the magnitude of facial movement. The execution of the facial emotion intensity judgment thus requires the integration of affective and magnitude representations (hypothesized to occur within dorsolateral prefrontal cortex; (Gray et al. 2002)). In terms of the neural substrates underlying the influence

of one's own expression on the perception of the emotion state of another, I predicted that IP would evoke an affective influence on the connectivity between regions engaged during salience judgments of faces. I tested this directly using dynamic causal modelling (DCM; (Friston et al. 2003)), incorporating the results of the first task as constrained regions-of-interest to probe functional neural connectivity patterns mediating judgments of facial emotion intensity and the interaction with the observer's facial expression from the data obtained in the second task. The underlying theorem of DCM is detailed in chapter 2.

5.2 MATERIALS AND METHODS

5.2.1 Subjects, experimental stimuli and tasks

Fourteen volunteers were recruited for the fMRI study (mean age, 22.7 years; 7 M, 7F). They were screened to exclude history or evidence of neurological, medical, or psychological disorder including substance misuse. None of the participants was taking medication. All participants provided written informed consent to participate in this study which was approved by the Local Ethics Committee.

Since facial emotional expressions are intrinsically dynamic signals (Kilts et al. 2003), I utilized short movies instead of static pictures as stimuli. Experimental stimuli consisted of video clips (700 ms duration) of two dynamic facial expressions, anger and happiness, portrayed by twelve male and twelve female models. Each video clip was further processed by SmartMorph (http://meesoft.logicnet.dk/SmartMorph/) to create 2 different intensities of emotional expression: 75% and 100%. In total, I therefore constructed 96 different video clips from 24 different identities. The stimulus set was also used in the earlier studies (Fig. 5.1 (i)). Visual instructions, dynamic face stimuli and rating scales were presented to the participant using an LCD media projector via a screen that was viewed through a mirror box place on the MRI headcoil.

5.2.1.1 Task 1: Emotional versus non-emotional judgment

I first set out to define brain regions supporting explicit judgments of the emotional intensity of faces. In a blocked design task, performed over one session, the participant was required either to rate the positive and negative emotional intensity of dynamic face stimuli or to rate both gender and age of the models depicted in the stimuli. This was possible because the stimuli were emotion-laden material from both male and female models; the subjects were instructed at the beginning of each block either to focus on the emotion or focus on the age. The contrast of these two conditions provided a means of identifying brain regions ('nodes') engaged specifically during explicit emotional appraisal of the faces. Participants viewed a total of six stimulus blocks representing cued judgments of the emotional intensity of the stimuli alternating with judgments of age of the stimuli. Each block consisted of 16 trials (Fig. 5.1 (ii)). The participant maintained a neutral facial expression throughout the task. Each participant was instructed to concentrate on the

relevant dimension (emotion or age) at the start of each block. At the end of each video clip, the participant was then prompted to rate their judgment. The participant signalled the perceived intensity of facial expressions using a two-button, hand-held response pad via a visual-analogue-scale (VAS) displayed on the screen. Positive emotional ratings were made to the right and negative emotion to the left. Similarly, age judgments were made in a similar way, the direction of responses made according to the sex of the stimulus model (right for female, left for male). Thus, both emotion and age judgments were signalled parametrically and bi-directionally. The video clips were replicated across both judgment conditions in randomized order. I expected that the contrast of the two conditions would highlight the critical components supporting explicit appraisal of emotional intensity. The leading block, either judging emotional intensity or age, was counterbalanced across participants.

5.2.1.2 Task 2: Influence of posed facial expression on emotional judgment

I next set out to examine how subjective ratings of emotional intensity may be biased by the emotional expression of the observer. In this task, the participant was cued to hold a specific facial expression at the start of each trial, and then rate the emotional intensity of the dynamic facial expression depicted by the stimulus. I therefore tested, first, for brain regions where activity varied parametrically with subjective judgments of perceived emotional intensity of the stimuli and, second for a modulatory influence of posed facial expression on activity underlying this explicit emotional appraisal. The emotion intensity judgment and modulatory influence were explored in greater depth using dynamic causal modelling (DCM), a connectivity analysis approach.

Figure 5.1

Fig. 5.1 Examples of experimental stimuli (i), and the structure of a single trial for emotion intensity and age judgment task (ii) and emotion intensity judgment task with actively posed expression (iii). The VAS scale used is illustrated in (iv).

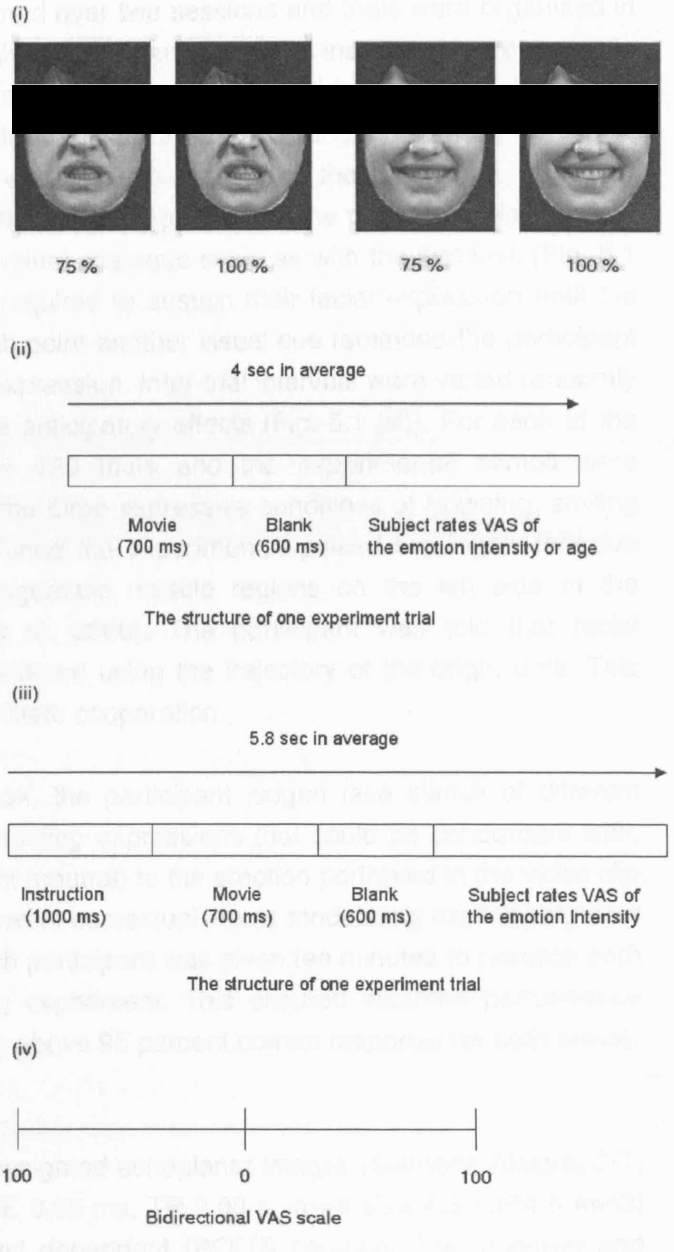

This main task was performed over two sessions and trials were organized in a randomized way. On each trial, the participant was instructed to frown, smile or keep neutral in response to a 1s visual cue. This cue was followed by presentation of a movie clip depicting a happy or angry facial expression of varying intensity. At the end of each video clip, the participant was then prompted to make an emotion intensity judgment. The participant signalled an intensity judgment via the visual-analogue-scale as with the first task (Fig. 5.1 (iv)). The participant was required to sustain their facial expression until the end of VAS rating, at which point another visual cue reminded the participant to relax back to a neutral expression. Inter-trial intervals were varied randomly from 5.3 to 6.3 s to reduce anticipatory effects (Fig. 5.1 (iii)). For each of the two sessions, there were 120 trials and the experimental stimuli were replicated across each of the three expressive conditions of frowning, smiling and neutral expression. During the experiment, I placed two highly-reflexive dots at corrugator and zygomatic muscle regions on the left side of the participant's face (Lee et al. 2006). The participant was told that facial responses were being monitored using the trajectory of the bright dots. This procedure was used to facilitate cooperation.

Overall, in this second task, the participant judged face stimuli of different emotional intensity while holding expressions that could be concordant with, discordant with or irrelevant (neutral) to the emotion portrayed in the video clip. This represented three different contextual inputs modulating explicit judgment of emotional intensity. Each participant was given ten minutes to practice both tasks before the scanning experiment. This ensured accurate performance (each participant achieving above 95 percent correct response for both tasks).

5.2.2 fMRI data acquisition

I acquired sequential T2*-weighted echoplanar images (Siemens Allegra, 3-T, 32 slices, 3.0 mm thick, TE 0.65 ms, TR 2.08 s, voxel size 4.5*4.5*4.5 mm3) for blood oxygenation level dependent (BOLD) contrast. Two hundred and eight images whole-brain images were obtained over 7 minutes for first task and 350 over 12 min for the two sessions of the second task. The first 6 echoplanar volumes of each session were not analyzed to allow for T1-equilibrium. A T1-weighted structural image was obtained for each participant to facilitate anatomical description of individual functional activity after co-registration with fMRI data.

5.2.3 fMRI data analysis

I used SPM5 analysis software on a Matlab platform (Mathwork, IL) to analyze acquired fMRI data. The analytic flows and underlying principles have been described in chapter 2. The 6 movement parameters (3 for translation and 3 for rotation) derived from realignment process were imported into the design matrix to account for confound from facial movement. Error responses were defined as the trials in which a participant misclassified the video clips (i.e. where happy movie was rated as angry), and were modelled within the design matrix as a separate column.

In the first task (explicit emotional judgment versus age judgment), I modelled each trial as a separate event convolved with a canonical haemodynamic basis function, categorized according to judgment type with the analytic design matrix (Mechelli et al. 2003). Within individual participant analyses, I computed the contrast for activity during explicit judgment of emotional intensity minus age judgment. This contrast provided a means of localizing neural centres specifically responsible for explicit emotional appraisal that could be used as constraint of neural nodes within DCM connectivity analysis. In addition, activity across the group was tested within second-level analyses using simple T-tests. Voxel-wise statistical threshold was set at $P < 0.001$, uncorrected.

In the main (second) task, I examined how judgments of perceived emotional intensity were processed and further modulated by the observer's posed facial expression. Trials were weighted parametrically according to the rated emotion intensity of the stimuli. A second parametric weighting of the trials reflected the degree of congruence between the emotion of the observed face stimulus and the facial expression posed by the participant. Thus, a value of 1 was assigned to concordant trials (when the participant held a frowning expression while viewing an angry video clip or held a smiling expression while viewing a happy video clip), the value 0 to neutral trials and -1 assigned to discordant trials (e.g. frowning to happy movies and smiling to happy movies). This weighting was predicated on the idea that congruence in expression would intensify the emotional impact of face stimuli and vice versa for incongruence in expression. Again stimulus events were modelled with a canonical haemodynamic response function (HRF). Contrast images were constructed at first-level (individual) analyses. I first explored regional brain activity showing a parametric relationship with judged emotional intensity.

This methodological approach is established as a means of examining neural correlates of affective behaviour through regional parametric covariation of the BOLD signal (Buchel et al. 1998; Lee et al. 2006; Phan et al. 2004; Winston et al. 2002). A second contrast directly probed the brain regions supporting the modulation of emotional intensity judgment by the participant's own directed facial expression. Again, group analyses were conducted to identify robust effects across the group using simple T-tests at a voxel-wise statistical threshold of $P < 0.001$, uncorrected.

5.2.4 Dynamic Causal Modelling (DCM) analysis

I applied DCM (Friston et al. 2003; Penny et al. 2004) to examine neural model mediating the judgment of emotional intensity of dynamic face stimuli, and further modulated by posed facial expression. A hypothetical brain network was proposed for this interaction that incorporated intrinsic, extrinsic and modulatory connections: I selected four neural nodes that were independently defined in the first task as supporting explicit judgment of emotional intensity; namely, superior temporal sulcus/gyrus (STS), post-central cortex (PC), premotor region (PM) and dorsolateral prefrontal cortex (PFC; see Results). STS was modelled as neural node receiving extrinsic input (see below), yet I specified fully connected models and compared the extrinsic connectivity strength and posterior probability (given the data) separately for STS and PC as input nodes (Ethofer et al. 2006).

For each participant, a large number (327) of models were constructed with discrete connectivity patterns. Each connectivity pattern represented a different hypothesis. In quantifying the validity of each model, haemodynamic BOLD time courses were extracted from voxels within the sphere of radius 8 mm at the coordinates with highest Z-score within the above four regions, for each session and for each participant. The first eigenvariates of these data were imported into the DCM analyses. The connectivity strengths and model evidence for each model were calculated using SPM DCM, to indicate the best data fit and the likelihood of the data given the model ($P(y|m)$ for model m and data y) respectively.

In this study, a model comparison procedure was adopted to determine which connectivity model represented an optimal balance between data fit and model complexity (Penny et al. 2004). Thus, to compare model a and model b, the Bayes factor (BF) was calculated for each participant by $Ba,b =$

P(y|m=a)/P(y|m=b). Ba,b > 1 favour model a over model b. Evidence for superiority of one model over another model is assumed if BF is bigger than 3 (Penny et al. 2004). To make inferences at group level, I first computed the individual BF by taking square root of the product of the BF for each session (number of session = 2), and then computed the average BF by taking 14th root of the product of the individual BF (number of subject =14). In this analysis (see Results), I found a cluster of models with highest BF shares similar intrinsic structure and close BF (in other words, the BF between these models is less than 3). To pick up the best model, I adopted a non-parametric procedure (Ethofer et al. 2006). The probability to obtain j or more BF >1 in n subjects under the null hypothesis Ho: P(y|m=a) = P(y|m=b) can be calculated by:

$$P = \sum_{k=j}^{n} C_k^n * 0.5^n$$

The alternative hypothesis P(y|m=a) ≠ P(y|m=b) was accepted if P <= 0.025 (two-sided test).

5.3 RESULTS

5.3.1 Neural substrates supporting explicit judgments of emotional intensity

In Task 1, four regions critical for emotion intensity judgment were identified in the comparison between emotion judgment and age judgment of the dynamic facial stimuli. These were the superior temporal sulcus/gyrus (STS), post-central cortex (PC), premotor cortex (PM) and dorsolateral prefrontal cortex (PFC). Enhanced engagement of these regions during explicit emotion judgement was interpreted as consistent with previous data. Thus, STS is implicated in the processing of dynamic information from faces (STS) (Allison et al. 2000; Haxby et al. 2000) and in the recognition of facial emotion (Narumoto et al. 2001); PC is implicated in both somatosensory and affective representations, and; PM is implicated in the 'mirror' representation of physical motoric aspects of observed facial expression (PM) (Adolphs et al. 1996; Fadiga et al. 2004; Hari et al. 1998; Heberlein et al. 2004; Iacoboni et al. 1999; Narumoto et al. 2001; Winston et al. 2003). Lastly, observed PFC activation was consistent with evaluative information processing (including the integration of inputs from PM and PC regions) for computation and execution of intensity judgments (Gray et al. 2002; Krawczyk 2002) (see Fig. 5.2 and Table 5.1). The identification of these regions informed the subsequent choice of ROIs for connectivity analyses, described below.

Figure 5.2

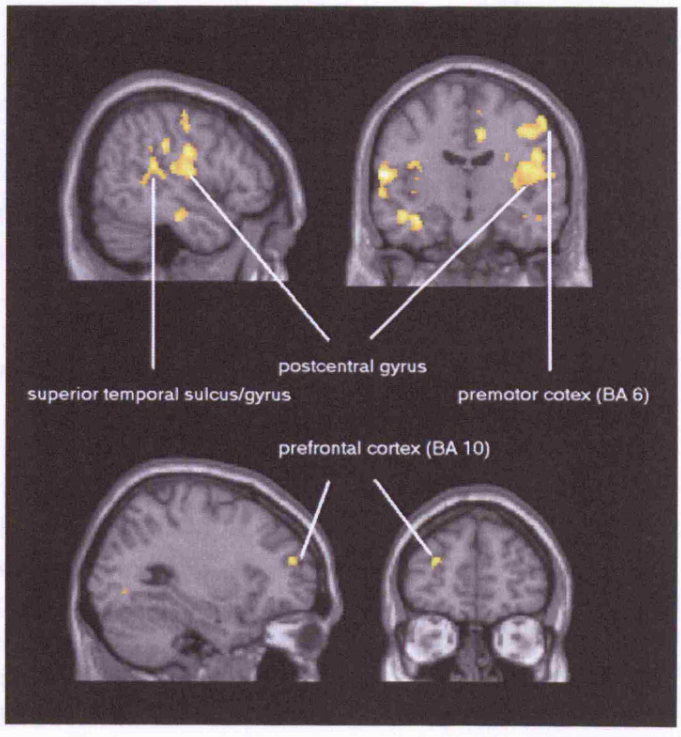

Figure 5.2 Brain regions showing significant activities for contrast of emotion intensity judgment minus age judgment (Task 1). For coronal sections, right is right and left is left.

Table 5.1 Brain regions showing activation for the contrast of emotion minus age judgment

Brain area (BA) [a]	Stereotaxic coordinates [b]			Z score
Premotor cortex (6/R)	42	-4	33	4.50
Premotor cortex (6/L)	-46	-8	32	3.58
Postcentral gyrus (43/R)	59	-7	17	4.78
Postcentral gyrus (43/L)	-59	-11	12	4.84
Rostral cingulate cortex (32)	2	21	-9	4.17
Anterior cingulate cortex (24/R)	2	22	21	3.59
Posterior cingulate cortex (23/L)	10	-15	41	4.10
Paracentral Lobule (4/L)	-14	-36	53	3.62
Middle frontal gyrus (10/L)	-28	49	16	3.97
Inferior parietal lobule (40/R)	48	-37	30	3.41
Inferior parietal lobule (40/L)	-59	-32	22	3.82
Cuneus (19/L)	-8	-86	30	3.72
Superior temporal sulcus/gyrus (22/R)	51	-34	16	4.17
Superior temporal sulcus (22/L)	-44	-40	15	3.69
Posterior insula (L)	-36	-15	12	3.93
Posterior insula (R)	46	-21	16	4.34
Lingual gyrus (19/L)	-28	-74	0	3.47
Fusiform gyrus (20/L)	-38	-17	-23	4.36
Fusiform gyrus (20/R)	46	-20	-16	3.42

[a] BA, Brodmann designation of cortical areas

[b] Values represent the stereotaxic location of voxel maxima above uncorrected threshold ($P < 0.001$)

5.3.2 Behavioural modulation of emotional intensity judgment by posed facial expression

Behavioural data from Task 2 revealed an overall intensity rating across participants for the angry and happy video clips of 43.3% (SD 5.2%). No gender effects were observed between participants in the rating of stimulus intensity. As predicted, the emotional facial expression of the observer influenced judgments of emotional intensity. For concordant trials, where the valence of the dynamic face stimuli (happy or angry) corresponded to the posed facial expression (smile or frown), there was an enhancement of intensity ratings by 6.6 % relative to the 'normal' (posed neutral expression)

condition (P = 0.018, df = 13). Similarly, for discordant trials (observing angry faces when smiling or happy faces when frowning), there was an attenuation of intensity ratings by 6.0 % (P = 0.029, df = 13).

5.3.3 Regional brain activity covarying with perceived emotion intensity

From the neuroimaging data, I identified brain regions that showed positive and negative parametric relationships with the rated emotional intensity of the stimuli. Regions showing a positive relationship with perceived intensity of faces were predominantly cortical, and included bilateral occipito-temporal cortices, premotor (PM) cortices, the inferior and middle frontal gyri and a region of anterior cingulate cortex. Interestingly, brain regions that showed a negative relationship with emotional intensity ratings of face stimuli included bilateral posterior insula, right anterior insula, precuneus, and several subcortical structures, including bilateral thalamus, bilateral amygdala and the nucleus accumbens, see Fig. 5.3 and, Table 5.2 and 5.3.

Figure 5.3

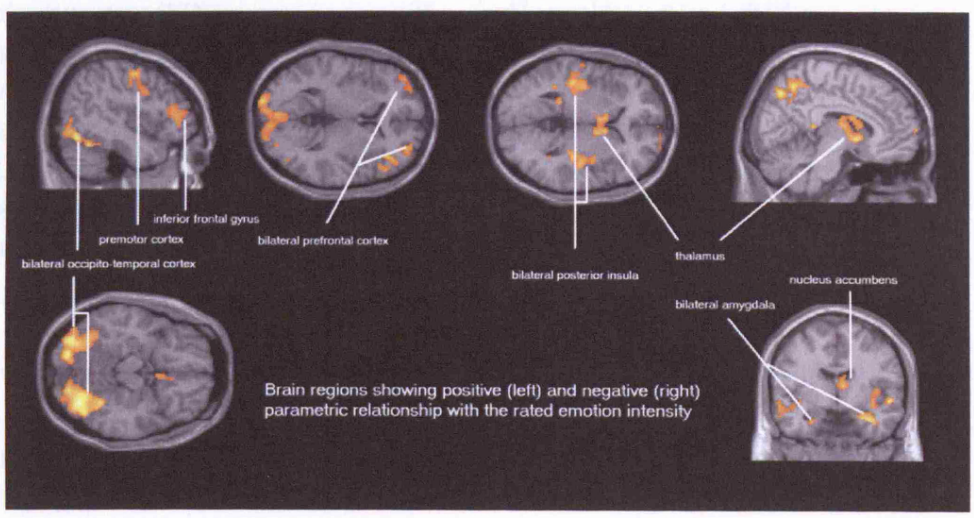

Fig. 5.3 Brain regions showing significant parametric relationship with rated emotion intensity (Task 2).

For coronal sections, right is right and left is left.

For axial sections, down is right and up is left.

Table 5.2 Sites where neural activation was positively associated with rated emotion intensity

Brain area (BA)[a]	Stereotaxic coordinates[b]			Z score
Precentral Gyrus (4/6/R)	48	-5	50	4.47
Precentral Gyrus (4/6/L)	-42	-4	39	3.97
Inferior frontal gyrus (47/R)	40	33	0	4.26
Inferior frontal gyrus (46/L)	-50	28	13	3.42
Middle frontal gyrus (10/R)	32	52	1	4.05
Middle frontal gyrus (10/L)	-42	50	-1	3.92
Medial frontal gyrus (10/L)	-10	59	10	3.55
Medial frontal gyrus (9/L)	-8	50	36	3.47
Anterior cingulate gyrus (24/L)	-8	8	47	3.95
Rostral cingulate gyrus (25/R)	6	11	-14	3.77
Lingual gyrus (18/R)	34	-72	-6	5.56
Lingual gyrus (18/L)	-28	-78	-11	4.99
Fusiform gyrus (37/R)	36	-47	-13	5.02
Fusiform gyrus (37/L)	-40	-61	-12	4.98
Cerebellum, Declive	10	-71	-13	3.93
Cerebellum, Semi-Lunar Lobule	14	-72	-38	3.70

[a] BA, Brodmann designation of cortical areas

[b] Values represent the stereotaxic location of voxel maxima above uncorrected threshold ($P < 0.001$)

Table 5.3 Sites where neural activation was negatively associated with rated emotion intensity

Brain area (BA)[a]	Stereotaxic coordinates[b]			Z score
Middle frontal gyrus (10/R)	4	66	2	3.96
Inferior parietal lobule (40/R)	46	-40	54	4.65
Inferior parietal lobule (40/L)	-57	-33	48	3.54
Precuneus (7/R)	14	-71	51	4.92
Precuneus (7/R)	-10	-51	62	4.40
Superior temporal gyrus (22/R)	55	-6	-5	4.88
Superior temporal gyrus (22/L)	-63	-13	4	3.41
Middle temporal gyrus (21/L)	59	-32	-12	4.79

Inferior temporal gyrus (20/R)	57	-55	-12	3.82
Superior occipital gyrus (19/L)	-38	-78	35	4.25
Posterior insula (R)	38	-25	3	4.12
Posterior insula (L)	-42	-23	5	4.78
Anterior insula (R)	40	9	-12	5.41
Caudate	-18	21	-4	4.02
Ventral striatum (nucleus accumbens)	-4	8	0	4.38
	8	6	-2	4.26
Thalamus (pulvinar)	14	-25	7	3.59
Thalamus (pulvinar)	-12	-33	9	4.90
Brain stem (medulla)	-6	-25	-39	3.84
Cerebellum, tuber	-38	-75	-28	3.99

[a] BA, Brodmann designation of cortical areas

[b] Values represent the stereotaxic location of voxel maxima above uncorrected threshold ($P < 0.001$)

5.3.4 Neural correlates of modulation of emotional intensity judgment by posed facial expression

I next determined the correlates of regional neural activity for this behavioural observation. First, I observed enhanced activity within bilateral amygdala in trials for which the observed emotion of face stimuli was concordant with the posed facial expression of the participant (which amplified ratings of perceived emotional intensity). In contrast, activity within the middle frontal gyrus (BA 9/10) and right posterior superior temporal sulcus (STS; BA 22) was enhanced where the stimulus and posed expressions were discordant (Tables 5.4 and 5.5; Figure 5.4).

Table 5.4 Sites where neural activation of emotion intensity judgment was positively modulated by actively posed facial expressions

Brain area (BA) [a]	Stereotaxic coordinates [b]			Z score
Inferior parietal lobe (40/R)	34	-41	39	4.07
Precuneus (7/L)	-22	-69	51	3.69
Precuneus (31/L)	-10	-36	57	3.50
Cuneus (18/L)	-20	-86	26	3.40
Superior temporal gyrus (38/L: pole)	-36	16	-29	3.34
Middle temporal gyrus (38/R: pole)	-48	16	-24	3.96

Middle temporal gyrus (21/R)	-59	-10	-10	3.88
Inferior temporal gyrus (19/L)	-53	-70	-2	3.55
Parahippocampal gyrus (36/R)	30	-30	-12	3.25
Parahippocampal gyrus (35/L)	-26	-28	-14	3.48
Posterior insula (R)	38	-4	-5	3.66
Amygdala (R)	32	3	-25	4.19
Amygdala (L)	-22	-3	-22	3.55

[a] BA, Brodmann designation of cortical areas

[b] Values represent the stereotaxic location of voxel maxima above uncorrected threshold ($P < 0.001$)

Table 5.5 Sites where neural activation of emotion intensity judgment was negatively modulated by subjective facial expressions

Brain area (BA) [a]	Stereotaxic coordinates [b]			Z score
Middle frontal gyrus (10/L)	-25	54	19	3.45
Middle frontal gyrus (9/R)	40	24	19	3.76
Middle frontal gyrus (9/L)	-42	12	36	3.37
Medial frontal gyrus (9/R)	6	51	20	3.53
Superior temporal sulcus (22/R)	55	-65	29	4.43
Cerebellum, Declive	28	-63	-19	4.06

[a] BA, Brodmann designation of cortical areas

[b] Values represent the stereotaxic location of voxel maxima above uncorrected threshold ($P < 0.001$)

Figure 5.4

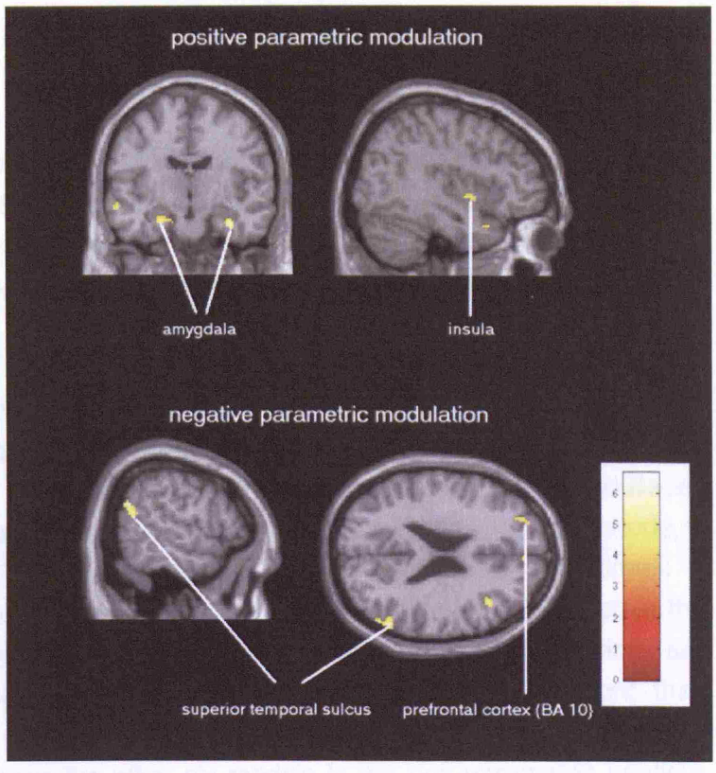

Figure 5.4 Brain regions showing significant positive and negative modulatory effect on emotion intensity judgment via actively posed facial expression (relating to judgment bias).
For coronal sections, right is right and left is left.
For axial sections, down is right and up is left.

5.3.5 Connectivity analyses using dynamic causal modelling

I included four neural nodes (STS, PC, PM and PFC) to represent the network for facial saliency judgment identified in the first task. This analysis of fully connected model confirmed STS is the appropriate neural node mediating extrinsic/perturbing input (extrinsic connectivity strength for STS = 0.27 with probability 100 percent, compared to PC = -0.01 with no statistical significance). I therefore treated STS as the only neural node receiving external input (dynamic facial expressions).

Beyond STS I suggest a putative role to PFC (BA 10) as the 'cognitive integrator' supporting a final conscious appraisal of the emotional intensity of the face stimuli (Gray et al. 2002; Krawczyk 2002). Correspondingly, I viewed PC and PM as intermediate relays representing respectively the sensory-emotional and physical motoric aspects of observed facial expression. I used DCM to test alternative hypotheses that could account for the observed neural responses. I quantified the efficiency of each model using the Bayes factors (BF). Eight models were clearly distinguished using this metric as being the most efficient. The remaining models reached BF criteria (greater than 3) for

further distinction. Thus the BF comparison between the highest model and the 9th model (B1,9) was 20.6, and the BF between the 8th model and the 9th model (B8,9) was 11. This group of eight models were internally consistent; the BF between the highest model and the 2nd model was 1.24 (B1,2 = P(y|m=1)/P(y|m=2)) and between the highest model and the 8th model was 1.80 (B1,8). Together these data indicate a cluster of models which have comparable model evidence that clearly surpass all the other 319 models.

Closer inspection of the top eight highest models revealed the same intrinsic structure. The only distinction lay in the site at which the modulatory effect of posed facial expression (IP) on regional connectivity was mediated (Fig. 5.5 (i)). The difficulty in further subdividing these models using a classical Bayes model comparison procedure was attributed to the relatively low magnitude of IP judgment bias (6 to 7 percent) on perceived intensity for the stimuli. I addressed this difficulty by applying a non-parametric approach to obtain the best model across all subjects. These non-parametric statistics are summarized in Table 5.6. Model 1 was significantly more efficient than models 3 to 8 ($P < 0.01$) but was indistinguishable from model 2. However, model 2 did not surpass the other six models in the non-parametric analysis (the inter-individual variance of model 2 BF is high). Both model 1 and model 2 shared the feature of modulatory connectivity at the posterior part of the network. Model 1, which had the highest explanatory value for the neuroimaging data, was characterized by the following structure: Unidirectional connections linked STS-to-PM, STS-to-PC, PC-to-PM, PM-to-PFC and PC-to-PFC (i.e. these were only feed-forward connections). The site of modulation was localized to the STS-to-PC connection. Fig. 5.5 (ii) illustrated the second-level (group) analysis of the estimated connection strengths and significance of the selected model.

Figure 5.5

(i)

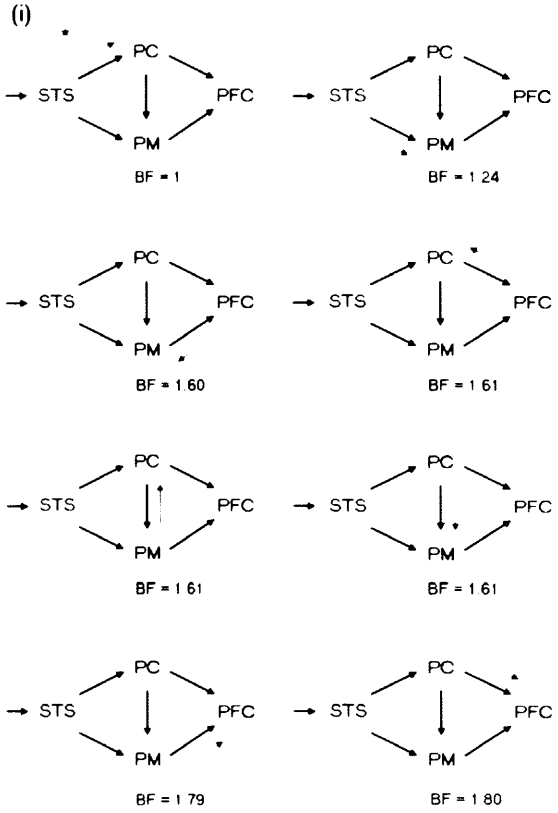

(ii)

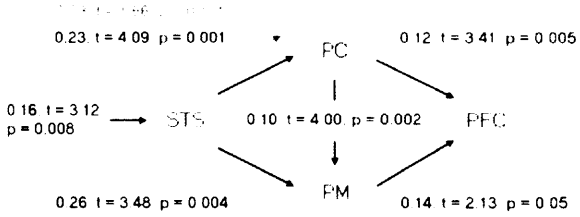

Fig. 5.5 Diagrammatic representations of the 8 competing models with highest model evidence, and the results of second-level analysis (simple t-test) of the selected model.

(i) The model with asterisk (*) is the one with highest model evidence, and is the selected model (upper left). Bayes Factor (BF) was calculated relative to this model. The black arrow to STS represents external/extrinsic input, and the other black arrows indicate the structure of intrinsic connections (the intrinsic structure is the same for all the 8 models). The orange arrows stand for the position and direction where modulatory effect by actively posed facial expression occurs.

(ii) The result of the second-level analysis of the selected model. The estimated parameters by Dynamic Causal Modelling are followed by t and P value, with d.f. 13.

Abbreviations: STS, superior temporal sulcus/gyrus; PC, post-central cortex; PM, pre-motor cortex; PFC, dorsolateral prefrontal cortex (BA 10).

Table 5.6 Non-parametric analysis of the 8 models with highest model evidence of DCM analysis

Modulation [a]	Model 1 STS->PC	Model 2 STS->PM	Model 3 PFC->PM	Model 4 PFC->PC	Model 5 PM->PC	Model 6 PC->PM	Model 7 PM->PFC	Model 8 PC->PFC
Model 1 [b]	1.000	0.788	0.910	0.910	0.910	0.910	0.994	0.994
Model 2	0.395	1.000	0.999	0.999	0.999	0.999	0.999	0.999
Model 3	0.006*	0.212	1.000	0.788	0.212	0.090	0.994	0.994
Model 4	0.006*	0.212	0.395	1.000	0.090	0.029	0.994	0.994
Model 5	0.006*	0.212	0.910	0.971	1.000	0.910	0.999	0.999
Model 6	0.006*	0.212	0.971	0.994	0.212	1.000	0.994	0.999
Model 7	0.006*	0.029	0.029	0.029	0.006*	0.029	1.000	0.910
Model 8	0.006*	0.029	0.029	0.029	0.006*	0.006*	0.212	1.000

[a] Site where emotion intensity judgment modulated by posed expression occurs. STS: superior temporal sulcus; PC: post-central cortex; PM: pre-motor cortex; PFC: dorsolateral prefrontal cortex (BA 10).

[b] Values represent the non-parametric statistics testing whether the column model is superior to the row model.

* Indicates significant ($P < 0.025$, two-tailed)

5.4 DISCUSSION

I used functional neuroimaging to identify neural mechanisms supporting the explicit judgment of the intensity of facial emotion and how this judgment is influenced by the congruence of the observer's own facial expression. In this data analyses, I used both conventional and DCM approaches. I first identified brain regions specifically supporting the judgment of emotion intensity (compared to age/gender judgment) in the default 'neutral' state of the observer. I next tested the influence of posed facial expression on the behavioural ratings of dynamic face stimuli and highlighted a behavioural effect of congruence. Thus, holding an expression that matches an observed facial expression enhanced perceived emotional intensity. Similarly, holding a discordant expression attenuated the perceived intensity of dynamic emotional face stimuli. This observation was consistent with established empirical findings (Adelmann & Zajonc 1989), yet the effect was relatively small, biasing judgments of emotional intensity by around 6 to 7 percent. Neuroimaging findings obtained during this same experimental task revealed a discrete pattern of brain activity that correlated with perceived emotional intensity. Moreover, using DCM, I demonstrated that the influence of posed facial expression on observed ratings (interaction: observed/posed; IP) was mediated via changes in the effective connectivity between superior temporal sulcus (STS) and post-central cortex (PC).

In Task 1, I identified the neural substrates mediating an explicit judgment of facial emotional intensity (in contrast to a non-emotional judgment of age). I observed engagement of four main regions; the superior temporal sulcus (STS), postcentral cortex (PC), premotor cortex (PM) and dorsolateral prefrontal cortex (PFC, BA 10). The functional relationship between these areas was also examined in DCM analyses of Task 2. STS is strongly implicated in processing of dynamic social and emotional information (Allison et al. 2000; Haxby et al. 2000; Narumoto et al. 2001), and consequently I assigned STS as the perturbing/extrinsic input node within this dynamic causal model (DCM). Although activities at fusiform gyrus also increased to emotional facial stimuli (compared with neutral), much evidence has suggested that emotional enhancement of fusiform activity is secondary to salience detection within amygdala (preferentially activated by with fearful faces) (Amaral et al. 1992; Vuilleumier 2005). I therefore did not take fusiform region as input node. Early engagement of PC during explicit emotional

appraisal was not initially predicted since its role in explicit emotional representations (compared to STS) is less well established. Nevertheless, functional imaging and lesion data suggest a contribution of PC to affective processing (arguably through linking emotion perception/representation with feedback from engendered somatomotor states) (Adolphs et al. 1996; Heberlein et al. 2004; Narumoto et al. 2001; Winston et al. 2003). PM regions are engaged when observing actions and activity here mirrors the magnitude of perceived facial movement (Fadiga & Craighero 2004; Hari et al. 1998; Iacoboni et al. 1999; Lee et al. 2006). Both PC and PM therefore represented plausible neural centres for extracting information concerning affective intensity from sensorimotor "simulatory" representations. In addition, a predicted contribution of PFC to explicit judgments of emotional expression concorded with a general role ascribed to PFC in conscious integration of information for executive decision-making, in this case the declarative evaluation of emotional intensity (Gray et al. 2002; Krawczyk 2002). Based on the above, these four regions naturally served as the neural nodes within this subsequent DCM connectivity analyses.

Direct examination of brain activity relating to the magnitude of perceived emotional intensity revealed engagement of occipito-temporal visual areas (where both attention and arousal enhance neural responsivity; (Keil et al. 2003; Pessoa et al. 2002)), motor regions (premotor and precentral cortices) and, both medial and lateral prefrontal cortices. These cortical activations plausibly reflect recruitment of perceptual (Bradley et al. 2003; Liberzon et al. 2003), imitative (Lotze et al. 2006; Rizzolatti et al. 2004) and evaluative (Carter et al. 1999; Gray et al. 2002; Krawczyk 2002) centres during explicit processing of affective stimuli. Nevertheless, more typical 'emotional' regions showed an attenuation of activity with increasing perceived emotional intensity, notably within amygdala, nucleus accumbens, precuneus, insula and thalamus. These regions are frequently implicated in neural responses to emotional challenges, including emotion induction, emotional learning and implicit emotion processing with low cognitive load (Britton et al. 2006; Damasio et al. 2000; Liberzon et al. 2003; Maddock 1999). An explanatory account for the negative correlation of activity within these regions during explicit 'cognitive' appraisal of emotionality may relate conceptually to cognitive control. Thus, activity within subcortical affective centres such as amygdala is decreased during performance of tasks that demand the volitional or effortful engagement of 'higher' cognitive processes or higher attentional

load (Critchley et al. 2000; Drevets et al. 1998; Hariri et al. 2003; Liberzon et al. 2003; Ochsner et al. 2005; Phan et al. 2005; Taylor et al. 2003).

When I examined the influence of congruence between observed and posed emotional facial expression (IP) on the ratings of emotional salience, I observed significant effects within bilateral amygdala, right posterior STS and PFC (middle frontal gyrus; BA 10). The congruency effect and positive relationship between emotional intensity ratings and amygdala activity extends earlier empirical observations implicating amygdala function in processing stimulus saliency (Hamann et al. 2002; Hamann et al. 1999; Liberzon et al. 2003; Yang et al. 2002). In contrast, activity within STS and middle frontal gyrus reflected the mismatch between observed and posed expression, an effect that parallels this prior findings regarding the interference 'cost' of producing emotional facial expressions when viewing an incongruent emotional expressions (Lee et al. 2007). Together the present data tentatively suggest complementary contributions of amygdala and STS in emotional processing in the context of self/other congruence: When there is affective concordance enhanced amygdala activity may facilitate subsequent behavioural interaction (Cardinal et al. 2002), while activity within STS is tuned down after evaluative signal processing. In situations where there is affective discordance, enhanced STS activity reflects the demand for monitoring and reappraisal of social circumstances by instantiating a cognitive evaluation at a more cortical level. In this context, decreased amygdala activity may disengage response tendencies and evoked arousal to facilitate such evaluative processing. This observation of parallel engagement of BA 10 supports this speculative account. Consistently, enhanced STS neural response has been noticed in emotion expression interference (chapter 4), where the observed and posed emotion expression are discordant.

This study is directly relevant to facial feedback theory, which proposes that facial expressions influence emotional experience via sensory feedback from the musculature (Adelmann & Zajonc 1989). Empirical studies have tested the influence of facial feedback using both explicitly - directed facial action, or implicit tasks (e.g. holding a pencil in the mouth, where gripping with lips or teeth respectively mimic depressive pouting or happy smiling; (Ekman et al. 1983; Strack et al. 1988). Facial feedback provides a powerful account for interference and interaction between observed and posed expression during emotional intensity judgment in the present study. Nevertheless it is not an

exclusive proposition. Recruitment of brain regions supporting affective feelings when expressing a particular emotion may not require obligatory extrinsic feedback, and other processes such as mood congruency may influence the evaluative appraisal of emotional stimuli (Elliott et al. 2000; Gray 2001; Perlstein et al. 2002; Simpson et al. 2000). My analysis of positive/negative parametric modulatory effect by posed expression addressed this issue specifically. It is noteworthy that the IP judgment bias (revealed in this parametric modulation analysis) engaged amygdala rather than somatomotor/somatosensory regions (i.e. PM or PC). It is interesting that precuneus and limbic regions, supposedly relevant to emotion experience, both revealed positive modulation effect by posed expression (Maddock 1999). In other words, our IP analysis prefers that mood congruency is the major mechanism contributing to IP judgment bias. One or several of these regions are expected to exert influence on the connectivity strength in our DCM model, see below.

This DCM analysis provided further insight into facial emotion intensity judgment and the interaction with posed expression (IP). This choice of STS as a receiving (input) neural node within a fully connected reciprocal model, was verified by a posterior probability of nearly 100%, entirely consistent with the functional role of STS in processing dynamic emotional/social information including emotional expressions. Further processing of the dynamic face stimuli was optimally modelled by forward connectivity and information flow from STS to both PC and PM. These somatomotor regions projected onto PFC, the likely neural substrate for integration of information necessary to reach the declarative judgment of emotion intensity. This DCM analysis further revealed that the modulatory effect of posed facial expression on emotional judgments occurred at the level of STS-to-PC connection, not PM-to-PC or PM-to-PFC, which only partly consistent with a sensory-motor facial feedback account of IP judgment bias. Integrating the results of this conventional and DCM analysis of explicit facial emotion intensity judgment, I infer that the neural mechanism underlying IP judgment bias is mediated either via backward projections from amygdala that tune affective perceptual processing or from the influence of precuneus regions (Amaral et al. 1992).

Several limitations of my design and DCM model were addressed here. First, although the expression and gender/age tasks were matched in terms of presented stimuli and required responses they were not equivalent in a

number of aspects. The judgment of emotion was perhaps more difficult, excited different attention/arousal levels, and triggered different degrees of imitating and empathetic proneness. Thus our localizing task (task 1 and Table 5.1) could be contaminated by neural networks reflecting task difficulty, attention/arousal (occipito-temporal visual areas), imitating (pre- and post-central gyri) and social brain (STS). Selection of neural nodes in my DCM model was thus partly based upon prior knowledge where controversial debates still exist (especially STS and fusiform area). Second, my DCM model only hosted 4 neural nodes which was possibly not an exhaustive neural representation of emotion judgment. For example, fusiform area could also participate in the process of emotion intensity judgment. What should be clarified is that DCM itself is not an exclusive account (Friston et al. 2002; Friston et al. 2003). The number of neural nodes which was restricted to four was purely a practical consideration of the validity of algorithm behind DCM (suggested maximum number of nodes is six but most studies take the number of neural nodes no greater than four) and reduction of calculation burden. In other words, DCM inherently welcomes parsimonious model but could possibly sacrifice model complexity. Besides, DCM cannot distinguish direct and indirect connections between distant brain regions. Taking STS as a starting node to receive input of experimental stimuli does not exclude that STS receives input from fusiform area which was a well-recognized region to manage facial information. It is also possible that STS receives joint inputs, say from fusiform area and middle temporal gyrus (MT) which handles the information of moving signals. Since highly reciprocal connectivity has been found in primates brains, the issues of direct and indirection connections is difficult to verify in human brains (Bitan et al. 2005; Bullmore et al. 2000; Chaminade et al. 2003; Mechelli et al. 2002). Although the plausibility of my DCM model was tested explicitly and survived statistical challenge it is still possible that there exists a better model.

5.5 CONCLUSION

In this study, I focused on the declarative appraisal of dynamic facial expressions and its modulation by voluntarily posed facial expressions. In particular I highlight regions involved in the biasing of emotional judgment by voluntarily posed facial emotion expression: The results of conventional voxel-wise analysis revealed reciprocal contributions from amygdala relative to STS and PFC, consistent with affective/cognitive interaction. Constrained connectivity analysis of the same dataset further highlighted changes in the connective strength between STS to PC. Together these findings provide insight into neural substrates shaping behavioural and evaluation of affective social signals of others in relation to the behavioural and emotional stance of the observer. Chapter 3 and 4 are the outward dimension (imitation and controlled expression to others) of emotional facial expression and this chapter highlights the neural mechanisms underpinning the effect that the expressive posers exert on themselves to make emotion intensity judgment.

Chapter 6

Context-sensitive influences of emotion on behaviour: An fMRI study of an eye gaze cued emotional GO/NOGO task

---

6.1 INTRODUCTION

The previous three chapters focus on emotion expression and its behavioural manifestation on the face. In the next two chapters, I address the behavioural influence elicited by emotion on response execution and inhibition using GO/NOGO paradigm.

Emotions are ultimately manifest as behavioural and physiological response tendencies that have been shaped through evolution and individual experience (Davidson et al. 1990; James 1894). In humans, the expression of emotions, particularly in the face, communicates inner feelings (Ekman 1972) and behavioural motives of an individual to conspecifics (Fridlund 1994). The facial expressions of others serve as social feedback cues to regulate directly ongoing behaviour. A smiling face can encourage or reinforce behaviour, while an angry face can demand behavioural modification or inhibition.

The brain mechanism underlying the recognition of facial emotion continues to be a strong focus of interest within affective neuroscience. In contrast, fewer studies in humans have addressed how perceived emotion influences behavioural responses. One methodological approach is the emotional GO/NOGO paradigm which links emotional processing to the execution (GO) and inhibition (NOGO) of behavioural responses. Extant studies of such tasks typically tag emotion valences onto GO and NOGO cues, for example using happy face stimuli to signal GO trials and angry faces to signal NOGO trials, consistent with the theoretical relationship between approach and withdrawal response tendencies and positive and negative emotions. In these studies, the perceived emotion is either concordant or discordant with GO/NOGO contingencies (Hare et al. 2005; Shafritz et al. 2006). This contingent coupling of emotional information with response ensures that these studies probe aspects of emotion regulation and emotion-cognition interaction. However this task design does not permit an independent assessment of emotional influences on response execution and inhibition.

The relationship between positive and negative emotional signals to approach and withdrawal behaviours actually represents an over-simplified dichotomy. Negative emotions, for example fear, may initiate fight, flight or freezing depending upon both the context and individual differences (Bracha 2004). Perceived fear may thus provide a flexible context wherein either response execution or response inhibition is conditionally facilitated. The former suggestion is indirectly supported by animal studies which demonstrated that the exploratory behaviours in rats can be increased rather than decreased by aversive stimulation (Halliday 1966; Russell 1973; Wong et al. 1976), while the latter is inferred from the well-documented phenomenon that fear can instigate freezing, avoidance reaction, submissive posture and immobilization (Misslin 2003). To test these hypotheses in humans, I developed a novel version of emotional GO/NOGO task that uncoupled response selection from emotional processing. I examined the behavioural and neural correlates of this task using functional magnetic resonance imaging (fMRI).

This design introduced fearful and neutral emotional face stimuli within a spatial GO/NOGO paradigm where the eye gaze direction of the face stimuli added a further level of behavioural demand (congruence with imperative cues). Thus, GO and NOGO signals were either concordant or discordant with eye gaze direction. On each trial, the participant fixated on the face stimulus and detected the GO or NOGO cue through peripheral attention. In all, the task embodied a 2 by 2 by 2 factorial design, providing 3 contexts 1) emotion (fearful vs. neutral), 2) cueing congruence (valid vs. invalid) and 3) response requirement (execution vs. inhibition). Valid spatial cueing is a well-established context wherein mental processing is facilitated via congruent spatial attention and interlinked motor pre-programming (Hietanen 1999; Rizzolatti et al. 1987; Rizzolatti et al. 1994; Rosen et al. 1999; Senju et al. 2004; Sheliga et al. 1997; Vecera et al. 2006). The inclusion of this cueing validity dimension within the emotional GO/NOGO task allowed me to test whether the behavioural influences engendered by processing fearful facial expressions were mediated through the same attentional and neural resources as spatial cueing. This design permitted the independent exploration of emotional influences on response execution and inhibition within one experiment.

This specific predictions were as follows: First, behaviourally, the response times (RTs) on fearful GO trials would be faster than on neutral GO trials;

correspondingly errors of commission on fearful NOGO trials would be lower than on neutral NOGO trials. Second, neural activity related to response execution on GO trials (engaging sensorimotor/premotor and anterior cingulate cortices; (Rosen et al. 1999)) would be enhanced by valid spatial cueing and by fearful face stimuli. Third, the 'inhibitory' neural activity during NOGO trials (engaging inferior frontal gyrus; (Konishi et al. 1999)) would also be enhanced in conditions of valid spatial cueing and fearful face stimuli. Last, the behavioural and neural interaction of emotion and cueing validity would reveal further emotion-specific effects on both response execution and inhibition.

6.2 MATERIALS AND METHODS

6.2.1 Subjects, experimental stimuli and tasks

I recruited fifteen female volunteers for the fMRI study (mean age, 24.7 years). Participants were screened to exclude a history or evidence of neurological, medical, or psychological disorder including substance misuse. None of the participants was taking medication. Written informed consent was provided for the study, which was approved by the Local Ethics Committee.

Experimental stimuli consisted of fearful and neutral faces portrayed by 11 male and 11 female models. Each face has 3 different eye gaze positions: central, looking to the left, looking to the right. In total, I constructed 132 different images from 22 different identities (Fig. 6.1 (i) & (ii)). The faces were positioned at the centre of the monitor and subtended 5 x 7.5 degree of visual angle. On each trial, I used either a green dot to signal GO; or a red dot to signal NOGO. The dot was located either at the same or opposite side to the stimulus eye gaze direction, at a visual angle of 4 degrees away from centre and radius 1 degree. Thus, the eye gaze provided valid and invalid spatial cueing of GO and NOGO imperative signal, within 2 emotional contexts: neutral or fearful expression. Each participant was instructed to fixate on the centre of the face stimuli. On fifteen percent of randomly chosen experimental trials the participant was required to identify the emotion and eye gaze direction of the face just viewed, and signal this using a four choice response scale (Fig. 6.1 (iii)). This ensured that the participant attended to each face stimulus. All stimuli, cues and instructions were presented to the participant using an LCD media projector via a screen that which was viewed through a mirror box placed on the MRI headcoil.

Figure 6.1

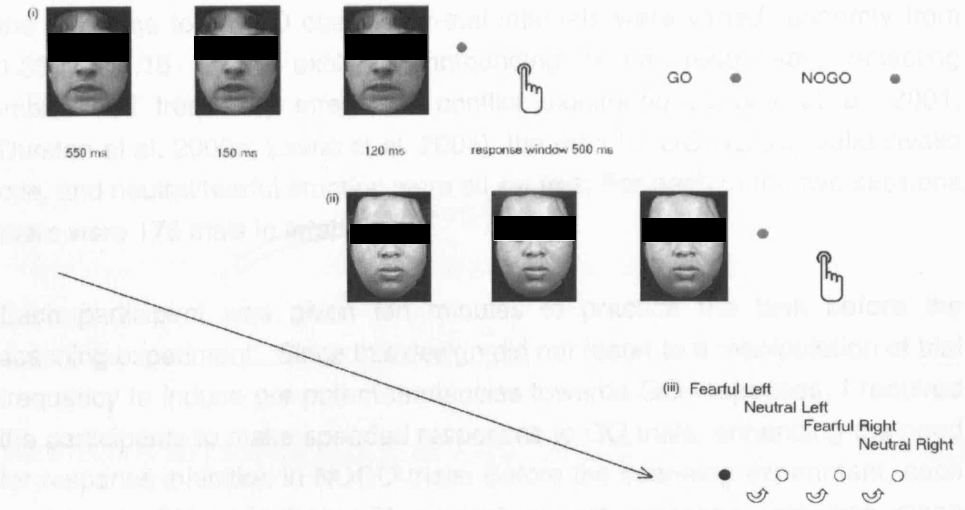

Figure 6.1 Sequence of events in the eye-gaze cued emotion GO NOGO task.
The structure of a single trial includes 4 successive phases: (1) a neutral/fearful face looking to the front (550 ms); (2) the same face as (1) with eye gaze looking to the right or to the left (150 ms); (3) GO or NOGO signal accompanying the face of (2) (120 ms), at either the same (valid cuing) or opposite position (opposite cuing) to the eye gaze direction; (4) responding using right index finger with response window 500 ms.

Illustration of trials:
(i) fearful face, validly cued NOGO trial, (ii) neutral face, invalidly cued GO trial, (iii) fifteen percent trails were followed by a simple judgment to identify the emotion and eye gaze direction on the face the participant just viewed

A 2x2x2 factorial design was adopted with three independent variables: emotions (neutral/fearful), eye gaze cueing validity (valid/invalid), and GO/NOGO. I thus had 8 different classes of trials. The task was performed over two sessions and the trials were organized in a fully randomized way. On each trial, the neutral or fearful face (with forward eye gaze) was presented for 550 ms then immediately followed by the same image with shift in eye gaze (left or right) for another 270 ms (Fig. 6.1 1 (i) & (ii)). The GO/NOGO cues were presented for the last 120ms for the trial at either the same or different side to the eye gaze direction. The brief duration of the GO/NOGO cue is

below the average latency for eye saccades (150 ms; (Carpenter 1988)). The participant was required to press a button quickly to GO cues and to withhold the response to NOGO cues. Inter-trial intervals were varied randomly from 1.35 to 2.15 s. To exclude confounding neural responses, reflecting imbalanced frequency effects or conflict monitoring (Braver et al. 2001; Durston et al. 2002a; Lavric et al. 2004), the ratio for GO/NOGO, valid/invalid cue, and neutral/fearful emotion were all set to 1. For each of the two sessions, there were 176 trials in total.

Each participant was given ten minutes to practice the task before the scanning experiment. Since this design did not resort to a manipulation of trial frequency to induce pre-potent tendencies towards GO responses, I required the participants to make speeded responses to GO trials, enhancing the need for response inhibition in NOGO trials. Before the scanning experiment, each participant achieved above 90 percent correct response rate and mean response time below 350 ms of 30 consecutive trials. Even though the participant was instructed to fixate on the faces, fifteen percent of the experimental trials required the participant to identify the emotion and eye gaze direction of the face just viewed to ensure that she actively processed the facial signals. The overall error rate on this control was 7.3 percent.

6.2.2 fMRI data acquisition

I acquired sequential T2*-weighted echoplanar images (Siemens Sonata, Erlangen, Germany; 1.5Tesla, 32 slices, 3.0 mm thick, TE 0.65 ms, TR 2.08 s, voxel size 4.5x4.5x4.5 mm3). One hundred and eight five whole-brain images were obtained for 9 minutes for each session. The first 6 echoplanar volumes of each session were not analyzed to allow for signal equilibrium. A T1-weighted structural image was obtained for each participant to facilitate anatomical description of individual functional activity after co-registration with fMRI data.

6.2.3 fMRI data analysis

I used SPM5 analysis software on a Matlab platform (Mathworks, Inc., Natick, MA) to analyze acquired fMRI data. Task-related brain activities were identified within the General Linear Model. The 6 movement parameters (3 for translation and 3 for rotation) derived from the realignment process were imported into the design matrix to account for movement-related confounds. Error trials were defined as the excessively slow responses in GO trials

(longer than 500 ms) and adjacent NOGO trials, failed inhibition in NOGO trials and misclassification of emotion and eye gaze direction of the face stimuli. Errors were independently modelled within the design matrix as a regressor of no interest.

I modelled each trial as a unique event, convolved with a canonical haemodynamic basis function and categorized according to each trial type within the analytic design matrix. For individual participant analysis, I constructed four classes of contrasts: (1) main effects of GO and NOGO, (2) comparison of cueing validity for GO and NOGO, (3) emotional influences on GO and NOGO constrained by the results from (1), (4) interaction of emotional effects and cueing validity for GO and NOGO. The interaction analyses allow specific control of emotion effect and cueing effect. For example, "[fearful invalid GO minus fearful valid GO] minus [neural invalid GO minus neutral valid GO]" would cancel differential brain activation by fearful emotion or by cueing validity and reveal unbalanced influence that fearful emotion exerts on cueing validity. Activity across the group was tested within second-level analyses of the above contrasts using simple T-tests for the first three classes and F-tests for the interaction analysis. Voxel-wise statistical threshold was set at $P < 0.001$, uncorrected and extent threshold of three voxels.

6.3 RESULTS

6.3.1 Behavioural Results

I analyzed GO and NOGO trials separately, within the factorial structure of the experimental design. The average reaction time (RT) was 354.4 ms for GO, and the average commission error (ER) was 6.4% for NOGO trials. The average slow GO was 3.2%. A multivariate repeated measures analysis revealed a significant effect of trial condition (4 pairs from emotion and eye gaze validity: fearful valid, fearful invalid, neutral valid, neutral invalid) for both RT (GO trials; $F(3,12) = 13.950$, $P < 0.001$ and ER (NOGO trials; $F(3,12)= 7.330$, $P = 0.005$). Consistent with my predictions, the fearful emotion condition compared with neutral condition was associated with reduced RTs (5 ms difference, $P = 0.192$) for GO and lower ER for NOGO (1 percent difference, $P = 0.048$) trials. Since the reduced GO RTs for fearful emotion did not reach statistical significance, the significant result from above multivariate repeated measurement analysis was at interaction level, see below. Similarly, there was a gain for valid, compared to invalid, eye gaze trials of 12.0 ms ($P = 0.008$) and 19.8 ms ($P < 0.001$) for neutral and fearful emotions respectively. This result also replicated the basic finding that eye gaze engenders a significant spatial cueing effect (Friesen et al. 1998).

Pair-wise comparison analyses revealed that the facilitatory effect of perceived emotional expression was not symmetrical over valid and invalid eye gaze cueing conditions; in other words, there was emotion by cueing interaction: Compared with neutral emotional expressions, fearful face stimuli facilitated GO responses in the valid cueing condition, but not in the invalid cueing condition, by an extra gain of RTs of 9.8 ms ($P = 0.012$). Fearful face stimuli also facilitated NOGO trials in the invalid cueing condition, but not in the valid cueing condition, by a reduction of ER by 1.4 percent ($P = 0.007$). The emotional GO/NOGO response was therefore modulated by the context provided by eye gaze cue. All the t-tests were two-tailed and the details of behavioural results are summarized in Table 6.1.

Table 6.1 The means and paired-sample t-tests of response times (RTs) and commission errors for GO and NOGO trials

Emotion	Cueing	SD	t	df	P value

GO: Reaction Times		*Mean (ms)*				
Neutral	Overall	357.3	34.5			
Fearful	Overall	351.7	32.6			
Neutral	Valid	351.3	36.5			
Neutral	Invalid	363.3	33.8			
Fearful	Valid	341.5	31.5			
Fearful	Invalid	361.3	34.4			
Pairwise Comparison						
Neutral – Fearful	Overall	5.6	16	1.370	14	0.192
Neutral	Invalid – Valid	12.0	15.1	3.090	14	0.008*
Fearful	Invalid – Valid	19.8	15.5	4.955	14	< 0.001*
Neutral - Fearful	Valid	9.8	13.1	2.889	14	0.012*
Neutral – Fearful	Invalid	2.0	22.1	0.347	14	0.734
NOGO: Commissions Errors		*Mean (%)*				
Neutral	Overall	6.9	3.4			
Fearful	Overall	5.9	2.3			
Neutral	Valid	6.8	3.1			
Neutral	Invalid	7.0	4.2			
Fearful	Valid	6.2	2.3			
Fearful	Invalid	5.6	3.0			
Pairwise Comparison						
Neutral – Fearful	Overall	1.0	1.8	2.162	14	0.048*
Neutral	Invalid – Valid	0.2	2.6	0.222	14	0.827
Fearful	Invalid – Valid	-0.6	2.6	-0.888	14	0.390
Neutral - Fearful	Valid	0.6	2.8	0.845	14	0.413
Neutral – Fearful	Invalid	1.4	1.7	3.153	14	0.007*

* indicates statistical significance ($P < 0.05$, 2-tailed t-test)

6.3.2 Functional imaging results

6.3.2.1 Main effects of GO and NOGO

GO minus NOGO

Across GO trials, the execution of speeded responses enhanced activity over

a distributed neural system covering motor-related regions (including precentral gyrus and supplementary motor area), frontostriatal pathways, anterior cingulate cortex (ACC), inferior parietal lobule, insula and thalamus; see Figure 6.2 and Table 6.2.

NOGO minus GO

In contrast to GO trials, response inhibition, NOGO, showed differential brain activation within several midline structures, including rostral ACC, precuneus, cuneus and posterior cingulate cortex. NOGO trials also engaged bilateral inferior frontal gyrus (Brodmann Area (BA) 47), posterior-lateral orbitofrontal cortices, middle temporal gyrus, angular gyrus and pons; see Figure 6.2 and Table 6.3.

Table 6.2 Brain activation for the contrast of GO minus NOGO

Brain area (BA) [a]	Stereotaxic coordinates [b]			Z score
Precentral Gyrus (4/L)	-38	-19	53	6.96
Postcentral Gyrus (3/L)	-34	-30	60	5.2
Middle Frontal Gyrus (9/L)	-55	7	25	3.88
(8/R)	48	10	40	3.69
Medial Frontal Gyrus (6/L)	-4	-7	63	4.54
Anterior Cingulate Cortex (24/32L)	-8	0	42	4.89
Inferior Parietal Lobule (40/L)	-42	-40	50	5.07
(40/R)	36	-44	45	4.96
Insula (13/L)	-44	-2	7	4.48
	-44	-22	18	4.45
Caudate Head (L)	-8	6	3	4.18
(R)	6	14	3	4.65
Thalamus (Medial Dorsal Nucleus/L)	-10	-15	8	4.06
Thalamus (Pulvinar/L)	-20	-25	12	3.9
Cerebellum (Semi-Lunar Lobule/R)	18	-64	-37	4.87
Cerebellum (Declive/R)	24	-59	-17	5.27

[a] BA, Brodmann designation of cortical areas

[b] Values represent the stereotaxic location of voxel maxima above uncorrected threshold ($P < 0.001$)

Figure 6.2

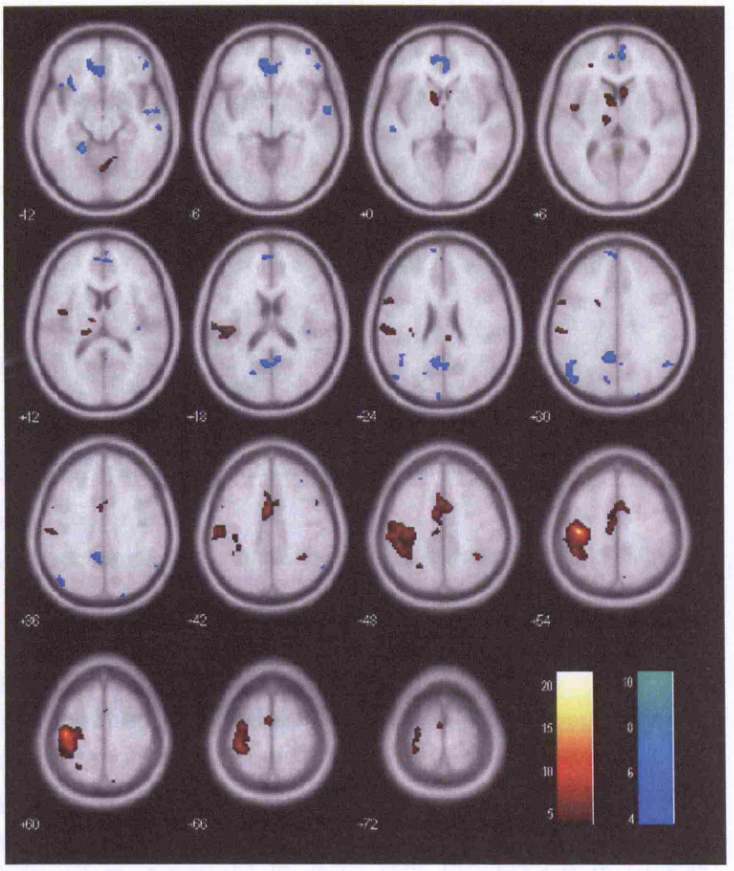

Figure 6.2 Brain regions showing significant activities for the main effect of GO and NOGO conditions. Bold contrasts of GO (hot) and NOGO (winter) are superimposed on a T1 structural image in axial sections from z = -12 to z = 72.

Table 6.3 Brain activation for the contrast of NOGO minus GO

Brain area (BA) [a]	Stereotaxic coordinates [b]			Z score
Medial Frontal Gyrus (10/L)	-10	61	21	3.84
(10/R)	4	51	7	4.25
Inferior Frontal Gyrus (47/L)	-38	24	-16	3.98
(47/R)	48	42	-11	3.71
Orbitofontal cortices (47/L)	-30	17	-14	3.76
(47/R)	28	14	-23	4.45
Anterior Cingulate Cortex (24/32/L)	-10	43	-4	4.55
(24/32/R)	4	43	-2	4.21
Angular Gyrus (39/L)	-44	-72	29	4.75
(39/R)	51	-55	29	3.75
Middle Temporal Gyrus (22/L)	-53	-23	-1	4.29
(22/R)	59	-6	-5	4.99

Parahippocampal Gyrus (37/L)	-22	-45	-8	5.45
Precuneus (31/L)	-18	-67	22	4.34
(23/R)	2	-61	23	4.43
Posterior Cingulate Cortex (30/R)	10	-51	19	3.48
(31/L)	-8	-57	21	4.14
(31/R)	4	-55	29	3.38
Cuneus (19/L)	-4	-92	29	3.56
(19/R)	22	-90	30	4.19
Insula (13/R)	38	-19	14	3.67
Pons (R)	6	-35	-34	3.55

[a] BA, Brodmann designation of cortical areas

[b] Values represent the stereotaxic location of voxel maxima above uncorrected threshold ($P < 0.001$)

6.3.2.2 Emotional effects on GO and NOGO processing

To focus on investigating the modulatory effects of emotion on GO and NOGO processes, I eliminated extraneous confounds related to emotion processing *per se* by constructing an inclusive mask, derived from the main effects of GO and NOGO processing. I set the statistical threshold of this mask at uncorrected $P < 0.005$. It is important to note that the contrasts of the inclusive mask and the following contrasts were orthogonal. This analysis was thus highly stringent (at an approximate threshold level of P value below 0.001*0.005).

Fearful GO compared to Neutral GO

Enhanced activity was observed for trials requiring GO responses in the context of fear processing in several motor-related regions, including precentral gyrus and medial frontal gyrus, and in the postcentral gyrus. 'Fearful' GO trials also enhanced brain activity within the superior parietal lobule; see Table 6.4. In contrast, there was an attenuation of activity within thalamus and cerebellum (Table 6.4). For neither of the above two contrasts, were I able to demonstrate a significant correlation between activity at these loci and RT or differences in RT.

Fearful NOGO compared to Neutral NOGO

In the case of NOGO trials, the processing of fearful facial expressions (compared to neutral expressions) was associated with an enhancement of activity within the inferior frontal gyrus (BA 47), angular gyrus (BA 39) and posterior cingulate gyrus. Concurrently, there was an attenuation of activity

within the parahippocampal gyrus (Table 6.4).

Table 6.4 Brain regions showing different activation between fearful and neutral emotions of GO and NOGO trials

Brain area (BA) [a]	Stereotaxic coordinates [b]			Z score
	GO [c]: Contrast Fearful > Neutral			
Precentral Gyrus (6/L)	-32	-9	59	2.61
Medial Frontal Gyrus (6/L)	-8	-13	49	2.69
Superior Parietal Lobule (7/L)	-24	-51	60	3
Postcentral Gyrus (40/L)	-40	-36	55	2.73
	GO [c]: Contrast Neutral > Fearful			
Thalamus (L)	-14	-15	6	3.32
	-14	-21	8	2.73
Cerebellum (R)	18	-48	-23	3.43
	NOGO [d]: Contrast Fearful > Neutral			
Inferior Frontal Gyrus (47/L)	-24	-51	60	3.64
Temporal Pole (38/L)	-40	16	-28	2.84
Angular Gyrus (39/R)	48	-57	29	2.64
Posterior Cingulate Gyrus (31/L)	-8	-51	23	2.60
	NOGO [d]: Contrast Neutral > Fearful			
Parahippocampal Gyrus (37/L)	-22	-45	-10	3.93

[a] BA, Brodmann designation of cortical areas

[b] Values represent the stereotaxic location of voxel maxima above uncorrected threshold ($P < 0.005$)

[c] Small volume correction was calculated using the contrast of GO minus NOGO (uncorrected, $P < 0.001$) as a mask.

[d] Small volume correction was calculated using the contrast of NOGO minus GO (uncorrected, $P < 0.001$) as a mask.

6.3.2.3 Comparison of cueing validity for GO and NOGO

This experimental design was fully balanced, allowing for the effects of emotion and response execution to be subtracted out. However, I still observed differential activation above and beyond these main effects attributable to differential influences of spatial cueing validity on GO and NOGO trials.

Valid GO compared to Invalid GO

'Valid' GO trials where stimulus eye gaze direction was concordant with the location of GO cues were associated with greater activation within visual associative cortices and frontal areas, which partially overlapped with the main effect of GO trial processing. These regions included primary visual cortices (cuneus and lingual gyrus; BA 18), middle occipital gyrus (BA 37), medial frontal gyrus (BA 6), middle frontal gyrus (BA 6 and BA 10) and precentral gyrus (BA 4). In addition, enhanced activity was also apparent within cingulate cortices notably dorsal (BA 32) and subgenual ACC (BA 25) and the cingulate gyrus (BA 31). Valid cuing GO also activated other motor related regions, including cerebellum, putamen and thalamus; see Table 5 and Figure 3. In contrast, invalid spatial cueing for GO trials was associated with relatively greater activity within the body of the caudate nucleus and the fusiform gyrus; see Figure 6.3 and Table 6.5.

Figure 6.3

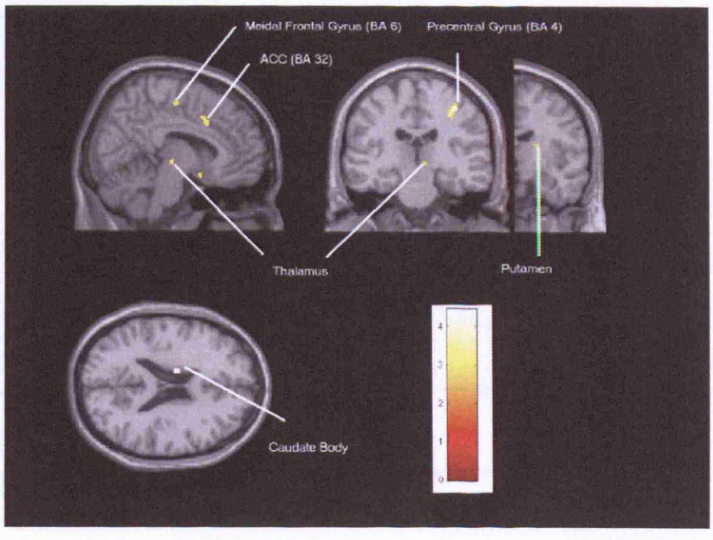

Figure 6.3 Brain regions showing significant difference of cuing validity in GO trials.
For coronal sections, right is right and left is left. For axial sections, down is right and up is left.

Upper: The contrast of valid cue greater than invalid cue.
Lower: The contrast of invalid cue greater than valid cue.

Table 6.5 Brain regions showing different activation between valid and invalid cuing conditions of GO trials

Brain area (BA) [a]	Stereotaxic coordinates [b]			Z score
	Contrast Valid > Invalid			
Precentral Gyrus (4/R)	38	-19	49	4.35
Middle Frontal Gyrus (10/L)	-34	52	-6	3.81
(10/R)	46	46	-4	4.21
Middle Frontal Gyrus (6/L)	-48	0	41	3.36
(6/R)	36	12	51	4.05
(6/R)	38	4	40	3.71
Medial Frontal Gyrus (6/R)	10	-13	52	3.94
Anterior Cingulate Cortex (32/R)	6	14	38	3.77
Subcallosal Gyrus (25/R)	8	7	-12	3.47
Cingulate Gyrus (31/R)	16	-41	44	3.66
Cuneus (18/L)	-26	-95	1	3.37
(18/R)	18	-57	18	3.92
(19/R)	14	-69	26	3.54
Lingual Gyrus (18/R)	32	-74	-5	4.12
Middle Occipital Gyrus (37/R)	38	-66	2	3.32
Cerebellum, Uvula (L)	-32	-77	-25	3.63
Putamen (R)	22	-9	15	3.29
Thalamus (R)	8	-19	-1	3.55
	Contrast Invalid > Valid			
Caudate Body (L)	-12	-5	21	3.45
Fusiform Gyrus (20/R)	46	-32	-17	3.39

[a] BA, Brodmann designation of cortical areas

[b] Values represent the stereotaxic location of voxel maxima above uncorrected threshold ($P < 0.001$)

Valid NOGO compared to Invalid NOGO

Valid NOGO trials, where stimulus eye gaze direction was concordant with the location of NOGO cues, in contrast to invalid NOGO trials, evoked an enhancement of BOLD signal within bilateral inferior frontal gyri (BA 47). Enhanced activity within this region was observed in the main effect of NOGO processing. In addition, valid NOGO trials evoked enhanced brain activity within the ACC, precentral gyrus, parahippocampal gyrus, cuneus, amygdala and cerebellum; see Figure 6.4 and Table 6.6. Correspondingly there was greater activity for spatially incongruent, invalid NOGO trials within regions that partially overlapped with activity changes evoked as a main effect of NOGO. These included the angular gyrus, insula and middle temporal gyrus; see Figure 6.4 and Table 6.6.

Figure 6.4

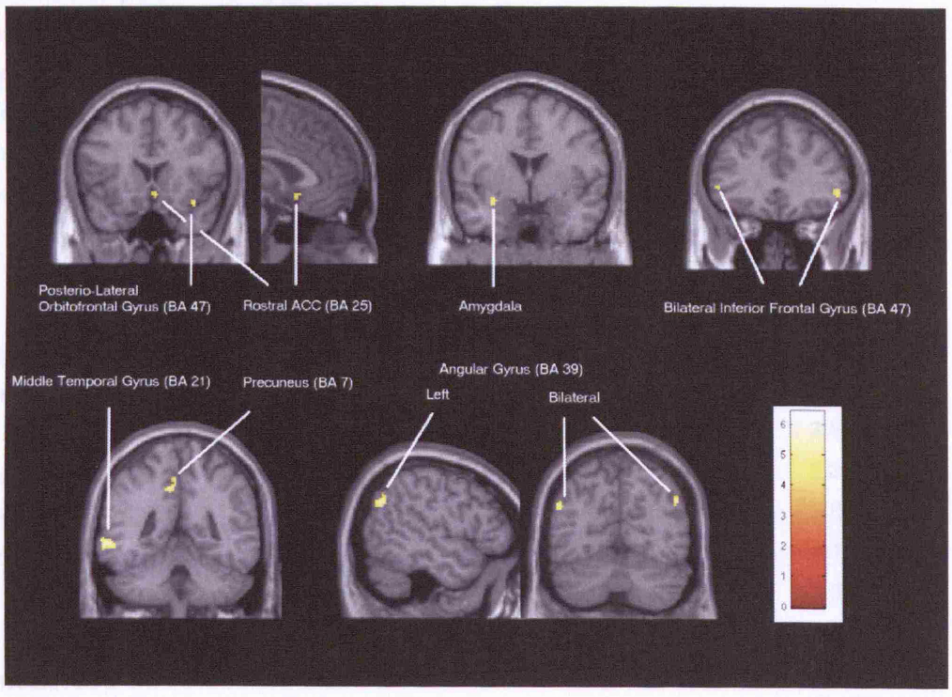

Figure 6.4 Brain regions showing significant difference of cuing validity in NOGO trials.

For coronal sections, right is right and left is left.

Upper: The contrast of valid cue greater than invalid cue.

Lower: The contrast of invalid cue greater than valid cue.

Table 6.6 Brain regions showing different activation between valid and invalid cuing conditions of NOGO trials

Brain area (BA) [a]	Stereotaxic coordinates [b]			Z score
	Contrast Valid > Invalid			
Precentral Gyrus (4/L)	-32	-17	52	3.54
Inferior Frontal Gyrus (47/L)	-51	33	0	3.33
Inferior Frontal Gyrus (47/R)	51	33	-3	3.54
	38	17	-16	3.63
Anterior Cingulate Cortex (25/R)	4	17	-8	3.4
Parahippocampal Gyrus (36/L)	-28	-15	-21	4.29
Cuneus (18/L)	-2	-91	12	3.72
Insula (13/L)	-46	-7	17	3.4
Dorsolateral Amygdala (L)	-32	1	-12	3.75
Cerebellum, Pyramis (R)	12	-79	-28	3.53
Cerebellum, Culmen (L)	-10	-55	-7	4.32
Cerebellum, Tonsil (R)	-6	-58	-34	3.39
	Contrast Invalid > Valid			
Middle Frontal Gyrus (9/R)	44	34	26	3.78
Angular Gyrus (39/L)	-50	-61	31	3.82
(39/R)	50	-62	34	3.69
Supramarginal Gyrus (40/L)	-61	-51	32	3.31
Precuneus (7/L)	-4	-38	46	3.87
Middle Temporal Gyrus (21/L)	-61	-45	-3	4.19
(21/L)	-63	-29	-5	3.52
Superior Occipital Gyrus (19/L)	-38	-78	37	3.91
Insula (13/R)	38	-7	11	3.63

[a] BA, Brodmann designation of cortical areas

[b] Values represent the stereotaxic location of voxel maxima above uncorrected threshold ($P < 0.001$)

6.3.2.4 Interaction of emotional processing and cueing validity for GO and NOGO trials

I next explored the interaction between emotional processing and cueing validity using the following two analytic contrasts; [valid fearful GO – invalid fearful GO] minus [valid neutral GO – invalid neutral GO] and [valid fearful NOGO – invalid fearful NOGO] minus [valid neutral NOGO – invalid neutral NOGO]. I used F-tests of the data (uncorrected P value < 0.001) to delineate brain regions showing activity changes that reflected these interactions.

For GO trials, the activity within inferior frontal gyrus (BA 44), bilateral putamen, middle occipital gyrus and cerebellum tracked the interaction between emotional processing and eye gaze-cueing. For NOGO trials, corresponding activity changes were observed within insula, caudate body, middle temporal gyrus, pregenual ACC (BA 33), superior frontal gyrus, inferior parietal lobule and parahippocampal gyrus; see Figure 6.5 and Table 6.7.

Figure 6.5

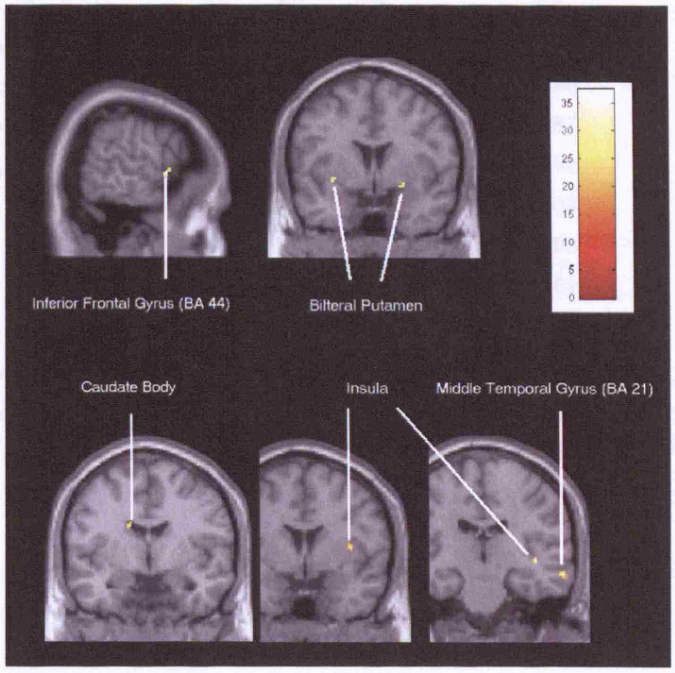

Figure 6.5 Brain regions showing 2-way interaction (2 emotions X 2 cue validity) for GO and NOGO trials.
For coronal sections, right is right and left is left.
Upper: Brain regions showing 2-way interaction for GO trials.
Lower: Brain regions showing 2-way interaction for NOGO trials.

Table 6.7 Brain regions showing 2-way interaction (2 emotions X cue-validity) for GO and NOGO trials

Brain area (BA) [a]	Stereotaxic coordinates [b]			Z score
	2-way interaction for GO trials			
Inferior Frontal Gyrus (44/L)	-59	8	5	3.67
Middle Occipital Gyrus (18/R)	34	-93	5	3.32
Putamen (L)	-32	2	-3	3.4
Putamen (R)	22	2	-8	3.34
Cerebellum, Culmen (R)	4	-61	-19	3.46
	2-way interaction for NOGO trials			
Anterior Cingulate (33/L)	-8	20	19	4
Superior Frontal Gyrus (10/L)	-12	60	25	3.3
Inferior Parietal Lobule (40/R)	53	-38	46	3.51
Middle Temporal Gyrus (21/R)	63	-20	-11	3.98
Parahippocampal Gyrus (35/R)	20	-32	-10	3.87
Middle Occipital Gyrus (19/R)	32	-93	8	3.82
Insula (R)	42	-19	-1	4.04
	38	4	9	3.63
Caudate Body (L)	-14	-3	24	3.62

[a] BA, Brodmann designation of cortical areas

[b] Values represent the stereotaxic location of voxel maxima above uncorrected threshold ($P < 0.001$)

6.4 DISCUSSION

I developed an eye gaze cued emotion GO/NOGO task to investigate an important though neglected theme within emotional neuroscience, namely the influence of affective processing on response execution and inhibition (James 1894). Fear was selected as this target emotion and spatial cueing of the imperative stimulus provided non-emotional comparison condition that also engages attentional resources. The paradigm was a balanced factorial design that excluded the potential confound of stimulus frequency (oddball) (Braver et al. 2001; Casey et al. 2001; de Zubicaray et al. 2000; Durston et al. 2002a; Lavric et al. 2004). This behavioural and neuroimaging results were grossly concordant with this prediction that perceived fearful emotion enhances both response execution (GO) and inhibition (NOGO). Since response execution and inhibition are two distinct and incompatible psychological constructs, the results argue against stereotyped approach/withdrawal response to perceived emotion.

Behaviourally, there were significant differences across conditions in both reaction times (for GO trials) and commission errors (for NOGO trials). This data robustly confirmed that eye gaze represents a reliable visuo-spatial cue (Friesen & Kingstone 1998) facilitating the appropriate behavioural response execution (GO) and showed that this facilitation was further enhanced by the concurrent perception of a fearful emotional expression. There was, moreover, an intriguing asymmetry in the observed behavioural interaction between emotion and cueing congruency on GO and NOGO trials. This observation argues against a non-specific mechanism, such as elevated attention or arousal, in mediating the emotional facilitation of behaviour since this would have impact equally on trials with valid and invalid spatial cues. Following the same logic, the observed interaction also argues against an unconditional pre-activation of either an approach or a withdrawal system by the perception of facial expressions of fear, implying instead that the behavioural consequence of perceiving fearful emotional expressions is dependent upon both the response requirement of (GO versus NOGO) and cueing congruency (valid versus invalid). These findings highlight the richness of interplay between cognitive and affective processing streams toward the control of stimulus-driven behaviour.

This fMRI results further confirmed that both fearful emotional and valid spatial (eye gaze) cueing conditions provide contexts that bias the magnitude and pattern of neural responses leading to either response execution or response inhibition. Across GO trials, the presence of fear stimuli generally enhanced activity within somatomotor cortices and the supplementary motor area (SMA). A similar effect was observed with spatial priming on GO trials, where valid (congruent) cues to the imperative stimulus enhance activity within somatomotor cortices, SMA, cingulate motor area and the putamen. Similarly across NOGO trials, the presence of fear stimuli or valid eye gaze cues enhanced neural activity within the inferior frontal gyrus (BA 47), a brain region implicated frequently in response inhibition GO/NOGO studies (Durston et al. 2002b; Matsubara et al. 2004; Menon et al. 2001; Nakata et al. 2005; Schulz et al. 2005). An adjacent cluster of activity, also within BA 47 extending into posterolateral orbitofrontal cortex, was observed as a main effect of response inhibition (NOGO minus GO trials). This region is implicated in both action selection in reversal (requiring a suppression of previously rewarded responses) and response inhibition during GO/NOGO task performance (Elliott et al. 2000; Horn et al. 2003). Interestingly in this task, the activity within lateral orbitofrontal cortex reflected the spatial congruency, but did not differentiate between the presence of fearful compared to neutral expressions in NOGO trials.

Emotional material may enhance visual perception and thus promote motoric responsivity, possibly through direct access to attention-motor pathways (Armony et al. 2002; Mogg et al. 1997; Ohman et al. 2001; Rizzolatti et al. 1994; Vuilleumier 2005). In other words, the emotional facilitation of behaviour may arise from activation of hard wired emotion-related response patterns and/or the capture of attention. This behavioural data demonstrated that the perception of fearful emotional expressions facilitated GO response in valid cueing condition (not invalid), and fearful emotion facilitated NOGO in invalid cueing condition (not valid). Consequently, I was able to test for a specific emotion-cueing interaction at the neural level. This interaction analysis was of particular interest since the behavioural difference of GO RTs and NOGO error rates were reflected at interaction level. The interaction analysis revealed activity within inferior frontal gyrus (BA 44) and bilateral putamen demonstrated emotion-by-cue interaction on GO trials. These regions are likely to support high level sensorimotor integration towards facilitatory motor control (Binkofski et al. 2004; Brown et al. 1997). The interaction between

emotional processing and spatial congruence during inhibitory NOGO trials presented an almost competitive effect. Brain regions associated with this interaction, including frontal pole, pregenual anterior cingulate gyrus, inferior parietal lobule, insula and caudate nucleus reflect the intricate engagement of sensory, emotion, motor and cognitive processes (Brown et al. 1997; Gray et al. 2002; Mattler et al. 2006). It is inappropriate to over-interpret the functional contributions and components of this matrix of NOGO related activity without further empirical data. Nevertheless the observation highlights the distributed complexity of behavioural control of response inhibition, an observation that may underlie patterns of clinical impairment observed in association with diffuse brain injury or neurodevelopmental perturbation.

Fundamental to this study was the use of face stimuli, potent social cues, both in spatial validity cueing and in providing emotional influence on the execution and inhibition of responses. A previous neuroimaging study contrasted the different neural correlates underlying the automatic orientating of attention to social and symbolic cues (Heinen et al. 2006). Eye gaze was the social orienting cue, evoking enhanced activation predominantly within visual associative cortices, including medial and inferior occipital gyri. Even within this own data, this pattern is notably distinct from the network of regions that reflected the emotion-by-cue interaction. Further, I demonstrate that the functional neuroanatomy mediating the interaction between emotional and eye gaze cues for GO and NOGO responses are non-overlapping, indicating that the mediation of facilitatory emotional influences embodies a goal-oriented neural specificity, instead of being a product of a generalized factor, for example spatial or social attention.

6.5 CONCLUSION

This study is distinct from investigations of the association between approach and withdrawal behaviours with different emotional states, for which there are data relating to hemispheric asymmetry (Davidson et al. 1990; Fox 1991). This design investigated the incidental influence of perceived emotion on cued responses, whereas in the human literature at least, approach and withdrawal tendencies are typically framed within context of subjective emotional experience. However the data do raise some questions in relation to broader areas of affective behaviour. This behavioural and fMRI analyses indicate that the perception of fearful emotion enhances neural responses dedicated to both response execution (GO) and inhibition (NOGO) (without marked lateralization of neural activity). I further revealed and dissociated interactions between emotional processing and spatial cueing on response execution and inhibition. The results implied that perceived fearful emotion provides an ambiguously flexible emotional/social challenge, to which implicit responsivity is shaped at both neural and behavioural levels by concurrent contextual demands of response requirement and spatial priming.

Chapter 7

Testing emotional influences on behaviour: An fMRI study of a bimanual GO/NOGO task during sustained affective states

---

7.1 INTRODUCTION

Complementary to chapter 6, which explores the influences of observed emotions on the observer's own behaviour; this chapter examines the influence of sustained affective states on behavioural (GO/NOGO) performance.

Positive and negative affective states have been linked to approach and withdrawal behaviours with corresponding neural substrates. The differential engagement of these facilitatory and inhibitory motivational systems is proposed to account for asymmetry in emotion-related brain activity (observed especially during electroencephalographic (EEG) studies) (Davidson 1995; Davidson et al. 1990). The extension of this model has been influential in accounting for neurobiological mechanisms underlying personality, affective disposition, psychopathology, and trait/state reactions to emotion- and motivation- related constructs (Coan et al. 2004; Davidson et al. 2000). However, adaptive social and motivational behaviours are also characterized by an ability to overcome stereotyped reactions and response patterns, permitting the expression of experiential learning in behavioural flexibility. Emerging evidence indicates a greater complexity to the relationship between discrete emotional states and response tendencies indicating the independence within emotional brain systems of dichotomized motivational approach/withdrawal mechanisms and positive/negative affective representations (Harmon-Jones et al. 1998; Wacker et al. 2003).

The conceptual framework of Davidson, accounting for lateralization of fronto-temporal activity (notably EEG alpha power), proposes that the subjective experience of affective valence maps onto approach and withdrawal responses. However this model does not especially address other dimensions of emotional processing, including the perception of emotion in others. Frontal EEG asymmetry may therefore relate to circumscribed aspects of affective regulatory processing rather than extending to all emotion-contingent behavioural responses (Davidson 1995). A parallel account of emotion-related response tendencies proposed by

Gray (Gray et al. 2000), differentiates behavioural activation (BAS), behavioural inhibition (BIS) and fight-flight freezing systems (FFFS). Gray's hypothesis proposes the flexible differential engagement of responses in situations where there is competition between mutually incompatible goals, for example when approaching a source of danger under a contextual requirement to achieve reward.

Chapter 6 has illustrated a study that provides insight into the influences of emotional processing on behaviour. I observed that the perception of fearful emotional expressions modulates motor responses during a GO/NOGO paradigm in a manner inconsistent with predicted approach/withdrawal response tendencies. Instead, emotion perception conditionally facilitated two incompatible mental constructs – response execution (GO) and response inhibition (NOGO). These data suggest emotion to be a mental construct that flexibly exerts a behavioural influence beyond deterministic pre-programming. This finding is intriguing in the light of the close relationship between emotion and physiological resource mobilization, as shaped through evolution (James 1894). However, I did not observe an associated lateralization of brain activity as perhaps predicted by Davidson's model of motivational engagement, and, because this GO/NOGO paradigm did not relate directly to reward seeking and punishment avoidance, the findings could not be interpreted within Gray's BAS/BIS account. In the present study, I extended this previous work (behaviour modulation through the perception of emotion; chapter 6), to investigate how induced sustained affective states influence behaviours (behaviour modulation through the induction and experience of emotion).

Pertinent to this *motivation directional* model is the *valence hypothesis* of emotion (Demaree et al. 2005), which suggests that the left and right hemispheres differentially deal with positive emotion and negative emotion. In contrast, the *right hemisphere hypothesis* proposes that the right hemisphere is dominant for emotion processing (Borod 1992; Hagemann et al. 2005; Heller et al. 1998). Although meta-analyses of neuroimaging studies generally failed to support either discourse (Phan et al. 2002; Wager et al. 2003), it is acknowledged that only few imaging studies explicitly test for condition by hemisphere interactions in either the design or the analysis (Baas et al. 2004). Besides, evidence suggests that emotion-related asymmetry manifests at only part of a widely-distributed emotion network

and, consequently is more robust for some, not for all, emotion-related constructs (Borod 1992; Wager et al. 2003). This study explored the laterality of emotional processing by introducing a lateralized response demand (bimanual finger presses) in the experimental design.

I developed another novel version of an emotional GO/NOGO task in which extended presentations of emotional stimuli were used to induce sustained affective states while participants performed a GO/NOGO task (Sutton et al. 1997). I examined the behavioural and neural correlates of this task using functional magnetic resonance imaging (fMRI). This design included happy, fearful and neutral emotional face stimuli, and the imperative GO/NOGO signals were present at either right or left peripheral visual field. On each trial, the participant fixated on the face stimulus to initiate and facilitate the generation and induction of discrete emotions, and detected the GO or NOGO cue via peripheral attention. The participants were required to respond using left index finger to left GO cues and right index finger to right GO cues. This bimanual design further enabled me to explore potential asymmetry in emotional influences on behavioural responses (see below). In all, the task embodied a 3 by 2 by 2 factorial design, providing 3 contexts: 1) emotion (happy vs. fearful vs. neutral), 2) cueing position and response sides (right vs. left) and 3) response requirement (execution vs. inhibition).

A priori knowledge regarding the laterality activity associated with simple finger press responses (in contrast to the performance of complex motor sequences or responses requiring bimanual coordination) is central to the design of this study (Gerloff et al. 2002; Serrien et al. 2006; Solodkin et al. 2001). The contrast of left GO/NOGO minus right GO/NOGO (or right minus left) was anticipated to demonstrate lateralization in corresponding activity patterns with one brain hemisphere showing increased and the other decreased activation. I examined the lateralization of emotional influences on response by contrasting left and right GO and NOGO responses across emotional conditions (abbreviated as LR_GO and LR_NOGO or RL_GO and RL_NOGO in the subsequent text). This approach conveys two crucial advantages: First, the confounding neural correlates relating to the main effect of emotional processing are subtracted out. Second, the emotional influence on each hemisphere during both response execution and inhibition is revealed through the interaction between emotion and response sides. To

clarify the second point, I illustrate nine possible brain response patterns in Figure 7.1.

In Figure 7.1, the lines represent the LR contrast (either GO or NOGO) in neutral (blue) and emotional (red) states. Induced emotional states, when compared with neutral states, may influence the activity within each hemisphere in three possible ways: as a significant increase, a significant decrease or without a significant change of neural responses. I thus derived nine (3x3) different inter-hemispheric modes of emotion influence on activity associated with the lateralized GO/NOGO task. In Figure 7.1, Mode 1 represents the enhancement of neural responses within both hemispheres; while Mode 9 represents bilateral attenuation of activity. Modes 2, 4, 6 and 8 indicate that the emotional influence is unilateral whereas Modes 3 and 7 indicate an asymmetrical effect with one hemisphere showing increased and the other decreased brain activity.

In line with my previous study (chapter 6); I predicted that both positive and negative affective states can facilitate motor-related neural circuitry. This prediction is broadly in accordance with previous observations of non-specific somatosensory cortex engagement during mood induction states across different emotions (Damasio et al. 2000). When considering the interaction between emotion and response sides, the neural response pattern compatible with the *right hemisphere hypothesis* corresponds to Modes 2 and/or 3 across fearful and happy emotional states; while the neural response pattern supporting the *valence hypothesis* corresponds to Modes 2 and 3 during the experience of fearful emotions and Modes 4 and 7 for happy emotions.

Figure 7.1

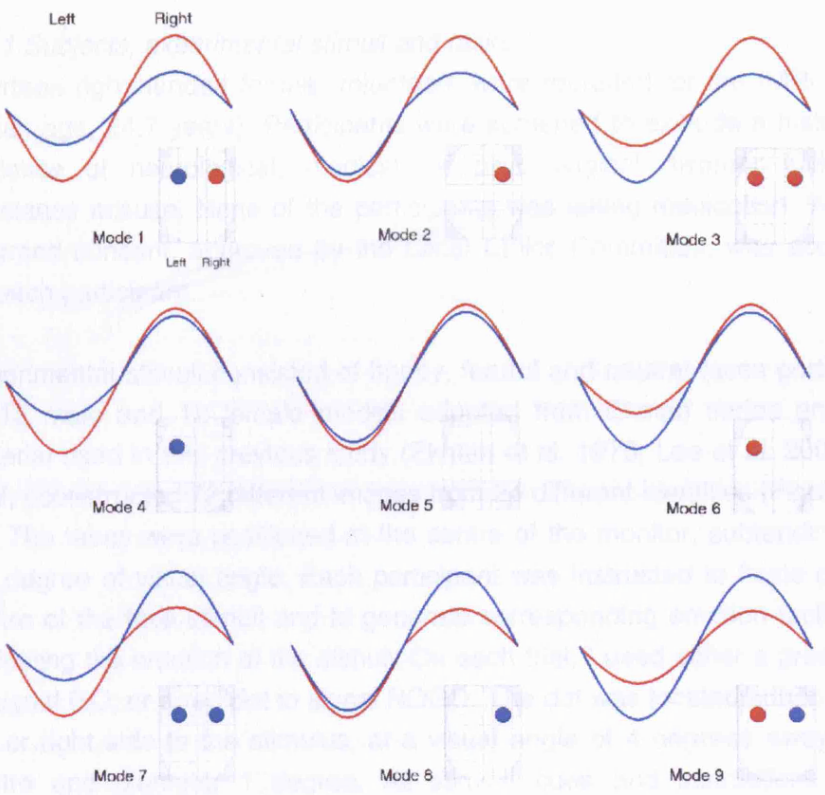

Figure 7.1 Illustration of different asymmetry patterns pertinent to emotion modulation.
The blue and red curves respectively stand for neural responses (ex. from the contrast of Left GO minus Right GO so that right side is positive and left side is negative) in neutral and emotional state. Compared with neutral state, the emotion influence on each hemisphere has 3 possibilities: significant increase, significant decrease or without significant change of neural responses. There are thus 3*3 (=9) different inter-hemispheric modes of emotion influence. Compared to neutral emotion, Mode 1 represents enhancement of neural responses at both hemisphere; while Mode 9 represents bilateral attenuation. Mode 2, 4, 6 and 8 indicate that the emotion influence is unilateral; and, Mode 3 and 7 indicate asymmetrical impact with one hemisphere showing increased and the other decreased brain activity.
The red and blue dots on the glass brain represent the expected brain map derived from subsequent contrast of "emotional state minus neutral state". For example, Mode 3 highlights a situation where emotional state exerts enhanced neural response at right hemisphere and attenuated neural response at left hemisphere. Calculation of the contrast "emotional minus neutral" engenders a brain map with bilateral positivity.

7.2 MATERIALS AND METHODS

7.2.1 Subjects, experimental stimuli and tasks

Fourteen right-handed female volunteers were recruited for the fMRI study (mean age, 24.7 years). Participants were screened to exclude a history or evidence of neurological, medical, or psychological disorder including substance misuse. None of the participants was taking medication. Written informed consent, approved by the Local Ethics Committee, was acquired for each participant.

Experimental stimuli consisted of happy, fearful and neutral faces portrayed by 12 male and 12 female models adopted from Ekman series and the material used in this previous study (Ekman et al. 1975; Lee et al. 2006). In total, I constructed 72 different images from 24 different identities (Figure 7.2 (i)). The faces were positioned at the centre of the monitor, subtending 5 x 7.5 degree of visual angle. Each participant was instructed to fixate on the centre of the face stimuli and to generate corresponding emotion facilitated by feeling the emotion of the stimuli. On each trial, I used either a green dot to signal GO; or a red dot to signal NOGO. The dot was located either at the left or right side to the stimulus, at a visual angle of 4 degrees away from centre and diameter 1 degree. All stimuli, cues and instructions were presented to the participant using an LCD media projector via a screen that was viewed through a mirror box placed on the MRI headcoil.

A 3x2x2 factorial design was constructed with 3 independent variables: emotions to be felt and generated (neutral/happy/fearful), response sides (left/right), and GO/NOGO. The task was performed over two sessions and the GO/NOGO trials were organized in a pseudo-randomized way so that the trial number was controlled for across each condition. The participant was instructed to engender a subjective emotional state corresponding to the viewed face through empathetic feeling, and while performing the task was required to make rapid button press responses to GO cues and to withhold responses to NOGO cues GO responses were made with the left index finger in response to left GO cues and right index finger to right GO cues (Figure 7.2 (ii)). In summary, the GO/NOGO task was performed bimanually during actively induced affective states. This procedure for engendering sustained emotions in the participant mirrored that used in a

previous study which adopted extended picture presentation to manipulate affective state (Sutton et al. 1997).

The induction of different affective states was achieved in a blocked manner. This design was structured to produce smooth transitions between different emotions i.e. blocks were arranged from positive to neutral then, to negative, and then back to neutral, then to positive emotions, and so on. Each session started with a block of either fearful or happy emotions. Each fearful/happy block lasted 70 s in average with 5 consecutively presented emotional stimuli portrayed by different identities. The emotion of the initial block was counter-balanced within and across subjects. There were 4 blocks of fearful and happy emotions for each session with neutral states interleaved in between. There were 7 neutral blocks, and each block lasted 50 seconds with 4 pictures of neutral facial expressions from different identities. Before each session and after each block, the participant was required to rate their emotional engagement using visual analog scales to score their subjective feelings as average levels of emotional arousal and valence (Figure 7.2 (ii)). After each rating period there was a 10 s break with a prompt reminding the subject to relax their emotional state back to neutral to reduce carry-over effects. The participants were also informed, by visual cue, of the emotion was to be felt (and subjectively generated) before each block.

Figure 7.2

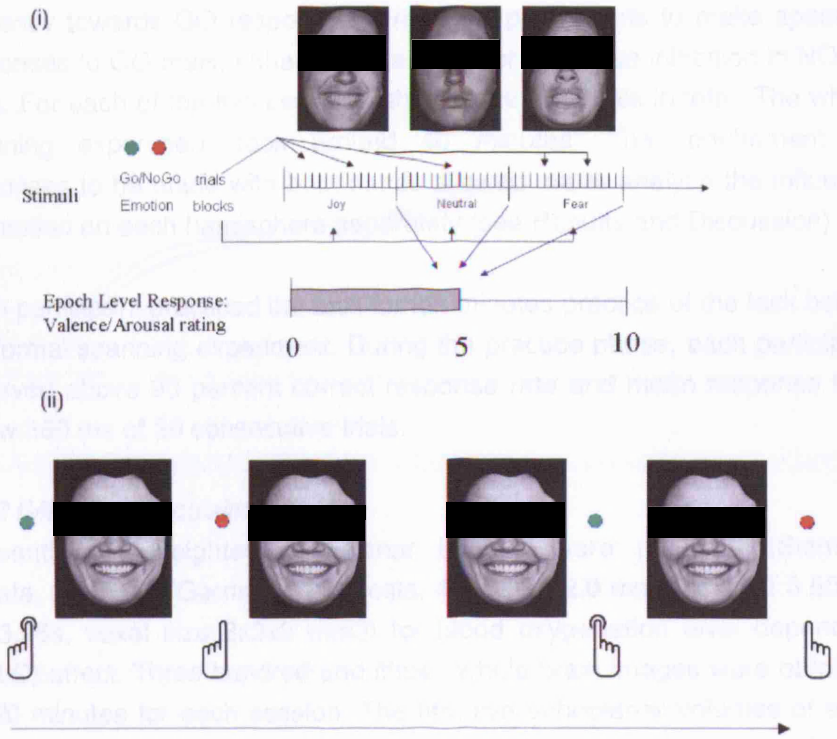

Figure 7.2 Experiment design and sequence of events in the emotion induction bimanual GO NOGO task.

Upper: The gross structure of the experiment design. There are 3 different emotion blocks: fearful, neutral and happy, where the participants perform GO/NOGO task (represented by small vertical lines) during active affective states. After each emotion block, a VAS scale of valence and arousal was rated.

Lower: The illustration of event sequence within an emotion (happy) block. The GO/NOGO cues are located either at the left or right side to the emotion stimuli; and the participants respond using either left or right index finger correspondent to the position of the cues.

From left to right: left GO, left NOGO, right GO, right NOGO.

The GO/NOGO cues were presented for 120ms, intentionally below the average latency for eye-saccades (150 ms; (Carpenter 1988)). Inter-trial intervals of GO/NOGO were varied randomly from 1.5 to 2.5 s (mean 2 s). To exclude confounding neural responses arising from imbalanced frequency effects (Braver et al. 2001; Durston et al. 2002a; Lavric et al.

2004), the proportion of GO and NOGO trials was equal. Since this design did not resort to a manipulation of trial frequency to induce pre-potent tendency towards GO responses, I required participants to make speeded responses to GO trials, enhancing the need for response inhibition in NOGO trials. For each of the two sessions, there were 380 trials in total. The whole scanning experiment took around 40 minutes. The requirement for responses to be made with both hands allowed me to analyze the influence of emotion on each hemisphere separately (see Results and Discussion)

Each participant practiced the task for ten minutes practice of the task before the formal scanning experiment. During the practice phase, each participant achieved above 90 percent correct response rate and mean response time below 360 ms of 30 consecutive trials.

7.2.2 fMRI data acquisition

Sequential T2*-weighted echoplanar images were acquired (Siemens Sonata, Erlangen, Germany; 1.5 Tesla, 44 slices, 2.0 mm thick, TE 0.50ms, TR 3.96s, voxel size 3x3x3 mm3) for blood oxygenation level dependent (BOLD) effect. Three hundred and fifteen whole-brain images were obtained for 20 minutes for each session. The first five echoplanar volumes of each session were not analyzed to allow for signal equilibrium. A T1-weighted structural image was obtained for each participant to facilitate anatomical description of individual functional activity after co-registration with fMRI data.

7.2.3 fMRI data analysis

I used SPM5 analysis software (on a Matlab platform (Mathworks, Inc., Natick, MA) to analyze acquired fMRI data. Task-related brain activities were identified within the General Linear Model. The six movement parameters (3 for translation and 3 for rotation) derived from the realignment process were imported into the design matrix to account for movement-related confounds. Error trials were defined as the excessively slow responses in GO trials (longer than 500 ms), response to GO trials with wrong hand and failed inhibition in NOGO trials. Errors were independently modelled within the design matrix as a regressor of no interest.

I modelled each trial as a unique event, convolved with a canonical haemodynamic basis function and categorized according to each trial type within the analytic design matrix. In each individual participant analysis, I

constructed four classes of contrasts: (1) main effects of GO and NOGO; (2) comparison of response sides (left vs. right) for GO and NOGO; (3) emotional influences on GO and NOGO (constrained by the results from (1)); and, (4) the interaction between emotional effects and response sides for GO and NOGO. Activity across the group was tested within second-level analyses of the above contrasts using simple T-tests. Voxel-wise statistical threshold was set at $P < 0.001$, uncorrected and extent threshold of 3 voxels in these group analyses.

Right hemisphere hypothesis was tested by non-parametric statistics. Assume there are n' regions (regardless of left or right sides) showing significant activation and among them s^+ regions did not show right side preference (in other words, not model 2 and model 3):

The possibility of null hypothesis was

$$P = \sum_{k=0}^{s^+} \binom{n'}{k} (0.5)^{n'}$$

The statistical threshold was set at 0.05.

7.3 RESULTS

7.3.1 Behavioural Results

One participant was excluded due to a failure to generate emotions in the scanner (i.e. subjective ratings showed no change in emotional intensity and valence inn happy and fearful conditions, relative to neutral). Thirteen participants were included in the subsequent analysis. I analyzed GO and NOGO trials separately within the factorial structure of the experiment (emotions (happy/fearful/neutral) by response sides (left/right)). The average reaction time (RT) was 378.4 ms for GO, and the average commission error rate (ER) was 5.8% for NOGO trials. GO trials with RTs greater than 500 ms was 5.3%. The total ER rate was 6.7%. Repeated measures analyses of RTs revealed a significant effect of trial condition (6 pairs from emotions and response sides: fearful right, fearful left, neutral right, neutral left, happy right, happy left) for GO trials ($F(2.986,35.831) = 12.110$, $P < 0.001$ under Greenhouse-Geisser correction). Pair-wise comparison analyses revealed that the RT difference in GO trials was attributable to the slowed response of right index finger in happy state, suggesting that joyful emotion imposes asymmetrical influence on response execution. There was a trend that RTs were faster when the cue of GO was present at left side regardless of emotions (Table 7.1). There was no significant differential effect on ER across NOGO trial conditions. The details of behavioural results are summarized in Table 7.1. In the thirteen participants who were entered into these analysis, arousal and valence ratings confirmed that the participants could engender appropriate emotional states as directed by the task requirements and prompted by the emotional face stimuli (these data are summarized in Table 7. 2).

Table 7.1 The means and paired-sample t-tests of response times (RTs) and commission errors for GO and NOGO trials (df = 12)

Emotion		t	P value
GO: Reaction Times	Mean (SD) ms		
Neutral	Overall 375.7 (15.4)		
Happy	Overall 381.0 (19.3)		
Fearful	Overall 378.4 (16.2)		

Pairwise Comparison	Response sides			
Happy – Neutral	Left	4.3 (13.5)	1.160	0.269
Fearful – Neutral	Left	3.4 (15.2)	0.803	0.438
Happy – Neutral	Right	6.4 (8.7)	2.639	0.022*
Fearful – Neutral	Right	2.0 (10.8)	0.681	0.509
Pairwise Comparison	Emotions			
Left – Right	Happy	15.9 (15.7)	3.647	0.003*
Left – Right	Fearful	19.3 (14.5)	4.789	< 0.001*
Left – Right	Neutral	18.0 (15.6)	4.186	0.001*
NOGO: Commissions Errors		Mean (SD) %		
Neutral	Overall	5.9 (3.5)		
Happy	Overall	6.0 (3.3)		
Fearful	Overall	5.6 (3.1)		
Pairwise Comparison	Response sides			
Happy – Neutral	Left	-0.4 (4.8)	-0.329	0.748
Fearful – Neutral	Left	-0.6 (4.7)	-0.436	0.671
Happy – Neutral	Right	0.6 (5.1)	0.444	0.665
Fearful – Neutral	Right	-0.1 (3.9)	-0.152	0.882
Pairwise Comparison	Emotions			
Left – Right	Happy	0.3 (6.1)	0.152	0.882
Left – Right	Fearful	0.9 (6.5)	0.479	0.628
Left – Right	Neutral	1.3 (5.2)	0.909	0.381

* indicates statistical significance ($P < 0.05$)

Table 7.2 The means and paired-sample t-tests of valence and arousal for different emotion conditions (df = 12)

Emotion	Valence (SD)	Arousal (SD)	t	P value
Neutral	4.8 (0.6)	2.3 (1.0)		
Happy	7.5 (0.9)	4.5 (1.9)		
Fearful	3.4 (1.1)	5.0 (2.0)		

7.3.2 Functional imaging results

7.3.2.1 Main effects of GO and NOGO

Across GO trials (compared to NOGO trials), the execution of speeded responses enhanced activity over a distributed neural system covering motor-related regions (including pre- and post- central gyrus and supplementary motor area), anterior cingulate cortex (ACC), inferior parietal lobule, insula, thalamus and cerebellum; see Table 7.3 and Figure 7.3. In contrast to GO trials, response inhibition (NOGO trials) were associated with differential activation within bilateral inferior frontal gyrus (Brodmann Area (BA) 47), bilateral middle frontal gyrus (BA 9), precuneus, cuneus, and middle temporal gyrus; see Table 7.4 and Figure 7.3.

Figure 7.3

Figure 7.3 Brain regions showing significant activities for the main effect of GO and NOGO conditions. Bold contrasts of GO (hot) and NOGO (winter) are superimposed on a T1 structural image in axial sections from z = -12 to z = 72.

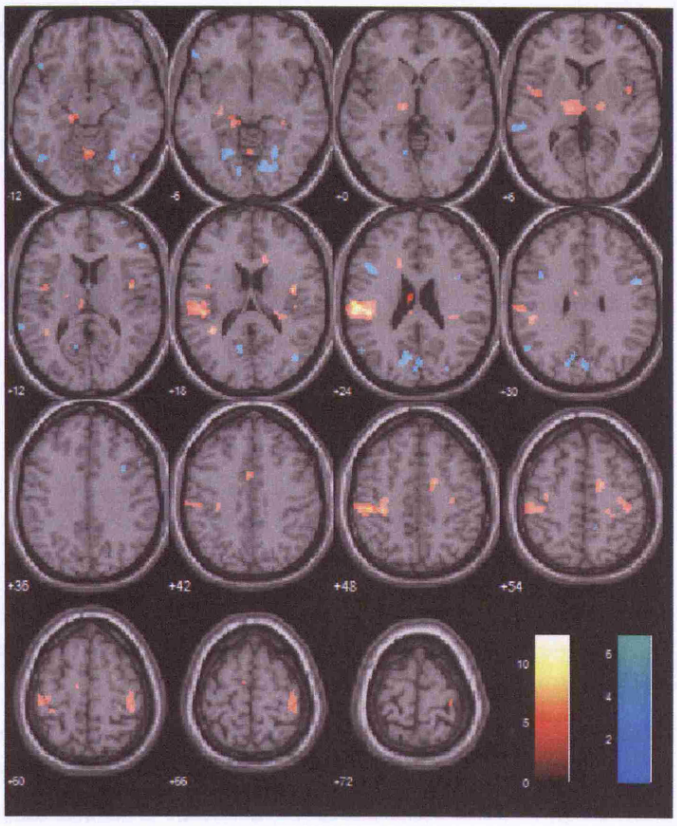

Table 7.3 Group mean activation for the contrast of GO minus NOGO (uncorrected, $P < 0.001$)

Brain area (BA) [a]	Stereotaxic coordinates [b]			Z score
Precentral Gyrus (4/L)	-30	-19	45	3.79
Precentral Gyrus (4/R)	36	-24	66	3.73
Medial Frontal Gyrus (6/L)	-6	-5	59	3.31
Medial Frontal Gyrus (6/R)	4	-3	54	3.21
Cingulate Gyrus (24/L)	-2	6	37	4.35
Cingulate Gyrus (24/R)	18	-1	48	4.51
Postcentral Gyrus (3/L)	-34	-32	57	3.23
Postcentral Gyrus (3/R)	22	-27	51	3.56
Postcentral Gyrus (43/R)	53	-18	21	3.39
Inferior Parietal Lobule (SII, 40/L)	-55	-20	25	5.53
Parahippocampal Gyrus (35/L)	-16	-29	-7	3.93
Hippocampus (R)	32	-33	-2	3.9
Insula (13/L)	-40	-3	15	3.72
Insula (13/R)	40	-5	17	4.61
Insula (13/R)	32	-28	22	3.79
Thalamus (Ventral Lateral Nucleus/L)	-12	-15	3	4.36
Thalamus (R)	18	-13	6	3.67
Pons (L)	-4	-40	-23	3.51
(R)	4	-34	-22	3.95
Cerebellum, Declive (L)	-20	-65	-15	3.41
Cerebellum, Declive (R)	26	-63	-20	4.72
Cerebellum, Culmen (L)	-8	-57	-11	3.44
Cerebellum, Culmen (R)	4	-61	-10	3.92
Cerebellum, Cerebellar Tonsil (L)	-28	-45	-38	3.7
Cerebellum, Cerebellar Tonsil (R)	24	-45	-38	3.84
Cerebellum, Uvula (L)	-8	-68	-34	3.52

[a] BA, Brodmann designation of cortical areas

[b] Values represent the stereotaxic location of voxel maxima above uncorrected threshold

Figure 7.4

Figure 7.4 Brain map derived from the contrasts of bimanual responses for GO trials.

Bold contrasts of index finger pressing derived from "left minus right" (hot) and "right minus left" (winter) are superimposed on a T1 structural image in axial sections from z = -12 to z = 72.

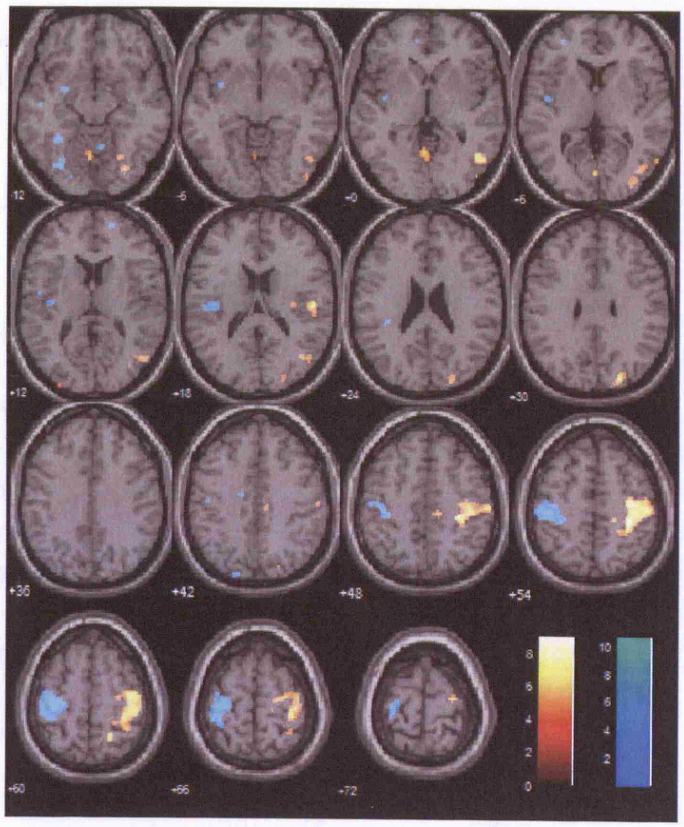

Table 7.5 Group mean activation for the contrast between Left and Right index finger for GO trials (uncorrected, $P < 0.001$)

Brain area (BA	Stereotaxic coordinates[b]			Z score
	Left minus Right			
Precentral Gyrus (4/R)	32	-27	47	4.88
Precentral Gyrus (6/R)	26	-10	65	4.4
Paracentral Lobule (6/R)	12	-23	47	4.25
Postcentral Gyrus (1,2,3,5/R)	32	-32	53	4.66
Postcentral Gyrus (43/R)	51	-17	17	3.99
Superior Parietal Lobule (7/R)	20	-49	60	3.99
Middle Temporal Gyrus (39/R)	50	-67	16	3.69
Inferior Temporal Gyrus (37/R)	48	-64	2	4.33
Fusiform Gyrus (19/R)	26	-64	-5	3.89
Superior Occipital Gyrus (18,19/R)	24	-80	32	3.88
Middle Occipital Gyrus (19/L)	-32	-94	14	3.59
Middle Occipital Gyrus (19/R)	46	-82	-1	3.58
Cuneus (18/L)	0	-75	9	3.75
Claustrum (R)	34	-15	15	3.81
Cerebellum, Culmen (L)	-12	-51	-14	4.33
	Rigth minus Left			
Precentral Gyrus (4/L)	-36	-20	56	4.88
Precentral Gyrus (6/L)	-40	-13	60	5.23
Middle Frontal Gyrus (10/L)	-30	47	7	3.83
Medial Frontal Gyrus (10/R)	16	55	8	3.96
Anterior Cingulate (24/R)	4	26	12	3.42
Paracentral Lobule (6/L)	-12	-10	41	3.52
Postcentral Gyrus (1,2,43/L)	-48	-24	56	4.99
Superior Parietal Lobule (7/L)	-18	-81	45	3.57
Middle Temporal Gyrus (21/L)	-50	-16	-8	3.26
Fusiform Gyrus (19/L)	-30	-72	-6	4.54
(37/L)	-34	-47	-8	4.28
Insula (13/L)	-38	-17	19	4.21
Amygdala (L)	-28	-2	-10	3.95
Claustrum (L)	-36	6	-4	3.51
Cerebellum, Culmen (R)	26	-55	-21	4.97

Cerebellum, Pyramis (R)	8	-73	-23	4.34
Cerebellum, Inferior Semi-Lunar (R)	12	-64	-39	3.65

[a] BA, Brodmann designation of cortical areas

[b] Values represent the stereotaxic location of voxel maxima above uncorrected threshold

When considering the laterality of NOGO cues, the contrast of left minus right NOGO (LR_NOGO) and right minus left (RL_NOGO) also revealed lateralization of brain activity. Both contrasts involved several regions located at posterior brain, including middle temporal gyrus, lingual gyrus and inferior occipital gyrus. Right index finger response inhibition (NOGO) engaged more cortical and subcortical neural correlates, including inferior frontal gyrus (BA 44), middle frontal gyrus, anterior cingulate cortex, superior parietal lobule, insula and thalamus. This neuroanatomical asymmetry between LR_NOGO and RL_NOGO may reflect the extra 'effort' required to inhibit the (dextral) dominant hand; see Table 7.6 and Figure 7.5.

Figure 7.5

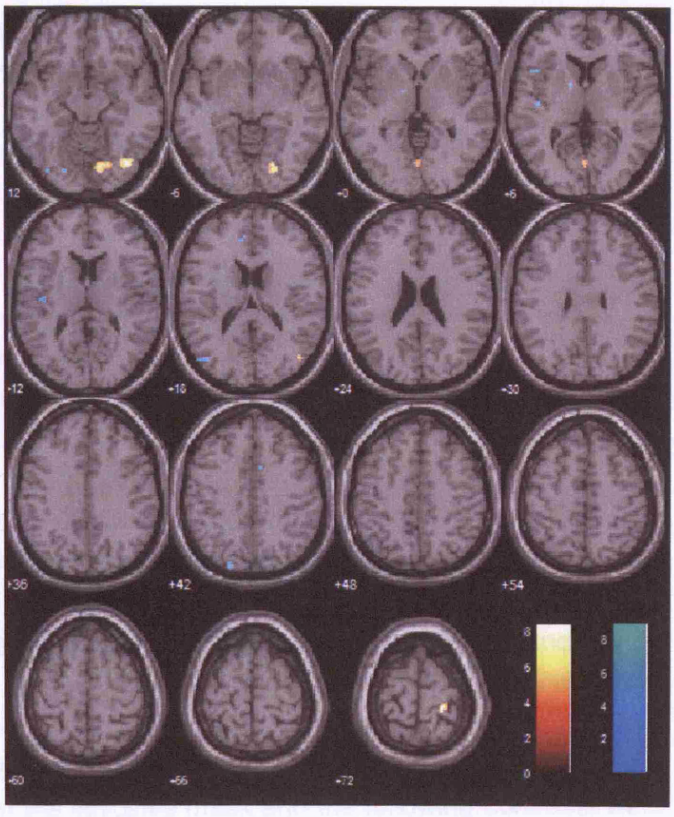

Figure 7.5 Brain regions showing the contrasts of bimanual responses for NOGO trials.

Bold contrasts of index finger response withholding from "left minus right" (hot) and "right minus left" (winter) are superimposed on a T1 structural image in axial sections from z = -12 to z = 72.

Table 7.6 Group mean activation for the contrast between Left and Right index finger for NOGO trials (uncorrected, $P < 0.001$)

Brain area (BA) [a]	Stereotaxic coordinates [b]			Z score
	Left minus Right			
Lingual Gyrus (18/R)	12	-76	-8	4.73
Postcentral Gyrus (3/R)	22	-28	68	4.64
Middle Temporal Gyrus (39/R)	44	-71	18	3.53
Fusiform Gyrus (37/R)	40	-57	-14	3.75
Inferior Occipital Gyrus (19/R)	38	-74	-6	4.54
Cuneus (30/L)	0	-72	5	3.74
	Right minus Left			
Inferior Frontal Gyrus (44/L)	-48	14	7	4.87
Middle Frontal Gyrus (8/L)	-38	22	47	3.57
Anterior Cingulate Gyrus (24/L)	-10	38	17	4.22
Anterior Cingulate Gyrus (24/R)	8	12	36	4.51
Superior Parietal Lobule (7/L)	-20	-79	43	3.72
Middle Temporal Gyrus (39/L)	-48	-73	18	3.49
Lingual Gyrus (18/L)	-20	-80	-8	3.51
Inferior Occipital Gyrus (19/L)	-40	-78	-3	3.45
Insula (13/L)	-42	-17	10	4.47
Thalamus (L)	-12	-6	2	3.91
Cerebellum, Declive (L)	-8	-69	-18	3.82

[a] BA, Brodmann designation of cortical areas

[b] Values represent the stereotaxic location of voxel maxima above uncorrected threshold

7.3.2.3 Emotional effects on GO and NOGO processing

To investigate the modulatory effects of emotion on GO and NOGO processes, I eliminated extraneous confounds related to emotion processing per se by constructing an inclusive mask, derived from main effects of GO and NOGO processing separately. I set the statistical threshold of this mask at uncorrected $P < 0.01$ and tested for the effects of emotion on GO and NOGO trials using small volume correction ($P < 0.01$, uncorrected). It is important to note that the contrasts of the inclusive mask and the following contrasts were

orthogonal. The thresholding of this analysis was therefore stringent (at an approximate threshold level of P value below 0.01*0.01).

When testing for emotional effects on GO trials, enhanced activity was observed for both happy and fearful trials within motor-related circuitry, including precentral gyrus, postcentral gyrus, globus pallidus, thalamus, pons and cerebellum (Table 7.7 and 7.8). For NOGO happy emotional states evoked an enhancement of neural responses relative to neutral, only within fusiform gyrus (BA 19; coordinate 26 -64 -4; Z score 2.82). Similarly, fearful NOGO processing enhanced neural response at only middle frontal gyrus (BA 9; -40 11 27; Z score 2.37). Interestingly, fearful NOGO, compared with neutral NOGO, was associated with attenuated activity within the inferior frontal gyrus (BA 47; coordinate 28, -60, -5; Z score 2.37), a region strongly implicated in the mediation of response inhibition (Durston et al. 2002b; Konishi et al. 1999; Matsubara et al. 2004; Menon et al. 2001; Nakata et al. 2005; Schulz et al. 2005).

Table 7.7 Happy emotion effect on GO (Happy vs. Neutral; uncorrected, $P < 0.01$[c])

Brain area (BA)[a]	Stereotaxic coordinates[b]			Z score
Activities in Happy > Activities in Neutral				
Precentral Gyrus (4/L)	-38	-19	52	3.08
Precentral Gyrus (4/R)	34	-13	50	2.34
Anterior Cingulate Gyrus (24/R)	16	-8	44	2.63
Postcentral Gyrus (3/L)	-40	-27	51	2.74
Postcentral Gyrus (3/R)	25	-25	51	2.43
Parahippocampal Gyrus (35/L)	-14	-26	-10	2.44
Thalamus, Ventral Lateral Nucleus (L)	-14	-9	6	3.75
Ventral Posterior Lateral Nucleus (L)	-18	-15	3	3.54
Thalamus, Ventral Lateral Nucleus (R)	14	-13	4	2.84
Thalamus (R)	22	-17	10	2.45
Pons (L)	-2	-39	-23	2.91
Pons (R)	2	-33	-20	3.46
Cerebellum, Culmen (L)	-2	-59	-5	2.52
Cerebellum, Culmen (R)	32	-53	-21	3.13
Cerebellum, Declive (L)	-22	-59	-16	2.52

Cerebellum, Declive (R)	26	-55	-17	2.9
Cerebellum, Inferior Semi-Lunar (L)	-10	-66	-37	2.87

[a] BA, Brodmann designation of cortical areas

[b] Values represent the stereotaxic location of voxel maxima above uncorrected threshold

[c] The contrast of GO minus NOGO derived at uncorrected $P < 0.01$ was taken as a mask for small volume correction.

No voxel showing activity in Neutral > activity in Happy

Table 7.8 Fearful emotion effect on GO (Fearful vs. Neutral; uncorrected, $P < 0.01$ [c])

Brain area (BA) [a]	Stereotaxic coordinates [b]			Z score
Activities in Fearful > Activities in Neutral				
Precentral Gyrus (4/L)	-36	-19	55	2.79
Precentral Gyrus (4/R)	29	-28	58	2.4
Postcentral Gyrus (2/L)	-36	-25	44	4.38
Inferior Parietal Lobule (40/L)	-52	-26	21	3.32
Inferior Parietal Lobule (40/R)	37	-28	24	3.2
Superior Temporal Gyrus (13/L)	-40	-44	17	3.12
Hippocampus (L)	-32	-24	-7	2.52
Insula (13/R)	42	-9	17	2.76
Thalamus (L)	-16	-11	4	2.94
Pons (L)	-12	-26	-10	2.39
Pons (R)	2	-34	-22	2.75
Cerebellum, Declive (R)	28	-61	-15	3.22
Cerebellum, Culmen (R)	32	-57	-22	2.59
Activities in Neutral > Activities in Fearful				
Postcentral Gyrus (3/L)	-59	-24	43	2.44
Postcentral Gyrus (40/L)	-59	-19	18	2.85
Postcentral Gyrus (2,3/R)	40	-29	64	3.33

[a] BA, Brodmann designation of cortical areas

[b] Values represent the stereotaxic location of voxel maxima above uncorrected threshold

[c] The contrast of NOGO minus GO derived at uncorrected $P < 0.01$ was taken as a mask for small volume correction.

7.3.2.4 Interaction of emotional processing and response sides for GO and NOGO trials

One of the main goals of this study was to investigate the emotion asymmetry hypothesis. I designed the bimanual task to address specifically this issue, via the contrast between left and right index finger in response execution (GO) and inhibition (NOGO) across different affective states and corresponding asymmetrical patterns of neural activity.

I explored the interaction between emotional processing and response sides for GO trials using the following two analytic contrasts: Happy LR_GO versus Neutral LR_GO, and Fearful LR_GO versus Neutral LR_GO. The interaction of happy emotional states with lateralised responses broadly revealed Mode 2 and Mode 3 activity patterns (as described in the introduction, see Figure 7.1) consistent with the *right hemisphere hypothesis* of emotion. Modes 2 and 3 both represent enhanced activities within the right hemisphere, (in Mode 2 there is no significant activity change within the left hemisphere and in Mode 3 there is attenuated activity within the left hemisphere). Brain structures showing a pattern of Mode 2 included precentral gyrus, cingulate gyrus, superior parietal lobule, middle occipital gyrus, posterior insula, cuneus and caudate tail. Brain structures revealing a pattern of Mode 3 included medial frontal gyrus, middle temporal gyrus, fusiform gyrus, middle insula, globus pallidus, putamen, claustrum and caudate tail (see Figure 7.6 and Table 7.9). Exceptions to this right predominance were observed in fusiform gyrus, superior occipital gyrus, postcentral gyrus, anterior insula and caudate body (increased activities at left hemisphere; Modes 4 and 7). The *P* value of non-parametric test was $0.032 < 0.05$, supporting right hemisphere hypothesis.

The overriding activity pattern associated with the interaction of fearful processing and lateralised GO responses (i.e. Fearful LR_GO vs. Neutral LR_GO) also corresponded to Modes 2 and 3 (see Figure 7.1), again supporting the *right hemisphere hypothesis*. Mode 2 pattern of activity was observed within medial frontal gyrus, anterior and posterior cingulate gyrus, ventromedial frontal gyrus, superior temporal gyrus and middle temporal gyrus while the Mode 3 pattern was observed within claustrum and globus pallidus. Middle occipital gyrus revealed a pattern of Mode 6 (decreased activities at left hemisphere); while lingual gyrus and fusiform gyrus revealed a pattern of Mode 4 (Figure 7.6 and Table 7.10). The *P* value of non-parametric test was $0.046 < 0.05$.

Figure 7.6

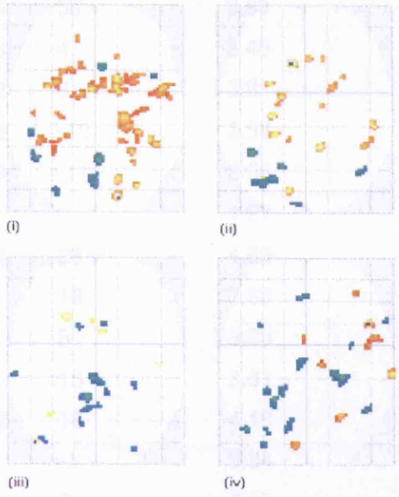

Figure 7.6 Brain regions showing interaction of "emotions X response sides" for GO and NOGO trials, projected onto a glass brain.

There are 4 contrasts compared. Hot: the contrast is positive; and Winter: the contrast is negative.

(i) (happy left GO minus happy right GO) vs. (neutral left GO minus neutral right GO)
(ii) (fearful left GO minus fearful right GO) vs. (neutral left GO minus neutral right GO)
(iii) (happy left NOGO minus happy right NOGO) vs. (neutral left NOGO minus neutral right NOGO)
(iv) (fearful left NOGO minus fearful right NOGO) vs. (neutral left NOGO minus neutral right NOGO)

Table 7.9 Group mean activation for the interaction between response side (Left/Right) and positive emotion (Happy/Neutral) for GO trials (uncorrected, $P < 0.001$)

Brain area (BA) [a]	Stereotaxic coordinates [b]			Z score
(Left Happy – Right Happy) minus (Left Neutral – Right Neutral)				
Precentral Gyrus (4/R)	26	-24	55	3.69
Precentral Gyrus (6/R)	57	-4	8	3.5
Middle Frontal Gyrus (8/L)	-30	10	36	3.73
Medial Frontal Gyrus (6/L)	-10	1	50	3.62
Medial Frontal Gyrus (6/R)	16	7	55	3.98
Ventromedial Prefrontal Cortex (10/L)	-12	42	-11	3.54
Cingulate Gyrus (24/R)	16	13	27	4.13
Postcentral Gyrus (2/L)	-46	-15	47	3.32

Superior Parietal Lobule (7/R)	28	-46	56	3.83
Middle Temporal Gyrus (21/L)	-44	-43	4	3.45
Middle Temporal Gyrus (21/R)	46	-42	8	3.9
Fusiform Gyrus (20/L)	-42	-39	-10	3.58
Fusiform Gyrus (20/R)	42	-39	-11	3.95
Middle Occipital Gyrus (19/R)	34	-78	2	4.27
Cuneus (19/R)	18	-84	28	4.63
Insula (13/L)	-36	5	16	3.83
Insula (Anterior, 13/R)	36	14	5	3.58
Insula (Middle, 13/R)	51	3	15	3.81
Insula (Posterior, 13/R)	34	-32	18	4.18
Globus Pallidus (L)	-12	-4	-1	3.34
Globus Pallidus (R)	18	0	0	4.02
Putamen (L)	-24	18	8	3.66
Putamen (R)	30	8	5	3.49
Claustrum (L)	-30	6	7	3.45
Claustrum (R)	30	8	5	3.49
Caudate, Caudate Body (L)	-14	-3	22	3.41
Caudate, Caudate Tail (R)	32	-39	6	3.36
Cerebellum, Declive (R)	18	-71	-17	4.13
Cerebellum, Cerebellar Tonsil (L)	-26	-41	-33	3.41
(Left Neutral – Right Neutral) minus (Left Happy – Right Happy)				
Medial Frontal Gyrus (8/R)	6	22	45	3.91
Postcentral Gyrus (2/L)	-48	-30	57	3.66
Precuneus (7/L)	0	-72	46	3.71
Precuneus (7/R)	4	-51	65	4.08
Fusiform Gyrus (37/L)	-44	-53	-16	4.11
Superior Occipital Gyrus (19/L)	-28	-80	39	3.5
Insula (13/R)	44	12	-2	3.44

[a] BA, Brodmann designation of cortical areas

[b] Values represent the stereotaxic location of voxel maxima above uncorrected threshold ($P < 0.001$)

Table 7.10 Group mean activation for the interaction between response side (Left/Right) and negative emotion (Fearful/Neutral) for GO trials (uncorrected, $P < 0.001$)

Brain area (BA) [a]	Stereotaxic coordinates [b]			Z score
(Left Fearful – Right Fearful) minus (Left Neutral – Right Neutral)				
Medial Frontal Gyrus (9/R)	14	29	30	3.49
Anterior Cingulate Gyrus (24/R)	12	-8	43	3.56
Posterior Cingulate Gyrus (31/R)	12	-43	30	4.07
Ventromedial Frontal Gyrus (32/R)	4	27	-11	3.62
Superior Temporal Gyrus (22/R)	53	-27	5	4.16
Middle Temporal Gyrus (21/R)	46	-43	4	3.43
Middle Occipital Gyrus (19/L)	-34	-71	20	3.79
Caudate, Caudate Head (L)	-10	23	-6	4.39
Claustrum (L)	-26	-19	18	4.12
Claustrum (R)	28	12	9	3.57
Globus Pallidus (L)	-18	-4	-5	3.96
	-20	-8	0	3.23
Globus Pallidus (R)	22	4	-2	3.44
Cerebellum, Declive (L)	-14	-80	-16	3.91
(Left Neutral – Right Neutral) minus (Left Fearful – Right Fearful)				
Lingual Gyrus (17/L)	-8	-90	-4	3.41
Fusiform Gyrus (19/L)	-32	-74	-11	3.57
Cerebellum, Culmen (L)	-42	-50	-21	3.98
Cerebellum, Declive (L)	-24	-71	-12	3.61
Cerebellum, Declive (R)	42	-65	-14	3.5
Cerebellum, Cerebellar Tonsil (L)	-18	-62	-32	3.95

[a] BA, Brodmann designation of cortical areas

[b] Values represent the stereotaxic location of voxel maxima above uncorrected threshold ($P < 0.001$)

I next explored the interaction between emotional processing and the spatial laterality of NOGO cues, using analytic contrasts: Happy LR_NOGO vs. Neutral LR_NOGO and Fearful LR_NOGO vs. Neutral LR_NOGO.

There was no generalized lateralization of the activity associated with interaction of processing happiness and lateralized response inhibition Happy LR_NOGO vs. Neutral LR_NOGO). The superior parietal lobule and middle temporal gyrus showed attenuation of activity within the left hemisphere (Mode 6); while insula and caudate showed enhancement of activity within the right hemisphere (Mode 2). The inferior parietal lobule showed left hemisphere enhancement (Mode 4) and middle occipital gyrus showed right hemisphere attenuation (Mode 8). Increased left sided and/or decreased right sided activities were noticed at several loci of posterior cingulate gyrus (see Figure 7.6 and Table 7.11). The non-parametric test of right hemisphere hypothesis did not reach significance (P = 0.930). The brain foci satisfying model 2 and 3 both contributed to the significance.

A mixed pattern of activity was associated with lateralized response inhibition in the context of fear processing (interaction Fearful LR_GO vs. Neutral LR_GO). There was no general trend in right hemisphere dominance. Mode 3 activity patterns were observed in superior frontal gyrus, middle frontal gyrus, postcentral gyrus, and temporal pole. Mode 4 activity patterns were observed in superior frontal gyrus, medial frontal gyrus, angular gyrus, superior parietal lobule, posterior cingulate gyrus, middle occipital gyrus, and lingual gyrus. Mode 8 activity patterns were observed in precentral gyrus, inferior frontal gyrus, inferior parietal lobule and insula (see Figure 7.6 and Table 7.12). The non-parametric test of right hemisphere hypothesis did not reach significance (P = 0.827). The brain foci satisfying model 2 and 3 both contributed to the significance.

Table 7.11 Group mean activation for the interaction between response side (Left/Right) and positive emotion (Happy/Neutral) for NOGO trials (uncorrected, $P < 0.001$)

Brain area (BA) [a]	Stereotaxic coordinates [b]			Z score
(Left Happy – Right Happy) minus (Left Neutral – Right Neutral)				
Anterior Cingulate (24/L)	0	19	23	3.45
Superior Parietal Lobule (7/L)	-34	-54	54	3.38
Middle Temporal Gyrus (39/L)	-46	-78	28	3.76
Insula (22/R)	46	-18	-1	3.52
Caudate, Caudate Head (R)	6	8	-4	3.48

(Left Neutral – Right Neutral) minus (Left Happy – Right Happy)				
Medial Frontal Gyrus (8/R)	6	18	49	3.71
Anterior Cingulate Gyrus (32/L)	-12	15	23	4.02
Inferior Parietal Lobule (40/L)	-61	-24	23	3.81
Posterior Cingulate Gyrus (31/L)	-6	-41	35	4.18
(31/L)	-2	-25	34	3.93
(31/L)	-6	-51	27	3.66
(23/R)	2	-49	25	3.37
(29/L)	-10	-44	10	3.43
(29/R)	10	-40	8	3.42
Middle Occipital Gyrus (18/R)	28	-85	3	3.31
Cerebellum, Tuber (L)	-40	-79	-26	3.44
Cerebellum, Uvula (L)	-10	-67	-29	3.42

[a] BA, Brodmann designation of cortical areas

[b] Values represent the stereotaxic location of voxel maxima above uncorrected threshold ($P < 0.001$)

Table 7.12 Group mean activation for the interaction between response side (Left/Right) and negative emotion (Fearful/Neutral) for NOGO trials (uncorrected, $P < 0.001$)

Brain area (BA) [a]	Stereotaxic coordinates [b]			Z score
(Left Fearful – Right Fearful) minus (Left Neutral – Right Neutral)				
Superior Frontal Gyrus (6/R)	12	-12	69	3.72
Middle Frontal Gyrus (46/R)	38	41	5	3.48
Anterior Cingulate Gyrus (24/L)	-2	9	29	3.39
Postcentral Gyrus (43/R)	65	-22	20	4.24
Temporal Pole (38/R)	48	16	-21	4.71
Superior Temporal Gyrus (38/R)	51	5	-9	3.66
Cuneus (17/L)	-8	-81	10	3.63
Cerebellum, Declive (R)	26	-59	-16	3.85
(Left Neutral – Right Neutral) minus (Left Fearful – Right Fearful)				
Precentral Gyrus (4/R)	22	-21	51	3.69
Superior Frontal Gyrus (9/L)	-36	17	38	3.36
Inferior Frontal Gyrus (45/R)	61	22	14	3.44

Medial Frontal Gyrus (9/L)	-4	40	31	3.82
Angular Gyrus (39/L)	-46	-67	29	3.81
Superior Parietal Lobule (7/L)	-16	-66	49	3.4
Inferior Parietal Lobule (40/R)	46	-50	41	3.67
Posterior Cingulate Gyrus (23/L)	-6	-16	36	3.43
Middle Occipital Gyrus (19/L)	-32	-81	10	3.41
Lingual Gyrus (L)	-12	-62	1	3.35
Insula (13/R)	36	1	15	3.64
Caudate, Caudate Tail (L)	-30	-38	9	3.34
Cerebellum, Culmen (L)	-24	-44	-18	4.04

[a] BA, Brodmann designation of cortical areas

[b] Values represent the stereotaxic location of voxel maxima above uncorrected threshold ($P < 0.001$)

7.4 DISCUSSION

I developed a bimanual emotion GO/NOGO task to investigate the influence of affective states on response execution and inhibition. Happy, fearful and neutral affective states were induced in subjects to provide emotional contexts for lateralized GO and NOGO responses. This cuing of responses bimanually to left and to right sides further enabled me to explore the neural lateralization of emotion and affective influences on behaviour. Enhanced neural activities within cortical and subcortical motor circuitry were noticed for response execution in both positive and negative affective states. The processing of fear was associated with attenuation (rather than enhancement) of activity within the brain region perhaps most strongly implicated in response inhibition (BA 47). In their interaction with response lateralization, happy and fearful emotional states demonstrated a right hemisphere dominant asymmetry. Thus the *right hemisphere hypothesis* was broadly supported (for both positive and negative emotions) but only for GO trials. These neuroimaging findings extended previous evidence for highly context-dependent influences of affective processes on behaviour.

Evidence that emotion permeates other psychological processes is apparent across studies quantifying declarative mental states, psychophysiological responses and observed behaviour. Subjective emotional states can enhance sensory perceptions, mobilize physiological resources, instigate and predict different behavioural patterns and bias attention, judgment and memory (Davidson et al. 2000; Dolan 2002). Correspondingly, the neural substrates supporting these diverse emotion-related processes are widely-distributed (Phan et al. 2002; Wager et al. 2003). Underpinning the motivation of the present study is the tenet that specific aspects of emotion are both context- and structure- specific (Borod 1992). Dichotomous theories that relate emotion to brain, including those addressing motivational direction and emotion asymmetry, are intrinsically constrained and may not generalize to all emotion-related contexts or structures. Nevertheless in this study, both positive and negative affective states enhanced neural responses associated with within response execution (GO), within somatosensory cortices, insula, thalamus and pons highlighting at a neural level the dependent relationship between emotional and homeostatic processes (Damasio et al. 2000). Evolutionary perspectives particularly link emotion to adaptive action-taking (James 1894). This is perhaps most apparent when considering fear.

Adaptive responses to threat have primacy and subjective feelings engender the desire to flee and corresponding preparatory autonomic changes facilitate the dominant skeleton-muscular response tendency (flight or fight (or faint)). Across emotions, the mobilization of motor-related neural circuitry in response to an emotional challenge adaptively facilitates action without necessarily compromising behavioural flexibility. The stereotyped approach/withdrawal response is thus conceptually dissociable from the behavioural manifestations of positive/negative emotion (Harmon-Jones & Allen 1998; Wacker et al. 2003).

I designed this experimental task to examine behavioural control, which is represented at perhaps the most fundamental level by response inhibition. A noteworthy finding was that neural response during NOGO trials within inferior frontal gyrus (BA 47), a frequently reported neural node of response inhibition (Durston et al. 2002b; Konishi et al. 1999; Matsubara et al. 2004; Menon et al. 2001; Nakata et al. 2005; Schulz et al. 2005), was attenuated by fear. This finding was not predicted, rather since fear typically engenders withdrawal or freezing behavioural responses, I anticipated the facilitation of response inhibition to be manifest as activity increases within BA 47. Nevertheless, in clinical 'fear' conditions, such as anxiety and PTSD, there is a characteristic enhancement of neural responsivity within BA47 and adjacent regions activity (Lanius et al. 2007; Liotti et al. 2000), yet in these conditions frequently manifest a failure of inhibition at multiple response levels. The inability to block pre-potent evolutionary responses to threat, including apprehension, avoidance, feelings of panic, hear rate increase may be aetiological. I have previously found that perception of fearful facial expressions in others enhances neural responses within BA 47 and lowers commission error on NOGO trials, see chapter 6. The present observation extends these findings to demonstrate that the subjective experience of the same fearful state engenders an opposite neural influence on the brain substrates supporting response inhibition.

The *right hemisphere hypothesis*' argues for a valence-independent association between emotional processing and right cerebral hemisphere function. I provide empirical evidence to support this hypothesis in both happy and fearful states, but only for response execution, GO trials, (again, arguing against a "universal" asymmetry hypothesis of emotion). In happy states, this lateralization was apparent across subcortical striatal regions associated with

facilitated execution of motor programs and these regions showed an attenuation of activity within left relative to right hemisphere (Figure 7.1, Mode 3). This may account in part for a prolongation of RT for right index finger responses. Counter-intuitively, the asymmetrical slow-down of RT also suggests that the experience of happiness engages more resources within left hemisphere (Davidson et al. 2000): Competition for cognitive modular resources may impact on performance, consistent with a *resources allocation model* (Ellis et al. 1985). This argument reconciles the Valence Hypothesis with the *right hemisphere hypothesis* and is compatible with the observation that emotion asymmetry is more robust for negative than for positive emotion (Hagemann et al. 2005; Tomarken et al. 1990). Overall, this observations highlight the engagement of differential neural systems by positive and negative emotions and highlights the context dependence of emotional processes.

Evidence for a right-hemisphere dominance of emotion processing comes from a wealth of empirical studies and is apparent in during the perception and expression of facial emotion and prosody, and in the experience of emotion (review; (Demaree et al. 2005)). This study provides a novel insight to this issue: Lateralization is not necessarily an anatomical question regarding the location of emotion centres within the right or left hemispheres, but may arise through the differential influence or modulation of behaviour exerted by emotional representations. In the analyses of this bimanual GO/NOGO design, I specifically targeted the influence of emotion on response execution and inhibition, while at the same time contrasting out primary effects of emotion per se. It is the influence of emotion on neuroanatomical structures that is asymmetrical. This findings therefore point to a parsimonious account of the right-lateralized activity patterns observed in across different dimensions of emotion: In studies of emotional expression emotional states impose asymmetrical (right-lateralized) bias on the neural correlates of facial muscle, such that the expression of the left hemi-face convey more emotion-related information (Borod et al. 1997). The same inference can be applied to the expressive affective aprosodia for right-hemisphere-damaged patients (Ross et al. 1997). I propose that the distributed representation of emotion states asymmetrically influences motoric systems in a context- dependent manner.

Two possible confounds need to be addressed: First, the index-finger response and imperative cues were lateralized to the same hemisphere and both can therefore potentially account for contra-lateral brain activation. I argue that, within this task, peripheral target detection is likely to have at most a trivial influence on overall activity lateralization. Consistent with this, I observed no consistent co-lateralization of activation and cue/response side in posterior early visual cortex regions in the contrasts of LR_GO, RL_GO, LR_NOGO and RL_NOGO. This is also perhaps consistent with earlier studies that note that high attention load at fixation causes an attenuation of responses to peripheral stimuli (Schwartz et al. 2005). This concern is potentially further confounded by the association of emotional (compared to neutral) stimuli with enhanced attention. However, this should in effect reduce the neural response to lateralized peripheral cues of GO trials (Rizzolatti et al. 1994), and I observed no significant difference in RTs between fearful (a well-known attention-attracting emotion (Georgiou et al. 2005; Moser et al. 2005)) and neutral trials.

7.5 CONCLUSION

Evaluating cognitive function and physiological profiles during various induced emotion states is a popular approach for exploring the interaction of emotion and other mental modules (Davidson et al. 1990; Gray 2001; Gross 1998; Wacker et al. 2003). This study addressed emotion-behaviour interaction by integrating emotion induction and bimanual GO/NOGO design. I focused on the general influence of induced emotion on behaviour (response execution and inhibition) to extend observations beyond emotion-related response tendencies related to approach/withdrawal, or fight/freeze/flight behavioural patterns. Stereotyped approach/withdrawal response and generalized emotion asymmetry hypotheses were both not supported in this study. The modulation of behaviour-related neural response by sustained affective state was context- and structure- dependent. I further showed that competing accounts of emotion lateralization may be clarified by framing the issue not in terms of anatomical asymmetry (the location of emotion centre is left or right) but functional asymmetry (whether emotion influence is lateralized).

Chapter 8
General Discussion

This thesis investigated an important, though neglected, theme within affective neuroscience; namely the facial somatomotor expression of the emotions and affective influences on behaviour (beyond physiological responsivity) (Critchley 2005; James 1894). To investigate the most prominent dimensions of overt emotion expressions, I have focused on face and body. My work provides novel insights to human emotional expression from neuroscientific perspectives and, complements studies of emotion perception and subjective affective experience to provide a more comprehensive understanding of human emotions.

8.1 THE EXPRESSION OF EMOTION ON THE FACE

8.1.1 Congruence effect for emotion expression

Emotional facial expressions can engender similar expressions in others. According to the theory of *emotional contagiosity* in face-to-face communication, congruence between viewed and expressed facial emotion would be facilitated; and similarly incongruence predicts an interference effect that impairs the ability to express a different emotion to that perceived. In my experiments, the pairing of actively posed expressions with viewed emotional faces simulated the dyadic nature of social interaction. Behaviourally, I demonstrated congruence and incongruence effects at both the response level (facial EMG onset; chapter 4) and the perceptual level (facial emotion intensity rating; chapter 5) (Adelmann et al. 1989; Dimberg et al. 2002).

During facial emotion imitation (a congruence condition examined in the first experiment), brain regions in which activity was observed to be correlated with the magnitude of facial movement included the motor network, the putative *mirror neuron system* and emotion-specific neural substrates (chapter 3). In other words, the neural matrix engaged and facilitated during emotion imitation encompassed both motoric and affective components. Correspondingly, overriding pre-potent imitative responses in order to express an emotion of the opposite valence on the face (emotional expression interference; EEI) engaged the inferior frontal gyrus (BA 47) and right insula, regions respectively implicated in the inhibition of motoric responses and in

the subjective experience of affective feelings (Critchley et al. 2004; Durston et al. 2002; Matsubara et al. 2004; Menon et al. 2001; Nakata et al. 2005; Reiman et al. 1997; Schulz et al. 2005). To be able to volitionally control the expression of emotion on one's face obviously possesses an adaptive social value, permitting individuals sometimes to suppress, conceal or override pre-potent imitative responses. Furthermore, the interference caused by overriding imitative tendencies (which I termed EEI) is conceptually related to the volitional act of suppressing emotional expressions as part of emotional self-regulation (Gross 1998) I empirically highlighted the relationship between the two concepts by demonstrating a significant correlation between interference-related activity within BA 47 and individual differences in a questionnaire measure of the suppression dimension of emotion regulation (Gross et al. 2003). This observation implicates the ventrolateral prefrontal cortex as the bridge between the reactive control of emotion expression and individual emotion regulatory style. My EMG data (in chapter 4) revealed that participants who scored higher on a measure of interpersonal empathy expressed facial emotions with greater speed in congruence conditions; they found it easier to smile to smiling faces, than less empathetic individuals. Together these findings extends the various notions of emotion being "expressed", "transmitted", or "communicated" by changes in the face (where the face represents a passive painted canvas), the exchange of emotional expressions actively contribute to emotional self- regulation and can be viewed as machinery tuned in accordance with personal empathy.

I unveiled the neural mechanisms engaged during congruence of posed and perceived facial emotions (chapter 5), the behavioural phenomenon having been established (Adelmann & Zajonc 1989). At the neural level, congruence between self (posing) and other (perception) facial expression was paralleled in complementary contributions of amygdala and STS. This observation supports a view of the amygdala as an emotion regulation centre and the STS as a social signal processor (LeDoux 2000; Puce et al. 1998). When there is affective concordance, the enhancement of amygdala activity may facilitate subsequent behavioural interactions (Cardinal et al. 2002), while activity within STS is tuned down for the concordant social signal evaluation, suggesting reduced demands at the perceptual level. In opposite situations where there is affective discordance, enhanced STS activity reflects perhaps neural recruitment for monitoring and reappraisal of social stimuli by instantiating a cognitive evaluation at a more cortical level. In this context, decreased

amygdala activity may disengage response tendencies and uncouple evoked arousal responses to facilitate such evaluative processing.

My DCM analysis (chapter 5) provided further insight into the appraisal of facial emotions (through intensity judgments of faces) and how this interacts with posed expressions. Behaviourally, the observer's facial expression modulated the judgment of perceived emotion by 6 to 7%. I showed this modulatory effect to be associated with neural changes at the level of STS-to-PC connectivity. Integrating *a priori* neuroanatomical knowledge of the amygdala (Amaral et al. 1992) with the results from conventional voxel-based and DCM connectivity analyses, I suggested that the neural mechanism underlying the judgment bias is likely to be mediated via backward projections from the amygdala that tune affective perceptual processing.

8.1.2 Active roles of superior temporal sulcus (STS) and insula in emotion expression

STS is implicated in sensory processing of changeable aspects of face stimuli, including facial expressions (Puce et al. 1998; Winston et al. 2004) and corresponding social representations (rather than motoric expression). Enhanced STS neural response was noticed in all my studies of facial emotion expression: STS activity correlated positively with the magnitude of facial movement when imitating happiness and sadness; STS activity was also enhanced when the observed and posed emotion expressions were discordant. What is worthy of note, in this interference (EEI) task, the participants were not required to rate the viewed facial emotion intensity immediately. In other words, the STS neural response appeared to be elicited automatically as a function of online expression-perception incompatibility. In addition to the STS, enhanced activity within the insula was observed during both the imitative expression of facial emotions and also in EEI task, where requirements of the experiment bear only an indirect relationship to interoceptive and emotion experiential functions (Critchley et al. 2004; Reiman et al. 1997). In this thesis, right anterior insula is related to second-order representations of emotional state, including feelings arising from the interpretation of interoceptive responses and self-generated emotion (Critchley et al. 2004; Phan et al. 2002; Reiman et al. 1997). However, recognition and experience of disgust also engages insula but at a more ventral region (Calder 2003; Calder et al. 2000; Krolak-Salmon et al. 2003),

suggesting somatotopical organization of primitive and higher-order emotion processing at anterior insula.

Accordingly, the empirical observations of my thesis extend the conventional roles of STS and insula from perceptual/experiential perspectives to the interface between expression, experience and perception; three fundamental yet inter-related sub-modules of emotion systems. My work endorses their active participation in the expressive dimension of social interaction.

8.1.3 Central hardwiring or facial feedback?

The modulatory role of posed facial emotions on affective judgment bias is explicitly tested and described in chapter 5, in an experiment that is directly relevant to the *facial feedback hypothesis* (Adelmann & Zajonc 1989). The task I adopted did not eschew subjective awareness of posed emotion, but was an attempt to address the interplay between actively posed emotion expression and the appraisal of observed emotions, a process that happens in our daily social life. The underlying neural substrates for this interaction engaged amygdala and STS, rather than somatomotor/somatosensory regions (i.e. PM or PC). But my DCM analysis revealed that the same modulatory effect of posed facial expression on emotional judgments occurred most strongly at the level of STS-to-PC connection, not PM-to-PC or PM-to-PFC. This observation is only partly consistent with a sensory-motor facial feedback account. Generally, my thesis supports a more conservative contention that central, hard-wired connections between motoric and affective areas of the brain involved in emotion expression (Ekman 1992).

8.1.4 Emotional or social?

What information does an expression typically convey? Besides the classic affective interpretation (Ekman 1972), different theorists have attributed a wide range of meanings to facial movements. The strongest challenge to affective interpretation perhaps came from the *social motives-communicative hypothesis* (Fridlund 1994). In my work, emotion centres (including amygdala, rostral cingulate cortex and insula) and social-signal processing regions (notably STS) were also involved in the expression of emotion. Although these observations support both emotional and social accounts, there is a point that warrants addressing here: affective and social functions are not mutually exclusive, and their integrated contribution to "emotional" expression is reflected in their synchronized neural activation pattern. My work echoes the

close relationship between emotion expression and socialization shaped through evolution (Ekman 1997; Fridlund 1991).

8.2 EMOTIONAL INFLUENCES ON BEHAVIOUR

Emotion is traditionally defined at behavioural and physiology levels (Ekman 1972; James 1894). Positive and negative affective states are linked to approach and withdrawal behaviours. The differential engagement of these facilitatory and inhibitory motivational systems is proposed to account for asymmetry in emotion-related brain activity (observed especially during electroencephalographic (EEG) studies; (Davidson 1995; Davidson et al. 1990)). However, emerging evidence has called for the separation of emotion valences (positive vs. negative) and motivational states (approaching versus withdrawal) (Harmon-Jones et al. 1998; Wacker et al. 2003). Besides, even during face-to-face interactions, the emotion-laden face is not necessarily the target we react to. For example, watching a companion's fearful face generally indicates something fearful is nearby or approaching, and it is to this environmental stimulus that we need to tailor subsequent approach or withdrawal responses. I investigated this issue from a low level perspective by dissociating the emotion influences on the target which cued participants' reaction from the emotional face which the participants viewed.

I developed two new versions of an emotional GO/NOGO task, in which I could examine response execution and response inhibition separately. The first was an eye-gaze cued emotional GO/NOGO task that probed the influences of perceived emotional challenges on behaviour. The second 'emotion-induction GO/NOGO' task explored influence of sustained affective states on behavioural responses execution and inhibition.

8.2.1 Emotion influence on response execution (GO)

Both the presence of an emotional signal (fear) and the maintenance of affective states (fearful and happy) enhanced neural response within somatosensory regions, concordant with previous neuroimaging studies (Damasio et al. 2000). Emotion thus regulates internal organismic states partly through preparedness or mobilization of action resource. My results also speak to emotion specificity: The enhanced neural responses were not a product of a generalized factor, such like attention or arousal.

In the emotion-induction GO/NOGO design, cuing of responses bimanually to left and to right sides also enabled me to explore neural lateralization of affective influences on behaviour. Broadly the *right-hemisphere hypothesis* was supported for both happy and fearful emotions (Demaree et al. 2005). However, my finding provided a novel insight into the lateralization issue: Lateralization is not necessarily an anatomical question regarding the location of emotion centres within the right or left hemispheres, but may arise through the differential influence or modulation of behaviour exerted by emotional representations. In other words, it is the influence of emotion on neuroanatomical structures that is asymmetrical.

8.2.2 Emotion influence on response inhibition (NOGO)

The inferior frontal gyrus (BA 47) is frequently implicated as a neural node of response inhibition (Durston et al. 2002; Konishi et al. 1999; Matsubara et al. 2004; Menon et al. 2001; Nakata et al. 2005; Schulz et al. 2005). The neural response within BA 47 during NOGO trials was attenuated during a fearful mood state but enhanced when viewing a fearful face. Accordingly, the subjective experience of the same fearful state engendered an opposite neural influence on the brain substrates supporting response inhibition. The neural response of BA 47 during a happy mood state was not different from that observed in the neutral state. In contrast to GO trials, no obvious lateralization pattern was observed for emotion-modulated response inhibition.

Overall, the affective modulation of behaviour-related neural responses (either through emotion perception or via induced subjective affective states) was context and structure -dependent. My work extends understanding of the affective modulation of behaviour beyond the stereotyped approach/withdrawal response tendencies; and implies that 'emotion' provides a flexible emotional/social dynamic, to which implicit responsivity at both neural and behavioural levels is shaped by concurrent contextual demands of response requirement.

8.3 LIMITATIONS OF THIS THESIS AND IMPLICATION FOR FUTURE WORK

8.3.1 Limitation of this thesis

There are several limitations regarding conceptual frame and methodology of this thesis acknowledged here. This thesis focused on the response of central

nervous system to emotion and thus clarification of neural network and pathway was the main concern. To make inference based upon this work to behavioural or psychological disciplines is not always appropriate. The underlying difficulties arise from the mystery of body/mind relationship which was sometimes iterated as computer hardware/software analogy (de Zubicaray et al. 2000). Information processing at abstraction level (mind/psychology) does not necessarily depend on the physical property of a system (body/brain). Knowing the hardware implementation does not self-explain the diversity of software algorithm. The possibility of alternative interpretation always exists.

Study human emotion expression is accompanied with a challenge to the experiment design. Unlike perceptual studies where isolation of a psychological construct is tenable, it is not easy to find a facial expression concordant with a particular emotion but is not emotional. Take colour imaging study as an example, comparison of coloured- with black-and-white- objects is expected to isolate brain regions for colour processing. The confounding factors from form, shape and related semantics are contrasted out. However, it is hard to imagine to extract emotional "colour" from the face while still keep emotional configuration on the face. This thesis thus took ingestive movements (chapter 3), Simon task (chapter 4) and age judgment (chapter 5) as comparison, not an optimal control in a strict sense. Besides, facial emotion expression perhaps has adverse effect on the imaging signal quality because of the associated head movements. The power of my analysis could be lessened by these innate difficulties.

Summarizing imaging findings to fit a plausible brain model is an interesting and emerging field in neuroscience. My attempt to construct a DCM model encountered several conceptual challenges. First, DCM is a multi-nodal approach which innately cannot handle distributed parallel network/model (Morecraft et al. 2004; Zhang et al. 1999). In other words, DCM may not be able to reflect the true dynamics in the brain. Second, the number of neural nodes hosted in DCM model is limited, prohibiting from modelling an orchestrated network with larger number of neural nodes. My neural model of emotion judgment which is modulated by actively posed expression, could therefore miss the neural nodes of other face and perhaps emotion processing (fusiform gyrus), motion/movement assessment (middle temporal region), emotion experience (precuneus and insula) and semantic processing

(frontal regions and inferior parietal regions). Further, current DCM model is capable of managing the modulatory influence of psychological factors on the physiological signals. It would be of interest to examine how a particular anatomical structure, say amygdala, modulates the connectivity between distant brain regions. This approach of physiological-physiological interaction requires refinement of current DCM algorithm.

8.3.2 Implication for future work

This thesis clarifies a number of issues relating to emotional expression at "face" and "body" levels, and provides several methodological and conceptual implications for future work on emotion expression and related disciplines.

First, putting metrics of facial movement into neuroimaging analyses may help identify expression-related neural mechanisms in a more powerful and sensitive way. The method introduced in this thesis can be applied to Tourette syndrome, stroke with facial palsy or in addressing dimensional characteristics of non-fundamental emotions. Besides, some non-classical/atypical emotions, e.g. shame and guilt, lack universal facial expression. The central network of these emotions can be accessed by similar method by introducing correlated physiological responses into the analysis.

Second, connectivity analysis, especially DCM, represents a useful approach to elucidate the organization of the "hard-wired connections" between emotion expression and other mental modules. My work illustrates how the combination of DCM and Bayesian frameworks for model comparison can be used to examine the interplays between emotion expression and other cognitive and executive mental modules. My work also encourages refinement to enable hosting larger number of neural nodes.

Third, although the interference effect of emotion expression has been established, the underlying mechanisms need further exploration. To dissect various sources, emotion expression interference across different modalities is of interest. Non-face emotion-laden material, like words or pictures of animals/landscape, can be adopted to test the incongruence from semantics and non-face pathways.

Fourth, this thesis explored how posed expressions bias emotion judgment, which happened in daily life. It is also of interest to take various strategies

eschewing awareness, like direction facial action or non-obtrusive tasks (Ekman et al. 1983; Strack et al. 1988), and compare the results of different approaches. This will help to validate or reject "facial feedback hypothesis".

Fifth, prevalent approaches to interactions between emotion and behaviour should be re-appraised beyond stereotyped response patterns. It is of interest to investigate how different emotions influence response execution and inhibition, whether they work through common pathways or show emotion specificity.

Last, questions relating to emotion lateralization can be framed at a function level in contrast to traditional anatomical level. This finding is concordant with the general impression that emotion asymmetry is most consistent for psychological studies, less for brain-damaged patient studies, and least for neuroimaging studies.

References

Ackermann RF, Finch DM, Babb TL, Engel J, Jr. (1984) Increased glucose metabolism during long-duration recurrent inhibition of hippocampal pyramidal cells *J Neurosci* **4**, 251-64.

Adelmann PK, Zajonc RB (1989) Facial efference and the experience of emotion *Annu Rev Psychol* **40**, 249-80.

Adolphs R, Damasio H, Tranel D, Damasio AR (1996) Cortical systems for the recognition of emotion in facial expressions *J Neurosci* **16**, 7678-87.

Allison T, Puce A, McCarthy G (2000) Social perception from visual cues: role of the STS region *Trends Cogn Sci* **4**, 267-78.

Amaral DG, Price JL, Pktkanen A, Carmichael ST (1992) Anatomical organization of the primate amygdaloid complex, in: J. Aggleton (Ed.), The Amygdala: Neurobiological Aspects of Emotion, Memory, And Mental Dysfunction, Wiley-Liss, New York, 1-66.

Andersen RA, Buneo CA (2002) Intentional maps in posterior parietal cortex *Annu Rev Neurosci* **25**, 189-220.

Andersson JL, Hutton C, Ashburner J, Turner R, Friston KJ (2001) Modeling geometric deformations in EPI time series *Neuroimage* **13**, 903-19.

Arkadir D, Morris G, Vaadia E, Bergman H (2004) Independent coding of movement direction and reward prediction by single pallidal neurons *J Neurosci* **24**, 10047-56.

Armony JL, Dolan RJ (2002) Modulation of spatial attention by fear-conditioned stimuli: an event-related fMRI study *Neuropsychologia* **40**, 817-26.

Ashby FG, Isen AM, Turken AU (1999) A neuropsychological theory of positive affect and its influence on cognition *Psychol Rev* **106**, 529-50.

Baas D, Aleman A, Kahn RS (2004) Lateralization of amygdala activation: a systematic review of functional neuroimaging studies *Brain Res Brain Res Rev* **45**, 96-103.

Bargh JA, Chen M, Burrows L (1996) Automaticity of social behavior: direct effects of trait construct and stereotype-activation on action *J Pers Soc Psychol* **71**, 230-44.

Bentall RP, Thompson M (1990) Emotional Stroop performance and the manic defence *Br J Clin Psychol* **29 (Pt 2)**, 235-7.

Bermond B, Nieuwenhuyse B, Fasotti L, Schuerman J (1991) Spinal. cord lesions, peripheral feedback, and intensities of emotional feelings *Cognition and Emotion* **5**, 201-20.

Binkofski F, Buccino G (2004) Motor functions of the Broca's region *Brain Lang* **89**, 362-9.
Bitan T, Booth JR, Choy J, Burman DD, Gitelman DR, Mesulam MM (2005) Shifts of effective connectivity within a language network during rhyming and spelling *J Neurosci* **25**, 5397-403.
Blonder LX, Heilman KM, Ketterson T et al. (2005) Affective facial and lexical expression in aprosodic versus aphasic stroke patients *J Int Neuropsychol Soc* **11**, 677-85.
Bonvento G, Sibson N, Pellerin L (2002) Does glutamate image your thoughts? *Trends Neurosci* **25**, 359-64.
Borod JC (1992) Interhemispheric and intrahemispheric control of emotion: a focus on unilateral brain damage *J Consult Clin Psychol* **60**, 339-48.
Borod JC, Haywood CS, Koff E (1997) Neuropsychological aspects of facial asymmetry during emotional expression: a review of the normal adult literature *Neuropsychol Rev* **7**, 41-60.
Bracha HS (2004) Freeze, flight, fight, fright, faint: adaptationist perspectives on the acute stress response spectrum *CNS Spectr* **9**, 679-85.
Bradley MM, Sabatinelli D, Lang PJ, Fitzsimmons JR, King W, Desai P (2003) Activation of the visual cortex in motivated attention *Behav Neurosci* **117**, 369-80.
Braver TS, Barch DM, Gray JR, Molfese DL, Snyder A (2001) Anterior cingulate cortex and response conflict: effects of frequency, inhibition and errors *Cereb Cortex* **11**, 825-36.
Britton JC, Phan KL, Taylor SF, Welsh RC, Berridge KC, Liberzon I (2006) Neural correlates of social and nonsocial emotions: An fMRI study *Neuroimage* **31**, 397-409.
Brothers L (1990) The social brain: a project for integrating primate behaviour and neurophysiology in a new domain *Concepts of Neuroscience* **1**, 27-51.
Brown LL, Schneider JS, Lidsky TI (1997) Sensory and cognitive functions of the basal ganglia *Curr Opin Neurobiol* **7**, 157-63.
Buccino G, Binkofski F, Fink GR et al. (2001) Action observation activates premotor and parietal areas in a somatotopic manner: an fMRI study *Eur J Neurosci* **13**, 400-4.
Buchel C, Holmes AP, Rees G, Friston KJ (1998a) Characterizing stimulus-response functions using nonlinear regressors in parametric fMRI experiments *Neuroimage* **8**, 140-8.
Buchel C, Morris J, Dolan RJ, Friston KJ (1998b) Brain systems mediating aversive conditioning: an event-related fMRI study *Neuron* **20**, 947-57.

Bullmore E, Horwitz B, Honey G, Brammer M, Williams S, Sharma T (2000) How good is good enough in path analysis of fMRI data? *Neuroimage* **11**, 289-301.

Burgess PW, Scott SK, Frith CD (2003) The role of the rostral frontal cortex (area 10) in prospective memory: a lateral versus medial dissociation *Neuropsychologia* **41**, 906-18.

Bush G, Luu P, Posner MI (2000) Cognitive and emotional influences in anterior cingulate cortex *Trends Cogn Sci* **4**, 215-22.

Bush G, Whalen PJ, Rosen BR, Jenike MA, McInerney SC, Rauch SL (1998) The counting Stroop: an interference task specialized for functional neuroimaging--validation study with functional MRI *Hum Brain Mapp* **6**, 270-82.

Buxton RB, Frank LR (1997) A model for the coupling between cerebral blood flow and oxygen metabolism during neural stimulation *J Cereb Blood Flow Metab* **17**, 64-72.

Buxton RB, Wong EC, Frank LR (1998) Dynamics of blood flow and oxygenation changes during brain activation: the balloon model *Magn Reson Med* **39**, 855-64.

Calder AJ (2003) Disgust discussed *Ann Neurol* **53**, 427-8.

Calder AJ, Keane J, Manes F, Antoun N, Young AW (2000) Impaired recognition and experience of disgust following brain injury *Nat Neurosci* **3**, 1077-8.

Calder AJ, Lawrence AD, Young AW (2001) Neuropsychology of fear and loathing *Nat Rev Neurosci* **2**, 352-63.

Caplan D, Moo L (2004) Cognitive conjunction and cognitive functions *Neuroimage* **21**, 751-6.

Cardinal RN, Parkinson JA, Hall J, Everitt BJ (2002) Emotion and motivation: the role of the amygdala, ventral striatum, and prefrontal cortex *Neurosci Biobehav Rev* **26**, 321-52.

Carpenter RHS (1988) Movements of the eyes *London: Pion.*

Carr L, Iacoboni M, Dubeau MC, Mazziotta JC, Lenzi GL (2003) Neural mechanisms of empathy in humans: a relay from neural systems for imitation to limbic areas *Proc Natl Acad Sci U S A* **100**, 5497-502.

Carter CS, Botvinick MM, Cohen JD (1999) The contribution of the anterior cingulate cortex to executive processes in cognition *Rev Neurosci* **10**, 49-57.

Casey BJ, Forman SD, Franzen P et al. (2001) Sensitivity of prefrontal cortex to changes in target probability: a functional MRI study *Hum Brain Mapp* **13**, 26-33.

Chainay H, Krainik A, Tanguy ML, Gerardin E, Le Bihan D, Lehericy S (2004) Foot, face and hand representation in the human supplementary motor area *Neuroreport* **15**, 765-9.
Chaminade T, Fonlupt P (2003) Changes of effective connectivity between the lateral and medial parts of the prefrontal cortex during a visual task *Eur J Neurosci* **18**, 675-9.
Coan JA, Allen JJ (2004) Frontal EEG asymmetry as a moderator and mediator of emotion *Biol Psychol* **67**, 7-49.
Compton RJ, Banich MT, Mohanty A et al. (2003) Paying attention to emotion: an fMRI investigation of cognitive and emotional stroop tasks *Cogn Affect Behav Neurosci* **3**, 81-96.
Critchley HD (2005) Neural mechanisms of autonomic, affective, and cognitive integration *J Comp Neurol* **493**, 154-66.
Critchley HD, Elliott R, Mathias CJ, Dolan RJ (2000) Neural activity relating to generation and representation of galvanic skin conductance responses: a functional magnetic resonance imaging study *J Neurosci* **20**, 3033-40.
Critchley HD, Mathias CJ, Josephs O et al. (2003) Human cingulate cortex and autonomic control: converging neuroimaging and clinical evidence *Brain* **126**, 2139-52.
Critchley HD, Rotshtein P, Nagai Y, O'Doherty J, Mathias CJ, Dolan RJ (2005a) Activity in the human brain predicting differential heart rate responses to emotional facial expressions *Neuroimage* **24**, 751-62.
Critchley HD, Tang J, Glaser D, Butterworth B, Dolan RJ (2005b) Anterior cingulate activity during error and autonomic response *Neuroimage* **27**, 885-95.
Critchley HD, Wiens S, Rotshtein P, Ohman A, Dolan RJ (2004) Neural systems supporting interoceptive awareness *Nat Neurosci* **7**, 189-95.
Damasio AR, Grabowski TJ, Bechara A et al. (2000) Subcortical and cortical brain activity during the feeling of self-generated emotions *Nat Neurosci* **3**, 1049-56.
Darwin CR (1872) The expression of the emotions in man and animals *John Murray, London.*
Davidson RJ (1995) Cerebral asymmetry, emotion, and affective style. In R. J. Davidson & K. Hugdahl (Eds.) *Brain asymmetry (pp. 361-387). Cambridge, MA: MIT Press.*
Davidson RJ, Ekman P, Saron CD, Senulis JA, Friesen WV (1990) Approach-withdrawal and cerebral asymmetry: emotional expression and brain physiology. I *J Pers Soc Psychol* **58**, 330-41.

Davidson RJ, Jackson DC, Kalin NH (2000) Emotion, plasticity, context, and regulation: perspectives from affective neuroscience *Psychol Bull* **126**, 890-909.
de Zubicaray GI, Andrew C, Zelaya FO, Williams SC, Dumanoir C (2000) Motor response suppression and the prepotent tendency to respond: a parametric fMRI study *Neuropsychologia* **38**, 1280-91.
Deichmann R, Gottfried JA, Hutton C, Turner R (2003) Optimized EPI for fMRI studies of the orbitofrontal cortex *Neuroimage* **19**, 430-41.
Demaree HA, Everhart DE, Youngstrom EA, Harrison DW (2005) Brain lateralization of emotional processing: historical roots and a future incorporating "dominance" *Behav Cogn Neurosci Rev* **4**, 3-20.
Devinsky O, Morrell MJ, Vogt BA (1995) Contributions of anterior cingulate cortex to behaviour *Brain* **118 (Pt 1)**, 279-306.
Dimberg U (1982) Facial reactions to facial expressions *Psychophysiology* **19**, 643-7.
Dimberg U (1986) Facial reactions to fear-relevant and fear-irrelevant stimuli *Biol Psychol* **23**, 153-61.
Dimberg U (1987) Facial reactions, autonomic activity and experienced emotion: a three component model of emotional conditioning *Biol Psychol* **24**, 105-22.
Dimberg U (1990) Facial electromyography and emotional reactions *Psychophysiology* **27**, 481-94.
Dimberg U, Thunberg M, Grunedal S (2002) Facial reactions to emotional stimuli: Automatically controlled emotional responses *Cognition and Emotion* **16**, 449-71.
Dolan RJ (2002) Emotion, cognition, and behavior *Science* **298**, 1191-4.
Dougherty DD, Rauch SL, Deckersbach T et al. (2004) Ventromedial prefrontal cortex and amygdala dysfunction during an anger induction positron emission tomography study in patients with major depressive disorder with anger attacks *Arch Gen Psychiatry* **61**, 795-804.
Drevets WC, Raichle ME (1998) Reciprocal suppression of regional cerebral blood during emotional versus higher cognitive implications for interactions between emotion and cognition *Emotion & Cognition* **12**, 353-85.
Durston S, Thomas KM, Worden MS, Yang Y, Casey BJ (2002a) The effect of preceding context on inhibition: an event-related fMRI study *Neuroimage* **16**, 449-53.

Durston S, Thomas KM, Yang Y, Ulug AM, Zimmerman RD, Casey BJ (2002b) A neural basis for the development of inhibitory control *Developmental Science* **5**, F9-16.
Eisenberger NI, Lieberman MD, Williams KD (2003) Does rejection hurt? An FMRI study of social exclusion *Science* **302**, 290-2.
Ekman P (1972) Universal and cultural differences in facial expressions of emotion. In J. Cole (Ed.), Nebraska Symposium on Motivation (pp. 207-283). *Lincoln: University of Nebraska Press.*
Ekman P (1992) Facial expressions of emotion: an old controversy and new findings *Philos Trans R Soc Lond B Biol Sci* **335**, 63-9.
Ekman P (1993) Facial expression and emotion *Am Psychol* **48**, 384-92.
Ekman P (1997) Should we call it expression or communication? *Innovations in Social Science Research* **10**, 333.
Ekman P, Friesen WV (1975) Pictures of facial affect *Palo Alto, CA: Consulting Psychologists Press.*
Ekman P, Friesen WV, Ancoli S (1980) Facial signs of emotional experience *J Pers Soc Psychol* **39**, 1125-34.
Ekman P, Levenson RW, Friesen WV (1983) Autonomic nervous system activity distinguishes among emotions *Science* **221**, 1208-10.
Elliott R, Dolan RJ, Frith CD (2000a) Dissociable functions in the medial and lateral orbitofrontal cortex: evidence from human neuroimaging studies *Cereb Cortex* **10**, 308-17.
Elliott R, Friston KJ, Dolan RJ (2000b) Dissociable neural responses in human reward systems *J Neurosci* **20**, 6159-65.
Ellis HC, Thomas RL, McFarland AD, Lane JW (1985) Emotional mood states and retrieval in episodic memory *J Exp Psychol Learn Mem Cogn* **11**, 363-70.
Ethofer T, Anders S, Erb M et al. (2006) Cerebral pathways in processing of affective prosody: a dynamic causal modeling study *Neuroimage* **30**, 580-7.
Fadiga L, Craighero L (2004) Electrophysiology of action representation *J Clin Neurophysiol* **21**, 157-69.
Fellows LK, Boutelle MG, Fillenz M (1993) Physiological stimulation increases nonoxidative glucose metabolism in the brain of the freely moving rat *J Neurochem* **60**, 1258-63.
Ferrari PF, Gallese V, Rizzolatti G, Fogassi L (2003) Mirror neurons responding to the observation of ingestive and communicative mouth actions in the monkey ventral premotor cortex *Eur J Neurosci* **17**, 1703-14.

Fitts PM, Deininger RL (1954) S-R compatibility: correspondence among paired elements within stimulus and response codes *J Exp Psychol* **48**, 483-92.
Fox NA (1991) If it's not left, it's right. Electroencephalograph asymmetry and the development of emotion *Am Psychol* **46**, 863-72.
Fransson P, Kruger G, Merboldt KD, Frahm J (1998a) Physiologic aspects of event related paradigms in magnetic resonance functional neuroimaging *Neuroreport* **9**, 2001-5.
Fransson P, Kruger G, Merboldt KD, Frahm J (1998b) Temporal characteristics of oxygenation-sensitive MRI responses to visual activation in humans *Magn Reson Med* **39**, 912-9.
Fridlund AJ (1994) Human facial expression: An evolutionary view *San Diego, CA: Academic.*
Fridlund AJ, Cacioppo JT (1986) Guidelines for human electromyographic research *Psychophysiology* **23**, 567-89.
Friesen CK, Kingstone A (1998) The eyes have it! Reflexive. orienting is triggered by nonpredictive gaze. *Psychonomic Bulletin. & Review* **5**, 490-95.
Frijda NH (1986) The emotions *Cambridge, England: Cambridge University Press.*
Friston KJ (2003) Introduction: Experimental design and Statistical Parametric Mapping *Human Brain Function. London Academic Press, 2nd edition.*
Friston KJ, Ashburner J, Frith CD, Poline JB, Heather JD, Frackowiak RSJ (1995) Spatial registration and normalization of images *Hum Brain Mapp* **3**, 165-89.
Friston KJ, Frith CD, Frackowiak RS (1993a) Time-Dependent Changes in Effective Connectivity Measured With PET *Hum Brain Mapp* **1**, 69-80.
Friston KJ, Frith CD, Liddle PF, Frackowiak RS (1993b) Functional connectivity: the principal-component analysis of large (PET) data sets *J Cereb Blood Flow Metab* **13**, 5-14.
Friston KJ, Glaser DE, Henson RN, Kiebel S, Phillips C, Ashburner J (2002) Classical and Bayesian inference in neuroimaging: applications *Neuroimage* **16**, 484-512.
Friston KJ, Harrison L, Penny W (2003) Dynamic causal modelling *Neuroimage* **19**, 1273-302.
Friston KJ, Mechelli A, Turner R, Price CJ (2000) Nonlinear responses in fMRI: the Balloon model, Volterra kernels, and other hemodynamics *Neuroimage* **12**, 466-77.

Frith CD, Frith U (1999) Interacting minds--a biological basis *Science* **286**, 1692-5.
Gehring WJ, Fencsik DE (2001) Functions of the medial frontal cortex in the processing of conflict and errors *J Neurosci* **21**, 9430-7.
George MS, Ketter TA, Gill DS et al. (1993) Brain regions involved in recognizing facial emotion or identity: an oxygen-15 PET study *J Neuropsychiatry Clin Neurosci* **5**, 384-94.
Georgiou GA, Bleakley C, Hayward J et al. (2005) Focusing on fear: Attentional disengagement from emotional faces *Vis cogn* **12**, 145-58.
Gerloff C, Andres FG (2002) Bimanual coordination and interhemispheric interaction *Acta Psychol (Amst)* **110**, 161-86.
Girden E (1943) Role of the response mechanism in learning and in 'excited emotion' *Am J Physiol* **56**, 1-20.
Gorelick PB, Ross ED (1987) The aprosodias: further functional-anatomical evidence for the organisation of affective language in the right hemisphere *J Neurol Neurosurg Psychiatry* **50**, 553-60.
Gould RL, Brown RG, Owen AM, ffytche DH, Howard RJ (2003) fMRI BOLD response to increasing task difficulty during successful paired associates learning *Neuroimage* **20**, 1006-19.
Gray JR (2001) Emotional modulation of cognitive control: approach-withdrawal states double-dissociate spatial from verbal two-back task performance *J Exp Psychol Gen* **130**, 436-52.
Gray JR, Braver TS, Raichle ME (2002) Integration of emotion and cognition in the lateral prefrontal cortex *Proc Natl Acad Sci U S A* **99**, 4115-20.
Gray M, McNaughton N (2000) The neuropsychology of anxiety (2nd ed.) *New York: Oxford University Press.*
Grezes J, Decety J (2001) Functional anatomy of execution, mental simulation, observation, and verb generation of actions: a meta-analysis *Hum Brain Mapp* **12**, 1-19.
Gross JJ (1998) Antecedent- and response-focused emotion regulation: divergent consequences for experience, expression, and physiology *J Pers Soc Psychol* **74**, 224-37.
Gross JJ, John OP (2003) Individual differences in two emotion regulation processes: implications for affect, relationships, and well-being *J Pers Soc Psychol* **85**, 348-62.
Hagemann D, Hewig J, Seifert J, Naumann E, Bartussek D (2005) The latent state-trait structure of resting EEG asymmetry: replication and extension *Psychophysiology* **42**, 740-52.

Halliday MS (1966) Exploration and fear in the rat *Symposium of the Zoological Society of London* **18**, 45-59.
Hamann S, Mao H (2002) Positive and negative emotional verbal stimuli elicit activity in the left amygdala *Neuroreport* **13**, 15-9.
Hamann SB, Ely TD, Grafton ST, Kilts CD (1999) Amygdala activity related to enhanced memory for pleasant and aversive stimuli *Nat Neurosci* **2**, 289-93.
Hare TA, Tottenham N, Davidson MC, Glover GH, Casey BJ (2005) Contributions of amygdala and striatal activity in emotion regulation *Biol Psychiatry* **57**, 624-32.
Hari R, Forss N, Avikainen S, Kirveskari E, Salenius S, Rizzolatti G (1998) Activation of human primary motor cortex during action observation: a neuromagnetic study *Proc Natl Acad Sci U S A* **95**, 15061-5.
Hariri AR, Bookheimer SY, Mazziotta JC (2000) Modulating emotional responses: effects of a neocortical network on the limbic system *Neuroreport* **11**, 43-8.
Hariri AR, Mattay VS, Tessitore A, Fera F, Weinberger DR (2003) Neocortical modulation of the amygdala response to fearful stimuli *Biol Psychiatry* **53**, 494-501.
Harmon-Jones E, Allen JJ (1998) Anger and frontal brain activity: EEG asymmetry consistent with approach motivation despite negative affective valence *J Pers Soc Psychol* **74**, 1310-6.
Haxby JV, Hoffman EA, Gobbini MI (2000) The distributed human neural system for face perception *Trends Cogn Sci* **4**, 223-33.
Hayward G, Goodwin GM, Harmer CJ (2004) The role of the anterior cingulate cortex in the counting Stroop task *Exp Brain Res* **154**, 355-8.
Heberlein AS, Adolphs R, Tranel D, Damasio H (2004) Cortical regions for judgments of emotions and personality traits from point-light walkers *J Cogn Neurosci* **16**, 1143-58.
Heeger DJ, Boynton GM, Demb JB, Seidemann E, Newsome WT (1999) Motion opponency in visual cortex *J Neurosci* **19**, 7162-74.
Heinen SJ, Rowland J, Lee BT, Wade AR (2006) An oculomotor decision process revealed by functional magnetic resonance imaging *J Neurosci* **26**, 13515-22.
Heller W, Nitschke JB, Miller GA (1998) Lateralization in Emotion and Emotional Disorders *Current Directions in Psychological Science* **7**, 26-32.
Hennenlotter A, Schroeder U, Erhard P et al. (2005) A common neural basis for receptive and expressive communication of pleasant facial affect *Neuroimage* **26**, 581-91.

Hietanen JK (1999) Does your gaze direction and head orientation shift my visual attention? *Neuroreport* **10**, 3443-7.
Hoff EC, Green HD (1936) Cardiovascular reactions induced by electrical stimulation of the cerebral cortex *Am J Physiol* **117**, 411-22.
Hollerman JR, Tremblay L, Schultz W (2000) Involvement of basal ganglia and orbitofrontal cortex in goal-directed behavior *Prog Brain Res* **126**, 193-215.
Horn NR, Dolan M, Elliott R, Deakin JF, Woodruff PW (2003) Response inhibition and impulsivity: an fMRI study *Neuropsychologia* **41**, 1959-66.
Hornak J, Rolls ET, Wade D (1996) Face and voice expression identification in patients with emotional and behavioural changes following ventral frontal lobe damage *Neuropsychologia* **34**, 247-61.
Hu S, Wan H (2003) Imagined events with specific emotional valence produce specific patterns of facial EMG activity *Percept Mot Skills* **97**, 1091-9.
Hunter MD, Green RD, Wilkinson ID, Spence SA (2004) Spatial and temporal dissociation in prefrontal cortex during action execution *Neuroimage* **23**, 1186-91.
Hyder F, Chase JR, Behar KL et al. (1996) Increased tricarboxylic acid cycle flux in rat brain during forepaw stimulation detected with 1H[13C]NMR *Proc Natl Acad Sci U S A* **93**, 7612-7.
Iacoboni M, Woods RP, Brass M, Bekkering H, Mazziotta JC, Rizzolatti G (1999) Cortical mechanisms of human imitation *Science* **286**, 2526-8.
Izard CE, Kagan J, Zajonc RB (1984) *Emotions, congition and behavior* Cambridge, MA: Cambridge University Press.
James W (1894) The physical basis of emotion *Psychological Review* **101**, 205-10.
Keil A, Gruber T, Muller MM et al. (2003) Early modulation of visual perception by emotional arousal: evidence from steady-state visual evoked brain potentials *Cogn Affect Behav Neurosci* **3**, 195-206.
Kennedy C, Des Rosiers MH, Sakurada O et al. (1976) Metabolic mapping of the primary visual system of the monkey by means of the autoradiographic [14C]deoxyglucose technique *Proc Natl Acad Sci U S A* **73**, 4230-4.
Kesler-West ML, Andersen AH, Smith CD et al. (2001) Neural substrates of facial emotion processing using fMRI *Brain Res Cogn Brain Res* **11**, 213-26.
Kilts CD, Egan G, Gideon DA, Ely TD, Hoffman JM (2003) Dissociable neural pathways are involved in the recognition of emotion in static and dynamic facial expressions *Neuroimage* **18**, 156-68.

Kipps CM, Duggins AJ, McCusker EA, Calder AJ (2007) Disgust and happiness recognition correlate with anteroventral insula and amygdala volume respectively in preclinical Huntington's disease *J Cogn Neurosci* **19**, 1206-17.

Konishi S, Nakajima K, Uchida I, Kikyo H, Kameyama M, Miyashita Y (1999) Common inhibitory mechanism in human inferior prefrontal cortex revealed by event-related functional MRI *Brain* **122 (Pt 5)**, 981-91.

Krawczyk DC (2002) Contributions of the prefrontal cortex to the neural basis of human decision making *Neurosci Biobehav Rev* **26**, 631-64.

Krolak-Salmon P, Henaff MA, Isnard J et al. (2003) An attention modulated response to disgust in human ventral anterior insula *Ann Neurol* **53**, 446-53.

Lanius RA, Frewen PA, Girotti M, Neufeld RW, Stevens TK, Densmore M (2007) Neural correlates of trauma script-imagery in posttraumatic stress disorder with and without comorbid major depression: a functional MRI investigation *Psychiatry Res* **155**, 45-56.

Lavric A, Pizzagalli DA, Forstmeier S (2004) When 'go' and 'nogo' are equally frequent: ERP components and cortical tomography *Eur J Neurosci* **20**, 2483-8.

Lawrence EJ, Shaw P, Baker D, Baron-Cohen S, David AS (2004) Measuring empathy: reliability and validity of the Empathy Quotient *Psychol Med* **34**, 911-9.

LeDoux JE, Iwata J, Cicchetti P, Reis DJ (1988) Different projections of the central amygdaloid nucleus mediate autonomic and behavioral correlates of conditioned fear *J Neurosci* **8**, 2517-29.

Lee TW, Dolan RJ, Critchley HD (2007) Controlling emotional expression: Behavioural and neural correlates of non-imitative emotional responses *Cereb Cortex*, doi:10.1093/cercor/bhm035.

Lee TW, Josephs O, Dolan RJ, Critchley HD (2006) Imitating expressions: Emotion-specific neural substrates in facial mimicry *Social Cognitive and Affective Neuroscience* **1**, 122-35.

Leslie KR, Johnson-Frey SH, Grafton ST (2004) Functional imaging of face and hand imitation: towards a motor theory of empathy *Neuroimage* **21**, 601-7.

Levenson RW, Ekman P, Friesen WV (1990) Voluntary facial action generates emotion-specific autonomic nervous system activity *Psychophysiology* **27**, 363-84.

Liberzon I, Phan KL, Decker LR, Taylor SF (2003) Extended amygdala and emotional salience: a PET activation study of positive and negative affect *Neuropsychopharmacology* **28**, 726-33.

Liotti M, Mayberg HS, Brannan SK, McGinnis S, Jerabek P, Fox PT (2000) Differential limbic--cortical correlates of sadness and anxiety in healthy subjects: implications for affective disorders *Biol Psychiatry* **48**, 30-42.
Logothetis NK, Pauls J, Augath M, Trinath T, Oeltermann A (2001) Neurophysiological investigation of the basis of the fMRI signal *Nature* **412**, 150-7.
Lotze M, Heymans U, Birbaumer N et al. (2006) Differential cerebral activation during observation of expressive gestures and motor acts *Neuropsychologia* **44**, 1787-95.
MacLeod CM (1991) Half a century of research on the Stroop effect: an integrative review *Psychol Bull* **109**, 163-203.
Maclin EL, Gratton G, Fabiani M (2001) Visual spatial localization conflict: an fMRI study *Neuroreport* **12**, 3633-6.
Maddock RJ (1999) The retrosplenial cortex and emotion: new insights from functional neuroimaging of the human brain *Trends Neurosci* **22**, 310-6.
Magistretti PJ, Pellerin L (1999) Cellular mechanisms of brain energy metabolism and their relevance to functional brain imaging *Philos Trans R Soc Lond B Biol Sci* **354**, 1155-63.
Malhi GS, Lagopoulos J, Sachdev PS, Ivanovski B, Shnier R (2005) An emotional Stroop functional MRI study of euthymic bipolar disorder *Bipolar Disord* **7 Suppl 5**, 58-69.
Malonek D, Grinvald A (1996) Interactions between electrical activity and cortical microcirculation revealed by imaging spectroscopy: implications for functional brain mapping *Science* **272**, 551-4.
Mandeville JB, Marota JJ, Ayata C et al. (1999) Evidence of a cerebrovascular postarteriole windkessel with delayed compliance *J Cereb Blood Flow Metab* **19**, 679-89.
Marrett S, Meyer E, Kuwabara H, Evans A, Gjedde A (1995) Differential increases of oxygen metabolism in visual cortex *J Cereb Blood Flow Metab* **15**, S80.
Marsden CD, Deecke L, Freund HJ et al. (1996) The functions of the supplementary motor area. Summary of a workshop *Adv Neurol* **70**, 477-87.
Matsubara M, Yamaguchi S, Xu J, Kobayashi S (2004) Neural correlates for the suppression of habitual behavior: a functional MRI study *J Cogn Neurosci* **16**, 944-54.
Matsumoto D (1987) The role of facial response in the experience of emotion: more methodological problems and a meta-analysis *J Pers Soc Psychol* **52**, 769-74.

Mattler U, Wustenberg T, Heinze HJ (2006) Common modules for processing invalidly cued events in the human cortex *Brain Res* **1109**, 128-41.
Mayberg HS, Liotti M, Brannan SK et al. (1999) Reciprocal limbic-cortical function and negative mood: converging PET findings in depression and normal sadness *Am J Psychiatry* **156**, 675-82.
Mechelli A, Henson RN, Price CJ, Friston KJ (2003) Comparing event-related and epoch analysis in blocked design fMRI *Neuroimage* **18**, 806-10.
Mechelli A, Penny WD, Price CJ, Gitelman DR, Friston KJ (2002) Effective connectivity and intersubject variability: using a multisubject network to test differences and commonalities *Neuroimage* **17**, 1459-69.
Menon V, Adleman NE, White CD, Glover GH, Reiss AL (2001) Error-related brain activation during a Go/NoGo response inhibition task *Hum Brain Mapp* **12**, 131-43.
Misslin R (2003) The defense system of fear: behavior and neurocircuitry *Neurophysiol Clin* **33**, 55-66.
Mogg K, Bradley BP, de Bono J, Painter M (1997) Time course of attentional bias for threat information in non-clinical anxiety *Behav Res Ther* **35**, 297-303.
Morecraft RJ, Stilwell-Morecraft KS, Rossing WR (2004) The motor cortex and facial expression: new insights from neuroscience *Neurologist* **10**, 235-49.
Morris JS, Buchel C, Dolan RJ (2001) Parallel neural responses in amygdala subregions and sensory cortex during implicit fear conditioning *Neuroimage* **13**, 1044-52.
Morris JS, deBonis M, Dolan RJ (2002) Human amygdala responses to fearful eyes *Neuroimage* **17**, 214-22.
Moser JS, Hajcak G, Simons RF (2005) The effects of fear on performance monitoring and attentional allocation *Psychophysiology* **42**, 261-8.
Murphy FC, Nimmo-Smith I, Lawrence AD (2003) Functional neuroanatomy of emotions: a meta-analysis *Cogn Affect Behav Neurosci* **3**, 207-33.
Nakamura K, Kawashima R, Ito K et al. (1999) Activation of the right inferior frontal cortex during assessment of facial emotion *J Neurophysiol* **82**, 1610-4.
Nakata H, Inui K, Wasaka T, Akatsuka K, Kakigi R (2005) Somato-motor inhibitory processing in humans: a study with MEG and ERP *Eur J Neurosci* **22**, 1784-92.
Narumoto J, Okada T, Sadato N, Fukui K, Yonekura Y (2001) Attention to emotion modulates fMRI activity in human right superior temporal sulcus *Brain Res Cogn Brain Res* **12**, 225-31.

Norup N, Lauritzen M (2001) Coupling and uncoupling of activity-dependent increases of neuronal activity and blood flow in rat somatosensory cortex *J Physiol* **533**, 773-85.
Nudo RJ, Masterton RB (1986) Stimulation-induced [14C]2-deoxyglucose labeling of synaptic activity in the central auditory system *J Comp Neurol* **245**, 553-65.
O'Doherty JP, Deichmann R, Critchley HD, Dolan RJ (2002) Neural responses during anticipation of a primary taste reward *Neuron* **33**, 815-26.
Ochsner KN, Gross JJ (2005) The cognitive control of emotion *Trends Cogn Sci* **9**, 242-9.
Ochsner KN, Knierim K, Ludlow DH et al. (2004) Reflecting upon feelings: an fMRI study of neural systems supporting the attribution of emotion to self and other *J Cogn Neurosci* **16**, 1746-72.
Ohman A, Flykt A, Esteves F (2001) Emotion drives attention: detecting the snake in the grass *J Exp Psychol Gen* **130**, 466-78.
Okuda J, Fujii T, Yamadori A et al. (1998) Participation of the prefrontal cortices in prospective memory: evidence from a PET study in humans *Neurosci Lett* **253**, 127-30.
Parkinson B (2005) Do facial movements express emotions or communicate motives? *Pers Soc Psychol Rev* **9**, 278-311.
Paus T, Koski L, Caramanos Z, Westbury C (1998) Regional differences in the effects of task difficulty and motor output on blood flow response in the human anterior cingulate cortex: a review of 107 PET activation studies *Neuroreport* **9**, R37-47.
Penny WD, Stephan KE, Mechelli A, Friston KJ (2004a) Comparing dynamic causal models *Neuroimage* **22**, 1157-72.
Penny WD, Stephan KE, Mechelli A, Friston KJ (2004b) Modelling functional integration: a comparison of structural equation and dynamic causal models *Neuroimage* **23 Suppl 1**, S264-74.
Perlstein WM, Elbert T, Stenger VA (2002) Dissociation in human prefrontal cortex of affective influences on working memory-related activity *Proc Natl Acad Sci U S A* **99**, 1736-41.
Perrett DI, Rolls ET, Caan W (1982) Visual neurones responsive to faces in the monkey temporal cortex *Exp Brain Res* **47**, 329-42.
Pessoa L, Kastner S, Ungerleider LG (2002) Attentional control of the processing of neural and emotional stimuli *Brain Res Cogn Brain Res* **15**, 31-45.

Peterson BS, Kane MJ, Alexander GM et al. (2002) An event-related functional MRI study comparing interference effects in the Simon and Stroop tasks *Brain Res Cogn Brain Res* **13**, 427-40.
Phan KL, Fitzgerald DA, Nathan PJ, Moore GJ, Uhde TW, Tancer ME (2005) Neural substrates for voluntary suppression of negative affect: a functional magnetic resonance imaging study *Biol Psychiatry* **57**, 210-9.
Phan KL, Taylor SF, Welsh RC, Ho SH, Britton JC, Liberzon I (2004) Neural correlates of individual ratings of emotional salience: a trial-related fMRI study *Neuroimage* **21**, 768-80.
Phan KL, Wager T, Taylor SF, Liberzon I (2002) Functional neuroanatomy of emotion: a meta-analysis of emotion activation studies in PET and fMRI *Neuroimage* **16**, 331-48.
Phelps EA, O'Connor KJ, Gatenby JC, Gore JC, Grillon C, Davis M (2001) Activation of the left amygdala to a cognitive representation of fear *Nat Neurosci* **4**, 437-41.
Phillips ML, Young AW, Senior C et al. (1997) A specific neural substrate for perceiving facial expressions of disgust *Nature* **389**, 495-8.
Picard N, Strick PL (1996) Motor areas of the medial wall: a review of their location and functional activation *Cereb Cortex* **6**, 342-53.
Price CJ, Friston KJ (1997) Cognitive conjunction: a new approach to brain activation experiments *Neuroimage* **5**, 261-70.
Puce A, Allison T, Bentin S, Gore JC, McCarthy G (1998) Temporal cortex activation in humans viewing eye and mouth movements *J Neurosci* **18**, 2188-99.
Raichle ME (1998) Behind the scenes of functional brain imaging: a historical and physiological perspective *Proc Natl Acad Sci U S A* **95**, 765-72.
Rainville P, Bechara A, Naqvi N, Damasio AR (2006) Basic emotions are associated with distinct patterns of cardiorespiratory activity *Int J Psychophysiol* **61**, 5-18.
Reiman EM, Lane RD, Ahern GL et al. (1997) Neuroanatomical correlates of externally and internally generated human emotion *Am J Psychiatry* **154**, 918-25.
Rinn WE (1984) The neuropsychology of facial expression: a review of the neurological and psychological mechanisms for producing facial expressions *Psychol Bull* **95**, 52-77.
Rizzolatti G, Craighero L (2004) The mirror-neuron system *Annu Rev Neurosci* **27**, 169-92.

Rizzolatti G, Fogassi L, Gallese V (2001) Neurophysiological mechanisms underlying the understanding and imitation of action *Nat Rev Neurosci* **2**, 661-70.
Rizzolatti G, Riggio L, Dascola I, Umilta C (1987) Reorienting attention across the horizontal and vertical meridians: evidençe in favor of a premotor theory of attention *Neuropsychologia* **25**, 31-40.
Rizzolatti G, Riggio L, Sheliga BM (1994) Space and selective attention. In C. Umiltà & M. Moscovitch. (Eds.), Attention and performance XV. *Cambridge, MA: MIT Press.*
Rosen AC, Rao SM, Caffarra P et al. (1999) Neural basis of endogenous and exogenous spatial orienting. A functional MRI study *J Cogn Neurosci* **11**, 135-52.
Ross ED, Mesulam MM (1979) Dominant language functions of the right hemisphere? Prosody and emotional gesturing *Arch Neurol* **36**, 144-8.
Ross ED, Thompson RD, Yenkosky J (1997) Lateralization of affective prosody in brain and the callosal integration of hemispheric language functions *Brain Lang* **56**, 27-54.
Rubia K, Smith AB, Woolley J et al. (2006) Progressive increase of frontostriatal brain activation from childhood to adulthood during event-related tasks of cognitive control *Hum Brain Mapp.*
Rushworth MF, Nixon PD, Passingham RE (1997) Parietal cortex and movement. I. Movement selection and reaching *Exp Brain Res* **117**, 292-310.
Rushworth MF, Walton ME, Kennerley SW, Bannerman DM (2004) Action sets and decisions in the medial frontal cortex *Trends Cogn Sci* **8**, 410-7.
Russell PA (1973) Relationships between exploratory behaviour and fear: a review *Br J Psychol* **64**, 417-33.
Sappey-Marinier D, Calabrese G, Fein G, Hugg JW, Biggins C, Weiner MW (1992) Effect of photic stimulation on human visual cortex lactate and phosphates using 1H and 31P magnetic resonance spectroscopy *J Cereb Blood Flow Metab* **12**, 584-92.
Scherer KR (2001) Appraisal prosesses in emotion: Tehory, methods, research *London: Oxford University Press.*
Schulz KP, Newcorn JH, Fan J, Tang CY, Halperin JM (2005) Brain activation gradients in ventrolateral prefrontal cortex related to persistence of ADHD in adolescent boys *J Am Acad Child Adolesc Psychiatry* **44**, 47-54.
Schwartz GE, Fair PL, Salt P, Mandel MR, Klerman GL (1976) Facial muscle patterning to affective imagery in depressed and nondepressed subjects *Science* **192**, 489-91.

Schwartz S, Vuilleumier P, Hutton C, Maravita A, Dolan RJ, Driver J (2005) Attentional load and sensory competition in human vision: modulation of fMRI responses by load at fixation during task-irrelevant stimulation in the peripheral visual field *Cereb Cortex* **15**, 770-86.

Scott SK, Young AW, Calder AJ, Hellawell DJ, Aggleton JP, Johnson M (1997) Impaired auditory recognition of fear and anger following bilateral amygdala lesions *Nature* **385**, 254-7.

Scott TR, Plata-Salaman CR (1999) Taste in the monkey cortex *Physiol Behav* **67**, 489-511.

Senju A, Tojo Y, Dairoku H, Hasegawa T (2004) Reflexive orienting in response to eye gaze and an arrow in children with and without autism *J Child Psychol Psychiatry* **45**, 445-58.

Serrien DJ, Ivry RB, Swinnen SP (2006) Dynamics of hemispheric specialization and integration in the context of motor control *Nat Rev Neurosci* **7**, 160-6.

Shafritz KM, Collins SH, Blumberg HP (2006) The interaction of emotional and cognitive neural systems in emotionally guided response inhibition *Neuroimage* **31**, 468-75.

Sheliga BM, Craighero L, Riggio L, Rizzolatti G (1997) Effects of spatial attention on directional manual and ocular responses *Exp Brain Res* **114**, 339-51.

Simon JR, Berbaum K (1990) Effect of conflicting cues on information processing: the 'Stroop effect' vs. the 'Simon effect' *Acta Psychol (Amst)* **73**, 159-70.

Simpson JR, Ongur D, Akbudak E et al. (2000) The emotional modulation of cognitive processing: an fMRI study *J Cogn Neurosci* **12 Suppl 2**, 157-70.

Singer T, Kiebel SJ, Winston JS, Dolan RJ, Frith CD (2004a) Brain responses to the acquired moral status of faces *Neuron* **41**, 653-62.

Singer T, Seymour B, O'Doherty J, Kaube H, Dolan RJ, Frith CD (2004b) Empathy for pain involves the affective but not sensory components of pain *Science* **303**, 1157-62.

Solodkin A, Hlustik P, Noll DC, Small SL (2001) Lateralization of motor circuits and handedness during finger movements *Eur J Neurol* **8**, 425-34.

Sonnby-Borgstrom M (2002) Automatic mimicry reactions as related to differences in emotional empathy *Scand J Psychol* **43**, 433-43.

Soussignan R (2002) Duchenne smile, emotional experience, and autonomic reactivity: a test of the facial feedback hypothesis *Emotion* **2**, 52-74.

Strack F, Martin LL, Stepper S (1988) Inhibiting and facilitating conditions of the human smile: a nonobtrusive test of the facial feedback hypothesis *J Pers Soc Psychol* **54**, 768-77.
Stricker JL, Brown GG, Wetherell LA, Drummond SP (2006) The impact of sleep deprivation and task difficulty on networks of fMRI brain response *J Int Neuropsychol Soc* **12**, 591-7.
Sutton SK, Davidson RJ, Donzella B, Irwin W, Dottl DA (1997) Manipulating affective state using extended picture presentations *Psychophysiology* **34**, 217-26.
Tagamets MA, Horwitz B (2001) Interpreting PET and fMRI measures of functional neural activity: the effects of synaptic inhibition on cortical activation in human imaging studies *Brain Res Bull* **54**, 267-73.
Talairach P, Tournoux J (1988) A stereotactic coplanar atlas of the human brain *Stuttgart Thieme.*
Taylor SF, Phan KL, Decker LR, Liberzon I (2003) Subjective rating of emotionally salient stimuli modulates neural activity *Neuroimage* **18**, 650-9.
Tomarken AJ, Davidson RJ, Henriques JB (1990) Resting frontal brain asymmetry predicts affective responses to films *J Pers Soc Psychol* **59**, 791-801.
Tomkins SS (1981) Affect, imagery, consciousness: Vol. 1. Positive affects. *New York: Springer.*
Valle-Inclan F (1996) The Simon effect and its reversal studied with event-related potentials *Int J Psychophysiol* **23**, 41-53.
Vecera SP, Rizzo M (2006) Eye gaze does not produce reflexive shifts of attention: evidence from frontal-lobe damage *Neuropsychologia* **44**, 150-9.
Vuilleumier P (2005) How brains beware: neural mechanisms of emotional attention *Trends Cogn Sci* **9**, 585-94.
Wacker J, Heldmann M, Stemmler G (2003) Separating emotion and motivational direction in fear and anger: effects on frontal asymmetry *Emotion* **3**, 167-93.
Wager TD, Phan KL, Liberzon I, Taylor SF (2003) Valence, gender, and lateralization of functional brain anatomy in emotion: a meta-analysis of findings from neuroimaging. *Neuroimage* **19**, 513-31.
Waldvogel D, van Gelderen P, Muellbacher W, Ziemann U, Immisch I, Hallett M (2000) The relative metabolic demand of inhibition and excitation *Nature* **406**, 995-8.

Wascher E, Verleger R, Wauschkuhn B (1996) In pursuit of the Simon effect: The effect of S-R compatibility investigated by event-related potentials *J Psychophysiol* **10**, 336-46.
Wenzel R, Obrig H, Ruben J et al. (1996) Cerebral blood oxygenation changes induced by visual stimulation in humans *Journal of Biomedical Optics* **1**, 399-404.
Whalen PJ, Bush G, McNally RJ et al. (1998) The emotional counting Stroop paradigm: a functional magnetic resonance imaging probe of the anterior cingulate affective division *Biol Psychiatry* **44**, 1219-28.
Wicker B, Perrett DI, Baron-Cohen S, Decety J (2003) Being the target of another's emotion: a PET study *Neuropsychologia* **41**, 139-46.
Williams JM, Mathews A, MacLeod C (1996) The emotional Stroop task and psychopathology *Psychol Bull* **120**, 3-24.
Williams LM, Brown KJ, Das P et al. (2004) The dynamics of cortico-amygdala and autonomic activity over the experimental time course of fear perception *Brain Res Cogn Brain Res* **21**, 114-23.
Winston JS, Henson RN, Fine-Goulden MR, Dolan RJ (2004) fMRI-adaptation reveals dissociable neural representations of identity and expression in face perception *J Neurophysiol* **92**, 1830-9.
Winston JS, O'Doherty J, Dolan RJ (2003) Common and distinct neural responses during direct and incidental processing of multiple facial emotions *Neuroimage* **20**, 84-97.
Winston JS, Strange BA, O'Doherty J, Dolan RJ (2002) Automatic and intentional brain responses during evaluation of trustworthiness of faces *Nat Neurosci* **5**, 277-83.
Wong R, Bowles LJ (1976) Exploration of complex stimuli as facilitated by emotional reactivity and shock *The American Journal of Psychology* **89**, 527-34.
Woods RP, Grafton ST, Holmes CJ, Cherry SR, Mazziotta JC (1998) Automated Image Registration: I. General Methods and Intrasubject, Intramodality Validation *Journal of Computer Assisted Tomography* **22**, 139-52.
Wree A, Schleicher A (1988) The determination of the local cerebral glucose utilization with the 2-deoxyglucose method *Histochemistry* **90**, 109-21.
Yang TT, Menon V, Eliez S et al. (2002) Amygdalar activation associated with positive and negative facial expressions *Neuroreport* **13**, 1737-41.